SSD
SPACE SYSTEMS DIVISION

LMSC-D665410

NASA CR-
151859

Prepared for:
LYNDON B. JOHNSON SPACE CENTER
NATIONAL AERONAUTICS AND SPACE ADMINISTRATION

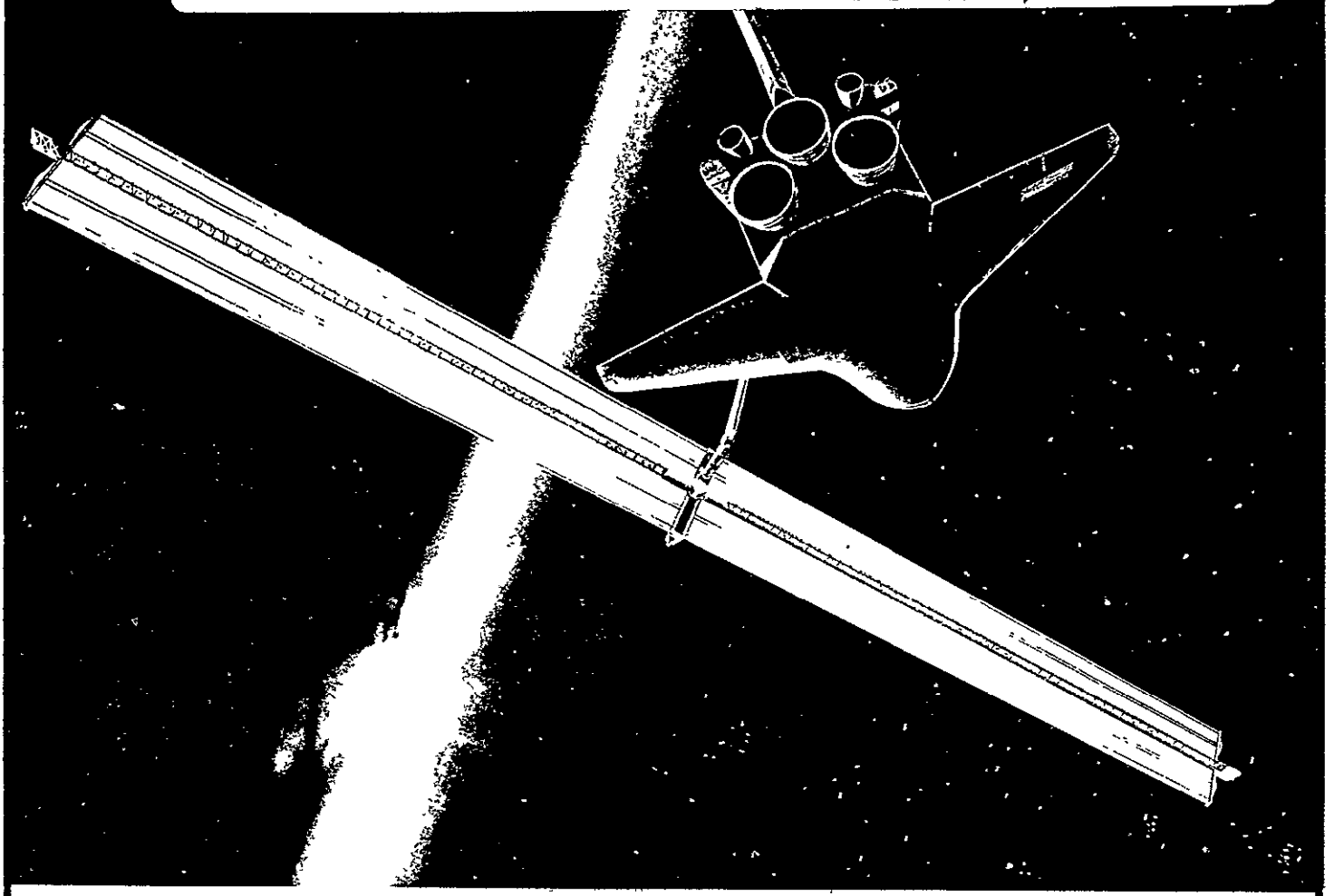

ASSESSMENT OF SEPS SOLAR ARRAY TECHNOLOGY FOR ORBITAL SERVICE MODULE APPLICATION

Final Topical Report

NAS 9-15595

30 OCTOBER 1978

Lockheed Missile & Space Company, Inc.
Sunnyvale, California

153

ASSESSMENT OF SEPS SOLAR ARRAY TECHNOLOGY FOR OSM APPLICATION

TOPICAL REPORT

NAS9-15595

Prepared for

National Aeronautics and Space Administration
Lyndon B. Johnson Space Center
Houston, Texas

by

Space Systems Division

LOCKHEED MISSILES & SPACE COMPANY, INC.

FOREWORD

This document is required by Contract NAS9-15595, Assessment of SEPS Solar Array Technology for OSM Application. It was prepared by the Space Systems Division of Lockheed Missiles & Space Company, Inc., for the National Aeronautics and Space Administration's Johnson Space Center, Houston, Texas.

TABLE OF CONTENTS

Section			Page
1.0	INTRODUCTION		1-1
2.0	REQUIREMENTS DEFINITION		2-1
	2.1	PEP SOLAR ARRAY WING DESIGN REQUIREMENTS	2-1
		2.1.1 Mechanical Performance	2-1
		2.1.1.1 Launch Systems	2-1
		2.1.1.2 Extension and Retraction	2-1
		2.1.1.3 Structural Rigidity	2-1
		2.1.1.4 Mast Design Load	2-4
		2.1.1.5 Weight	2-4
		2.1.1.6 Volume	2-4
		2.1.1.7 Rate of Array Extension	2-4
		2.1.2 Electrical Performance	2-4
		2.1.2.1 Power Requirement	2-4
		2.1.2.2 Power Degradation Limits	2-4
		2.1.3 Operating Environment	2-4
		2.1.4 Solar Array Mounting	2-4
		2.1.5 On-Orbit Loading	2-5
		2.1.6 Power Required by Solar Array	2-5
		2.1.7 Lifetime	2-5
3.0	DESIGN EVALUATION		3-1
	3.1	Configuration Definition	3-1
		3.1.1 Configuration 1	3-1
		3.1.2 Configuration 2	3-3
		3.1.3 Configuration 3	3-4
		3.1.4 Configuration 4	3-4
	3.2	Electrical Design Definition	3-6
		3.2.1 Cell Cover	3-11
		3.2.2 Solar Cell	3-11
		3.2.3 Interconnect	3-13
		3.2.4 Assembly Technique	3-13
		3.2.5 Substrate-Interconnect System	3-14

TABLE OF CONTENTS (Cont.)

Section			Page
	3.2.6	Electrical Panel Design	3-14
	3.2.7	Array Harness	3-16
	3.2.8	Electrical Sizing Analysis	3-16
	3.3	Mechanical Design	3-22
	3.3.1	Blanket Assembly	3-22
	3.3.2	Container Assembly	3-26
	3.3.3	Box Cover Locking Levers	3-29
	3.3.4	Tensioning Mechanisms	3-31
	3.3.5	Extension Mast	3-34
	3.3.6	Canister to Cover Linkage	3-39
	3.3.7	Canister Deployer	3-39
	3.3.8	Support Structure	3-39
4.0	DESIGN SUPPORT STUDIES		4-1
	4.1	DYNAMIC ANALYSIS	4-1
	4.2	THERMAL ANALYSIS	4-27
	4.3	RELIABILITY ANALYSIS	4-37
	4.4	CONTAMINATION CONSIDERATIONS	4-45
5.0	SUMMARY DISCUSSION OF MODIFICATION RECOMMENDATIONS		5-1
	5.1	CONFIGURATION RECOMMENDATION	5-1
	5.2	ELECTRICAL MODIFICATION RECOMMENDATIONS	5-1
	5.3	MECHANICAL MODIFICATION RECOMMENDATIONS	5-2
	5.3.1	Blanket Assembly Modifications	5-2
	5.3.2	Container Assembly Modifications	5-2
	5.3.3	Box Cover Locking Lever Modifications	5-3
	5.3.4	Tensioning Mechanism Modifications	5-3
	5.3.5	Extension Mast Modifications	5-3
	5.3.6	Canister to Cover Linkage	5-4
	5.3.7	Canister Deployer and Support Structure	5-4
6.0	ASSESSMENT CONCLUSIONS		6-1
7.0	REFERENCES		7-1

TABLE OF CONTENTS (Cont.)

Section		Page
APPENDIX A	Configuration Drawings	A-1
APPENDIX B	Automatically Deployable Able Booms	B-1
APPENDIX C	Mode Shape Plots	C-1

LIST OF ILLUSTRATIONS

Figure		Page
3-1	PEP Solar Array System (Stowed) Baseline	3-2
3-2	Array Extension Sequence	3-5
3-3	Power Radiation Degradation	3-9
3-4	Voltage Radiation Degradation	3-10
3-5	Integral Interconnect-Substrate Design	3-15
3-6	PEP Electrical Module	3-17
3-7	Array Panel Configuration .	3-17
3-8	10 x 306 Cell Panel Performance	3-18
3-9	6 x 510 Cell Panel Performance	3-20
3-10	Solar Array Elements	3-23
3-11	Proposed PEP Solar Array Blanket Design	3-27
3-12	Array Panel Stiffening	3-28
3-13	SEP Locking Levers	3-30
3-14	Blanket Tensioning	3-32
3-15	Blanket & Tension Bar Stowage	3-33
3-16	SEP Solar Array Extension Mast	3-35
3-17	PEP Extension Mast	3-38
3-18	Linkage Mechanism	3-40
3-19	Canister Deployer Drive	3-41
3-20	Canister Latching Mechanism	3-42
4-1	Natural Frequencies Case 1	4-5
4-2	Natural Frequencies Case 2	4-6
4-3	Cantilever Mode	4-9
4-4	Cantilever Mode	4-9
4-5	Dynamics Model	4-13
4-6	Base Reaction Moment - Step Translation Input	4-14
4-7	Base Reaction Moment - Step Rotational Input	4-15
4-8	Base Reaction Moment - Spike Translational Input	4-16
4-9	Base Reaction Moment - Spike Rotational Input	4-17
4-10	Relative Displacement Case 1	4-18
4-11	Relative Displacement Case 2	4-19
4-12	Relative Displacement Case 3	4-20
4-13	Relative Displacement Case 4	4-21

LIST OF ILLUSTRATIONS (Cont.)

Figure		Page
4-14	Lateral Deflection vs Blanket Preload	4-24
4-15	Lateral Deflection vs Blanket Preload	4-25
4-16	Fundamental Frequency vs Blanket Preload	4-26
4-17	Equatorial Orbits	4-28
4-18	Solar Cell Temperature Beta = 0°	4-29
4-19	Solar Cell Temperature Beta = 30°	4-30
4-20	Solar Cell Temperature Beta = 60°	4-31
4-21	Solar Cell Temperature Beta = 90°	4-32
4-22	Power/Cell Beta = 0°	4-33
4-23	Power/Cell Beta = 30°	4-34
4-24	Power/Cell Beta = 60°	4-35
4-25	Power/Cell Beta = 90°	4-36
4-26	Mechanical System Reliability Block Diagram	4-39
4-27	Negator Motor	4-42
4-28	Reliability Block Diagram - Redundant Elements	4-43
4-29	Reliability Per Extension/Retraction	4-44
4-30	Orbiter Reaction Control Subsystem	4-46
4-31	Change of Solar Absorptance	4-48
4-32	Change of Emissivity	4-49

LIST OF TABLES

Table		Page
2-1	General Requirements PEP Solar Array	2-2
3-1	PEP Array Blanket Characteristics	3-7
3-2	Mission Radiation Fluence	3-8
3-3	Solar Cell Characteristics	3-12
3-4	Parallel By Series Configuration Options	3-21
3-5	Solar Array Weight Summary	3-24
3-6	SEP Extension Mast Design	3-36
4-1	Power Level Configuration Table	4-2
4-2	MDAC Load Cases	4-2
4-3	Critical Bending Moments Case 1	4-3
4-4	Critical Bending Moments Case 2	4-4
4-5	Geometric and Frequency Characteristics	4-10
4-6	Boom Properties	4-11
4-7	Frequency Out-of-Plane Bending Case 1	4-11
4-8	Frequency Out-of-Plane Bending Case 2	4-11
4-9	Summary of Responses for Unitary Input Values	4-22
4-10	Scaled Response Results	4-23
4-11	Temperature Data Summary Table	4-37
4-12	Deploy/Extension/Retraction System Failure Rates	4-40
4-13	MMH-$HN0_3$ Mass Fluxes Along Orbiter	4-47
6-1	PEP Assessments Summary	6-2

1.0 INTRODUCTION

This report documents the major phases of the Assessment of SEPS Solar Array Technology for OSM Application. This study is being conducted with the NASA Lyndon B. Johnson Space Center (JSC), Houston, Texas, under Contract NAS9-15595. The principal goal of the study is to determine the adaptability of the SEPS Solar Array design for Shuttle application.

A two phase program has been defined as follows:

Phase I	-	Evaluation of Design
Phase II	-	Design Modification and Implementation

This report presents a summary of the effort performed on the following NASA-JSC assigned tasks for Phases I and II. A Program Plan, LMSC-D665402, (Reference 2) was developed which defined the efforts required to design, test, qualify and manufacture a PEP Solar Array System.

- Requirements Definition
- Electrical Design Evaluation
- Mechanical Design Evaluation
- Design Modification Analysis

Section 2.0 details the specific requirements applicable to the design of a solar array, designated the Power Extension Package (PEP) Solar Array, as the prime electrical power subsystem for Orbiter power use.

Section 3.0 discusses the evaluation of the electrical and mechanical design performed to assess compatibility of the SEPS solar array design to the performance requirements for the PEP Solar Array.

Section 4.0 discusses the design support studies and analyses performed in support of the compatibility assessment effort.

Section 5.0 contains recommendations relating to the design modification analysis performed.

Section 6.0 contains the assessment conclusions.

2.0 REQUIREMENTS DEFINITION

The general requirements upon which the design and analysis were based were derived as an iterative process by JSC, LMSC and McDonnell Douglas Astronautics Company (MDAC). From these general requirements, hardware requirements were derived. These extend to loads, packaging constraints, deployment rates, and performance goals upon which the detailed component assessments were based. Because the overall PEP Solar Array design has been and is in a highly iterative stage, it was necessary in many instances to assume design requirements. The major design requirements and constraints identified to date are presented in this section. Table 2-1 presents a summary of the general overall requirements for the PEP Solar Array.

2.1 PEP SOLAR ARRAY WING DESIGN REQUIREMENTS

2.1.1 Mechanical Performance

2.1.1.1 Launch Systems. The PEP Solar Array shall be capable of withstanding Shuttle launch environments in the stowed configuration in any orientation. The mast canisters shall be caged and the solar array blanket shall be preloaded and supported as required to prevent damage to the masts or blankets under the launch dynamic environment.

2.1.1.2 Extension and Retraction. Each wing shall be capable of automatic release of the canisters, the stowed extension masts and array blankets and full extension of both array blankets. The canisters and wings shall be capable of automatic full retraction and re-storage so that they are supported as required to prevent damage during the Orbiter reentry dynamic environment.

2.1.1.3 Structural Rigidity. The solar array wings natural vibration frequency, when fully deployed, shall be equal to or greater than 0.04 Hz in-plane, normal-to-plane and in a torsional mode. This requirement is in conflict with the MDAC requirement of equal to or less than .02 Hz. Based on preliminary dynamic analysis it appears that the blanket would contact the mast if an .02 Hz mast system were to be utilized. Therefore, it is LMSC's recommendation that the solar array/mast system be designed for $\geq$.04 Hz with frequency softening external to the solar array to reduce the system natural frequency to .02 Hz or less.

TABLE 2-1

GENERAL REQUIREMENTS - PEP SOLAR ARRAY

ITEM	REQUIREMENT
Design Requirements	
Output EOL, kWe	30
Altitude, km	370 - 556
Inclination, Deg	28.5, 57 & 90
Array Orientation	Normal to Solar Vector ± 10°
Life	
• Years	5
• Missions	30 (5 years)
• Retraction Cycles (100%)	Orbit - 1 Per Mission
• Retraction Cycles (Partial)	Ground - 1 Per Mission
Mission Duration, Days	30
Reliability (Extend/Retract)	0.999/Cycle
Voltage, Volts	
• Vmp at 70°C	~120
Intermediate Retraction Position	None
Replacement	Required
Max. Weight, kg	612
Max. Size, m	
• Box	Max. Length - 4.5 m
• Canister	
• Max. Blanket Length, m	50.0
• Max. Retracted Length, m	2.0

TABLE 2-1 (Cont.)

ITEM	REQUIREMENT
Deployed Natural Frequency, Hz	
• Bending	≧ .04
• Axial	≧ .04
• Torsion	≧ .04
Shuttle Launch Environment	Per 7700
• G-Loads	
• Vibration	
• Acoustics	
Post-Mission Checkout	Required
Technical/Schedule Risk	Low
Magnetic Moment	TBD
RCS Thruster Loads	TBD
Independent Array Jettison	None
On-Orbit Design Loads	
• Axial, Kg (Lb)	TBD
• Lateral, Kg (Lb)	TBD
• Bending, M-N (Ft-Lb)	135.58 (100)
• Torsion, M-N (Ft-Lb)	TBD

2.1.1.4 Mast Design Load. Due to the possibility of RCS thruster plume impingement on the deployed wing, the mast shall be capable of sustaining a moment of 100 ft-lbs.

2.1.1.5 Weight. The PEP Solar Array, including all deployment and caging mechanisms, and all mounting bracketry shall weigh no more than 612 kg (1350 lbs). This weight does not include any array tracking or jettison systems.

2.1.1.6 Volume. The total PEP Solar Array stowed volume shall not exceed 1.88 m (74 inches) wide by 4.27 m (168 inches) long by 1.40 m (55 inches) high.

2.1.1.7 Rate of Array Extension. The solar array masts shall be capable of extension and retraction rates of 1 in./sec. to 4 in./sec.

2.1.2 Electrical Performance

2.1.2.1 Power Requirement. The solar array wings shall have the area that is required to provide 30.6 kW at the solar array to RMS interface at one A.U. sun distance, normal illumination.

2.1.2.2 Power Degradation Limits. Electrical wing power shall not degrade as a result of launch environments or wing extension/retraction operations. Array power shall not degrade below 30 kW as a result of all degrading mechanisms after the accumulative exposure of 30 months in space.

2.1.3 Operating Environment

The solar array shall be capable of operating in the environment existent in free space at one A.U. from the sun.

2.1.4 Solar Array Mounting

The stowed mechanical attachment of the solar array shall be two sets of bolt patterns on opposing ends of its support structure parallel to the Orbiter's "Y" axis approximately 4.2 m (165 inches) apart.

The on orbit mechanical attachment of the solar array to the RMS gimbal assembly shall be parallel to the Orbiter's "Z" axis and easily accessible by the RMS when the solar array is stowed within the Orbiter bay.

2.1.5 On-Orbit Loading

The solar array in any extension configuration shall withstand the equivalent of 100 ft-lbs. of moment in any direction at the wing to structure interface. The fully retracted solar array package shall withstand a 0.5 g docking load acting in any direction at the system interface to the gimbal assembly.

2.1.6 Power Required by Solar Array

The solar array package shall require no more than 450 watts to operate at any time during its mission.

2.1.7 Lifetime

The solar array shall be capable of operating within the design constraints of 2.1.1 through 2.1.6 for a period not less than 5 years total with 2.5 years accumulative exposure in space.

3.0 DESIGN EVALUATION

This section summarizes the analyses performed to support the definition of the PEP Solar Array mechanical and electrical design.

3.1 CONFIGURATION DEFINITION

After evaluating the available Shuttle bay volume, minimizing the solar array stowed volume and maximizing its flexibility for placement guided the initial selection of configuration candidates. Conceptual layouts of four solar array configurations in terms of stowed volume, weight and complexity assessed to date are shown in Appendix A and itemized below. Configuration 1 is essentially the present SEP baseline structural design. Configuration 2 consists of two masts housed in a common canister with two sets of articulating container trays. Configuration 3 is the JSC baseline configuration which employs two articulating mast canisters. Configuration 4 is a single masted array with a set of articulated containment trays.

Configuration 3 (Figure 3-1) was selected as the array configuration baseline. This configuration was not chosen from a weight or complexity standpoint but rather from JSC's and MDAC's desire to minimize the array's stowed length. Configurations 1, 2 and 4 possess many advantages in other categories as itemized in the following sections and deserve further consideration should stowed length become less of a design driver.

3.1.1 Configuration 1

The integral mast/tray assemblies are mounted to a common support structure. The support structure supports the stowed array for the ascent and reentry phases of the Orbiter mission, positions the array wings for extension and retraction, and restows the locked and preloaded wings back to its original launch position. The wing support includes a structural beam that interfaces with the Orbiter pallet at four trunnion locations and two drive motors that rotate the wings to their ready-to-deploy position.

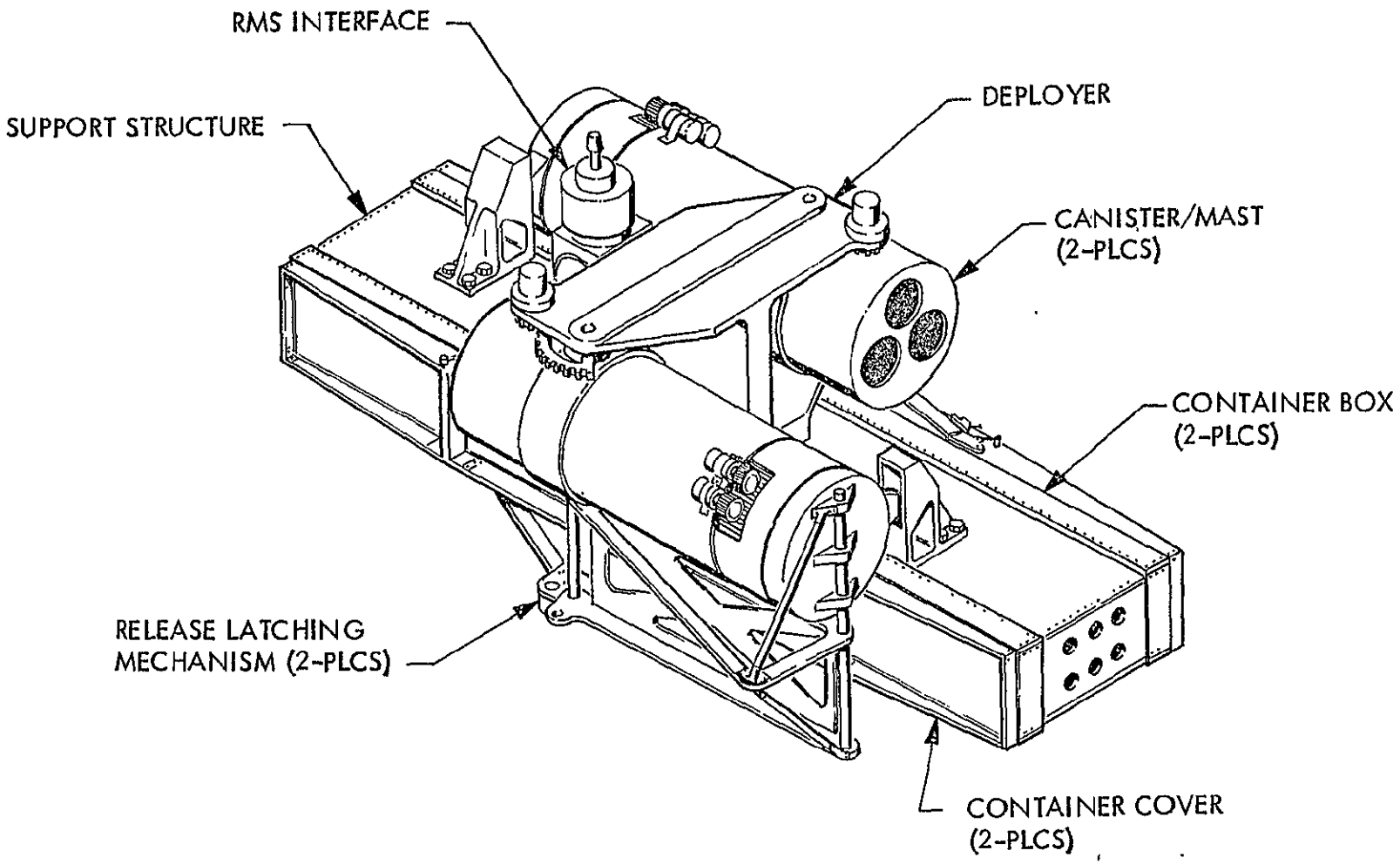

Figure 3-1 PEP Solar Array System (Stowed) Baseline

The major advantages of this configuration include:

- Takes maximum advantage of structural testing accomplished on SEP array due to close resemblance of structural design.
- With minor structural modification the mast and canister geometry can be varied without affecting other array elements.
- The existing SEP ground test techniques can be utilized.
- Easily stowed in existing SEP vehicle design.

Associated with this configuration are the following disadvantages:

- Large stowage length ($\approx$160 in.) minimizes placement alternatives within Shuttle bay.
- Requires continuous tracking about the array's maximum axis of inertia.
- Requires motors and latches for solar array/support orientation.

3.1.2 Configuration 2

This configuration concept utilizes a common canister to house two coilable lattice structure masts. The containment trays are cantilevered off each side and are rotated from their launch to ready-to-deploy positions.

This configuration encroaches upon the 180" dia. circle; however, since the PEP package is part of the basic Shuttle and not part of the payload package it is LMSC's understanding that these local protrusions are acceptable.

The major advantages of this configuration are:

- Permits blanket growth potential length wise
- Minimizes blanket offset from centerline of mast

Disadvantages of this configuration include:

- Cover difficult to preload without addition of independent motorized preload system
- Stowed volume in Shuttle allows only one MMU placement which requires array removal to access MMU
- Folded assembly requires deployment motors and latches
- Prohibits use of SEP ground test techniques at solar array wing level
- Requires continuous tracking about maximum axis of inertia
- Three special Shuttle bridges required for stowage in Shuttle bay.

3.1.3 Configuration 3

This concept consists of two independent hinged canisters which are rotated 90° and are caged in place in their stowed configuration as shown in Figure 3-2. This design offers the lowest packaged volume of all the configurations studied and provides for the maximum flexibility of solar array placement within the Orbiter payload bay. Additional advantages inherent to this configuration include:

- 2 MMU modules can be used
- Only 2 special Shuttle support bridges required

Disadvantages of this configuration include:

- Boom growth limited in diameter
- Mast rotation required for deployment with motors and release latches
- Continuous tracking about maximum axis of inertia
- Requires a 180° rotation about orbit drive axis for each passage through $\beta = 0$.

3.1.4 Configuration 4

This design consists of two independent 4 meter blankets symmetrically deployed on a common mast. This split blanket concept essentially eliminates the concern of the blankets contacting the mast as a result of dynamic excitation. Additional advantages to this configuration concept include:

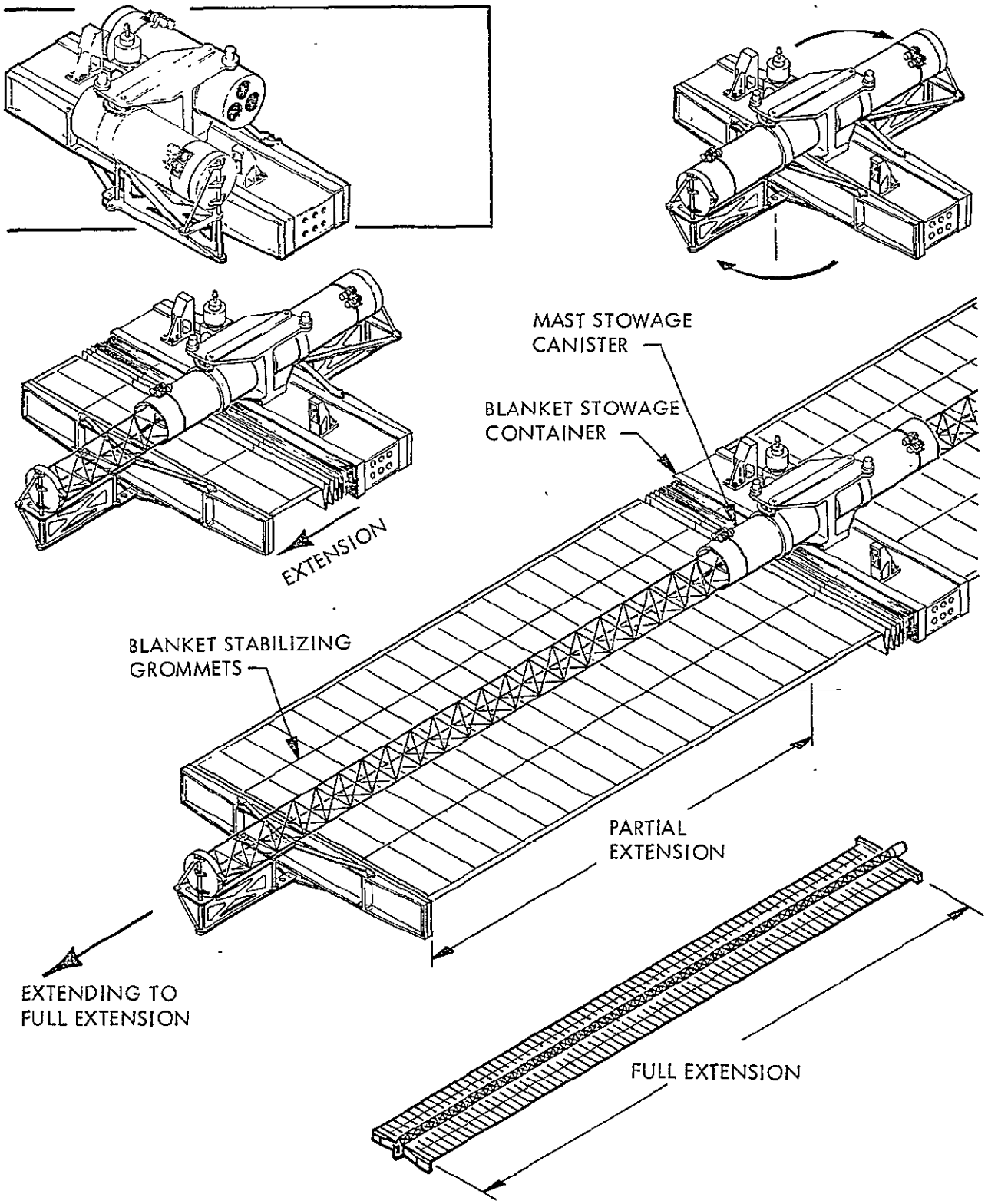

Figure 3-2 Array Extension Sequence

- Maximum mast diameter and length growth potential
- Allows continuous tracking about minimum axis of inertia
- No natural frequency control joint required

Disadvantages inherent to this configuration are:

- Two independent active preload systems required
- Four release points required
- Only one MMU allowable with solar array stowed

3.2 ELECTRICAL DESIGN DEFINITION

The basic electrical design has evolved from the overall requirements and from the derived requirements. MDAC defined the voltage required and LMSC then used the orbital and life parameters to determine the electrical configuration.

The electrical system baseline design is described in the following sections in a sequence progressing from the cell cover through the cell stack to the substrate.

The array blanket characteristics are summarized in Table 3-1.

The cell tentatively selected for the PEP array is a High Efficiency hybrid. This cell assembly will provide the most power in orbit due to its low solar absorptivity and low temperature coefficients. Higher efficiency cells are available, but they operate at higher temperatures which offsets their room temperature performance and typically degrade at a higher rate under mission radiation environments. Table 3-2 represents the predicted radiation fluence for the PEP mission.

The P+ (backside treatment) cell was not selected based on test data showing B.O.L. power gain being fairly sensitive to radiation. The allowed power degradation due to the mission radiation environments cannot be met with the use of the P+ technique. Figures 3-3 and 3-4 display the P+ and H.E. hybrid cell power and voltage characteristics as a function of electron fluence.

TABLE 3-1
PEP ARRAY BLANKET CHARACTERISTICS (ONE WING)

No. of Cell Assemblies/Electrical Module	1,530
No. of Electrical Modules/Wing	96
No. of Cell Assemblies/Wing	146,880
Single Cell Area	8.088 cm^2
Total Cell Area	118.80 m^2
Nominal Cell Spacing (on-array padding)	1.19 mm (0.047 in.)
Overall Blanket Area, 48 x 158 x 29.9 in.*	146 m^2 (1575 ft^2)
Cell Area Packing Factor (1.19 mm cell spacing)	0.887
Overall Blanket Area Cell Packing Factor	0.812
Printed Circuit Substrate Area Density (no cells)	0.1358 kg/m^2 (0.02776 lb/ft^2)
Substrate Plus Cell Assemblies Area Density	1.013 kg/m^2 (0.2072 lbs/ft^2)
Total Blanket Plus Harness Area Density**	0.9785 kg/m^2 (0.2001 lbs/ft^2)

*Includes area for array harness, panel stiffening, and panel-to-panel hinges

**Includes hinges, panel stiffening, on-array padding, and tension distribution bar

TABLE 3-2

MISSION RADIATION FLUENCE

LEO PEP SOLAR CELL FLUENCE PREDICTION (EQUIVALENT 1 MEV ELECTRON/$CM^2 \times 10^{13}$)					
Cell Thickness (mil)	Orbit Inclination Degrees	Orbit Altitude (NMI)	Coverslide Thickness (mil)		
			12	6	2
12	55	300	3.71 (0.531)	4.91 (0.654)	6.225 (0.805)
		235	2.88 (0.201)	3.9 (0.248)	4.96 (0.306)
	28	300	1.77 (0.707)	2.18 (0.872)	2.69 (1.074)
		235	0.5 (0.201)	0.62 (0.248)	0.76 (0.306)
[8]	55	300	4.46 (0.6)	5.67 (0.723)	6.96 (0.875)
		235	3.52 (0.228)	4.55 (0.274)	5.61 (0.332)
	[28]	300	2.0 (0.8)	2.41 (0.964)	2.92 (1.166)
		[235]	0.57 (0.228)	[0.69 (0.274)]	0.83 (0.332)

( ) Values in Parentheses are the trapped contribution per year. Time period 1982 - 1990

[ ] Values in Boxes for nominal PEP mission

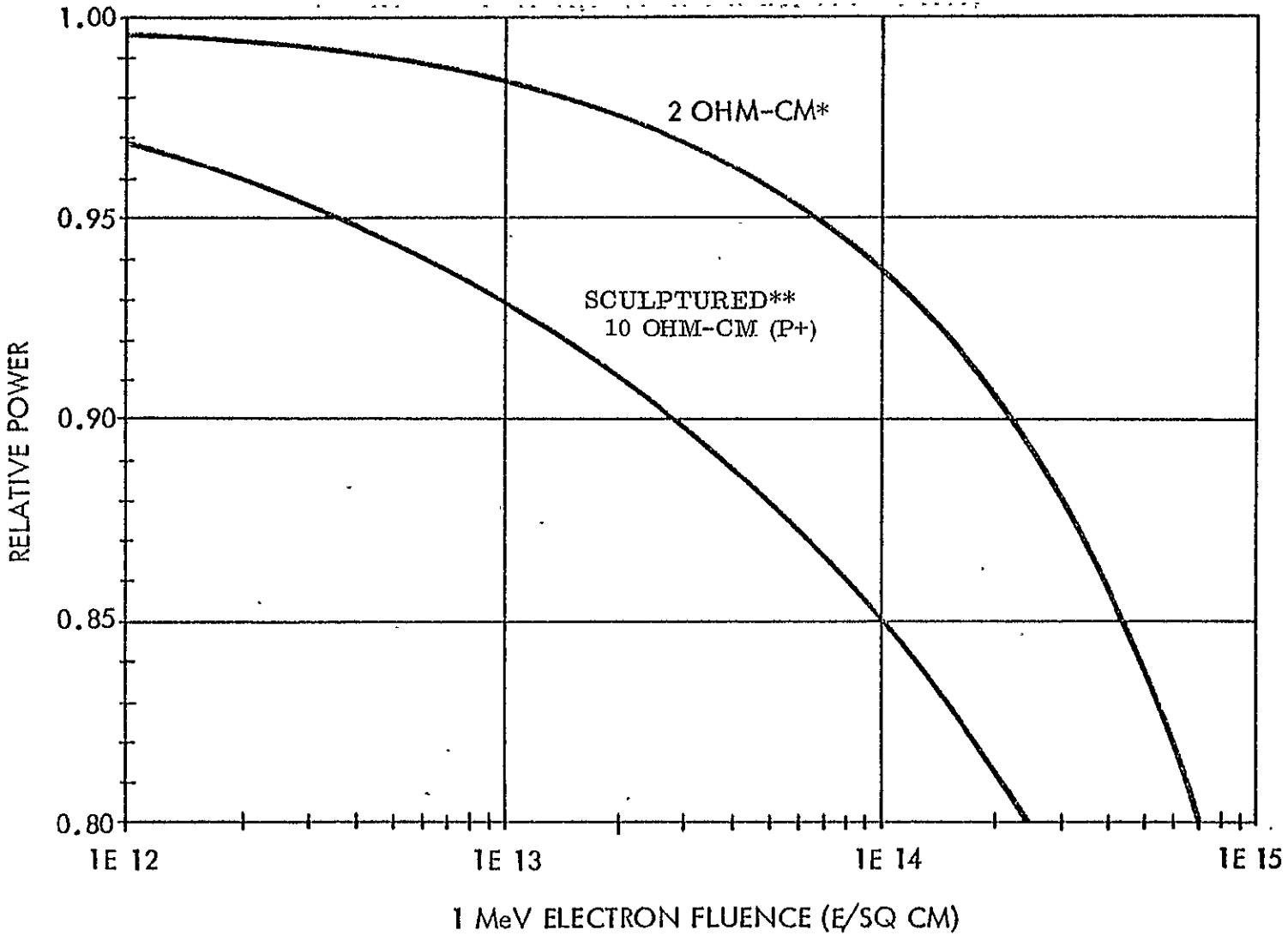

*LMSC TEST DATA

**REFERENCE 1

Figure 3-3 Power Radiation Degradation

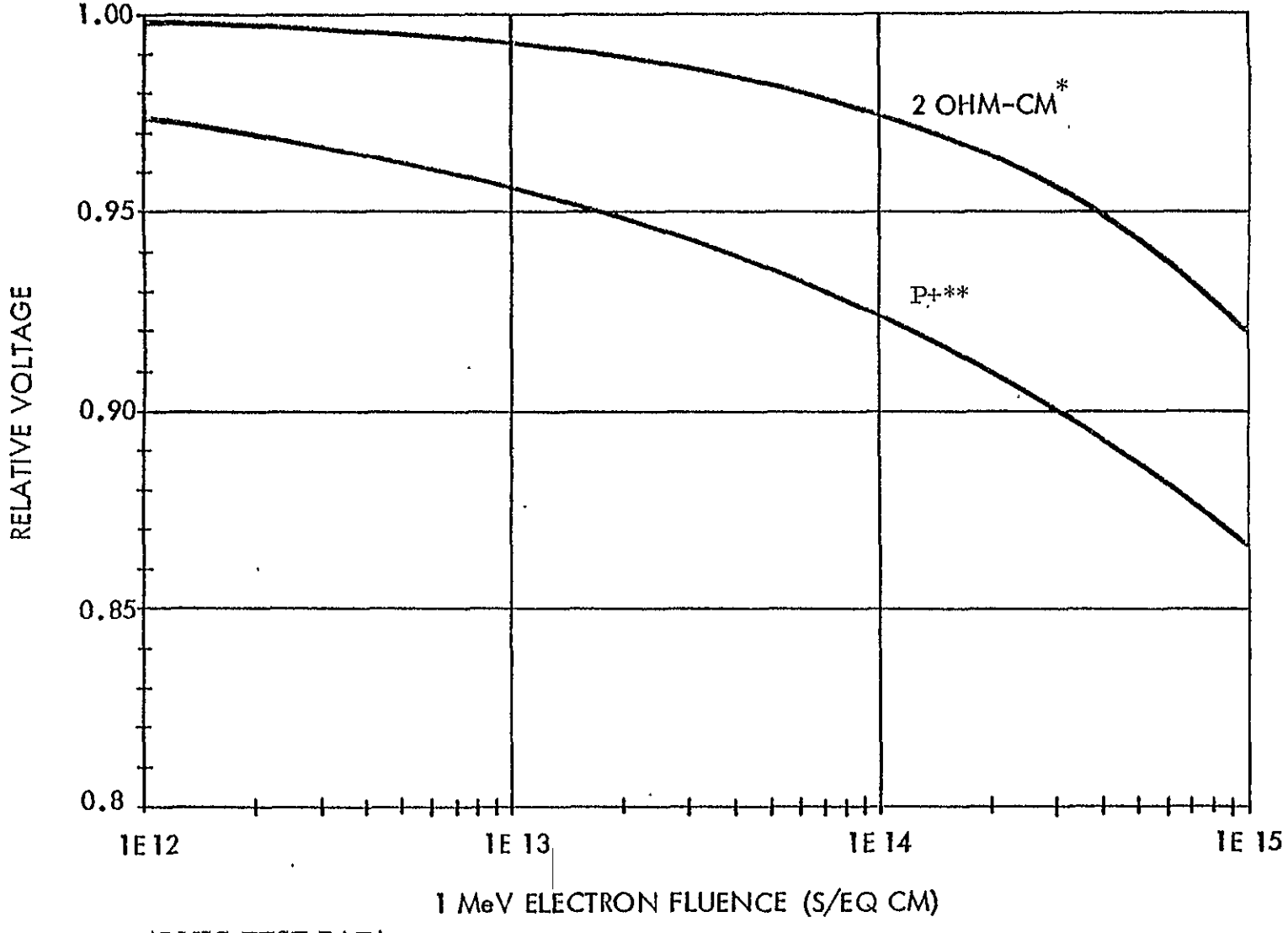

*LMSC TEST DATA

** REFERENCE 1

Figure 3-4 Voltage Radiation Degradation

The solar cell with cell cover bonded in place will be procured as an assembly so that the performance of the assembly is not modified by cell covering at LMSC's facility. Welding of the cell to substrate represents the only major cell handling step.

Table 3-3 summarizes the characteristics of the three solar cell candidates considered for the PEP Solar Array.

3.2.1 Cell Cover

The use of the SEP fused silica cover represents a qualified application of this material. A 0.350 micron UV cut-on filter (blue filter) is placed on the cell side of the cover to protect the cover-to-cell adhesive from UV caused darkening. An anti-reflective (AR) coating is put on the outside cover surface to limit the loss of power due to light reflection at the interface of space vacuum and the cell cover. Since the solar cell has wraparound N contacts, the cover size tolerances are such that the minimum size cover will completely cover the largest solar cell.

The SEP cover adhesive is DC 93-500. This material is a highly refined version of Sylgard 182 and has good transmission stability in the space environment and is applicable for use on the PEP Solar Array.

3.2.2 Solar Cell

The SEPS wraparound solar cell contact is recommended for the PEP array due to the following advantages:

- Eliminates the need for discretely formed, damage susceptible series tabs.
- Allows the cell bonding to the interconnect system to be a single function wherein series contacts can be made at the same time parallel contacts are made.
- Eliminates the N gap radiation problem by allowing the use of uniform covers over the entire cell surface.
- Allows a higher packing factor (more cells per unit area) by reducing the additional series spacing required for the series tab.

TABLE 3-3

SOLAR CELL CHARACTERISTICS

Parameters	SEPS	H.E. Hybrid (Baseline)	Sculptured P+
Base Resis Ohm-Cm	1-3	1-3	7-14
Sculptured	No	No	Yes
Junction Depth (m)	150-250	100-120	100-120
Cell Thickness (in.)	0.008	0.008	0.010
AR Coating	$Ta_2 0_5$	$Al_2 0_3/Ti0_2$	$Ta_2 0_5$
P+	No	No	Yes
Back Surface Reflec.	No	Yes	Yes
Metalization	Cr Pd Ag	Cr Pd Ag	Ti Pd Ag
Solar Absorptance	0.83	0.70	0.89
Coverslides	Fused Silica	Fused Silica	Fused Silica
Cell Emittance	0.81	0.81	0.81
Grid Pattern	10/cm	12/cm	12/cm
Grid Application	Metal Mask	Metal Mask	Metal Mask
28°C AM0 Eff. (%)	11.4	12.8	14.8
28°C Cell Power (mw/cm^2)	15.5	17.4	20.0
V_{mp} (mv)	480	490	490
P_{mp} Temp Coeff. %/OC	-0.467	-0.43	-.48
V_{mp} Temp Coeff. %/OC	-0.467	-0.44	-.46
P/P_o 6 x 10^{13} e/cm^2	0.94	0.94	0.87
V/V_o	0.98	0.98	0.93

- All cell-to-interconnect bonds are in line and in the same plane along the backside centerline of the cell forming a pivot axis such that interconnect flexure is minimized and cell load carrying capability is increased.

3.2.3 Interconnect

In an effort to achieve commonality with the existing SEPS design the tentative selection for interconnect material is copper. Of the other interconnect choices, molybdenum has the best electrical conductivity, is non-magnetic unlike Kovar, and has been successfully used in many flight applications in an independent (non-laminated) interconnect category. As a result, molybdenum is the current recommended interconnect material in the low thermal expansion category. Copper, silver and aluminum are in the higher thermal expansion category. The high cost, lower tensile strength, and higher density of silver as compared to copper, favor copper. Copper was selected for the SEPS design since a low density interconnect material was mandatory to meet SEPS weight requirements. One mil molybdenum with 0.5 mil Ag plating weighs 0.1042 kg/m^2 (0.0213 lbs/ft^2) while 1 oz. copper weighs 0.0611 kg/m^2 (0.0125 lbs/ft^2), both at 20% area. Further evaluation should be accomplished prior to the final interconnect material selection for the PEP solar array.

3.2.4 Assembly Technique

Parallel gap electric resistance welding is selected for interconnection of solar cells to the copper interconnect. Parallel gap electrical resistance welding is selected over soldering because welding offers a better potential for meeting the fatigue requirements induced by thermal cycle stresses. However, solder should not be ruled out at this time.

Parallel gap electric resistance welding was selected since:

- Common to SEPS
- More development work has been performed on this non-soldered bonding technique than on any other. Thermocompression bonding and conductive adhesive bonding techniques are under development but require considerable effort to demonstrate technology readiness for this application.

- The required welding equipment is available and compatible with requirements for production operations

3.2.5 Substrate-Interconnect System

The array substrate is a laminated printed circuit in which the printed circuit is exposed at four locations per solar cell for cell interconnection and at two locations per electrical module to allow electrical harness electrical connection. The substrate is composed of two sheets of 0.5 mil Kapton polyimide film (blanket strength member and printed circuit insulation) which encapsulate the one oz. copper printed circuit (20% area). A 0.5 mil of high temperature polyester adhesive is the laminating system adhesive. The use of the printed circuit or integral interconnect system has major advantages:

- Common SEPS technology.
- Weight and assembly functions are eliminated by not requiring adhesive to mechanically mount the interconnect cells to the substrate.
- The electrical joint is the mechanical joint.
- Thin foils of the interconnect metal are accommodated, protected and held in exact registration throughout the assembly process.
- A wide variety of interconnect stress relief-geometric patterns can be incorporated by precise step and repeat camera photographic processes to form the circuitry for the entire 76.2 x 200.7 cm (30 x 79 in.) electrical module (1530 solar cells).

The integral interconnect-substrate design is shown in Figure 3-5 along with the more conventional formed series tab approach.

3.2.6 Electrical Panel Design

The array wing blanket configuration proposed for the PEP solar array is composed of 48 panels. The panels are 401 x 76.2 cm (158 x 30 in.) in size and are mechanically hinged (fiberglass cloth piano hinge with fiberglass-epoxy hinge pin) to each other along their long dimension. Fiberglass cloth is bonded to the panel edges (short dimension) in a width of 1.27 cm (0.5 in.) for tear resistance. Each panel is composed of two electrical modules, 76.2 x 200.7 cm, that are lap bonded to each other along the

- GOOD JOINT ACCESS
- HIGHER PACKING FACTOR
- REDUCED ASSEMBLY STEPS AND COST
- ELIMINATES N-BUS GAP PROBLEM
- REDUCED WEIGHT

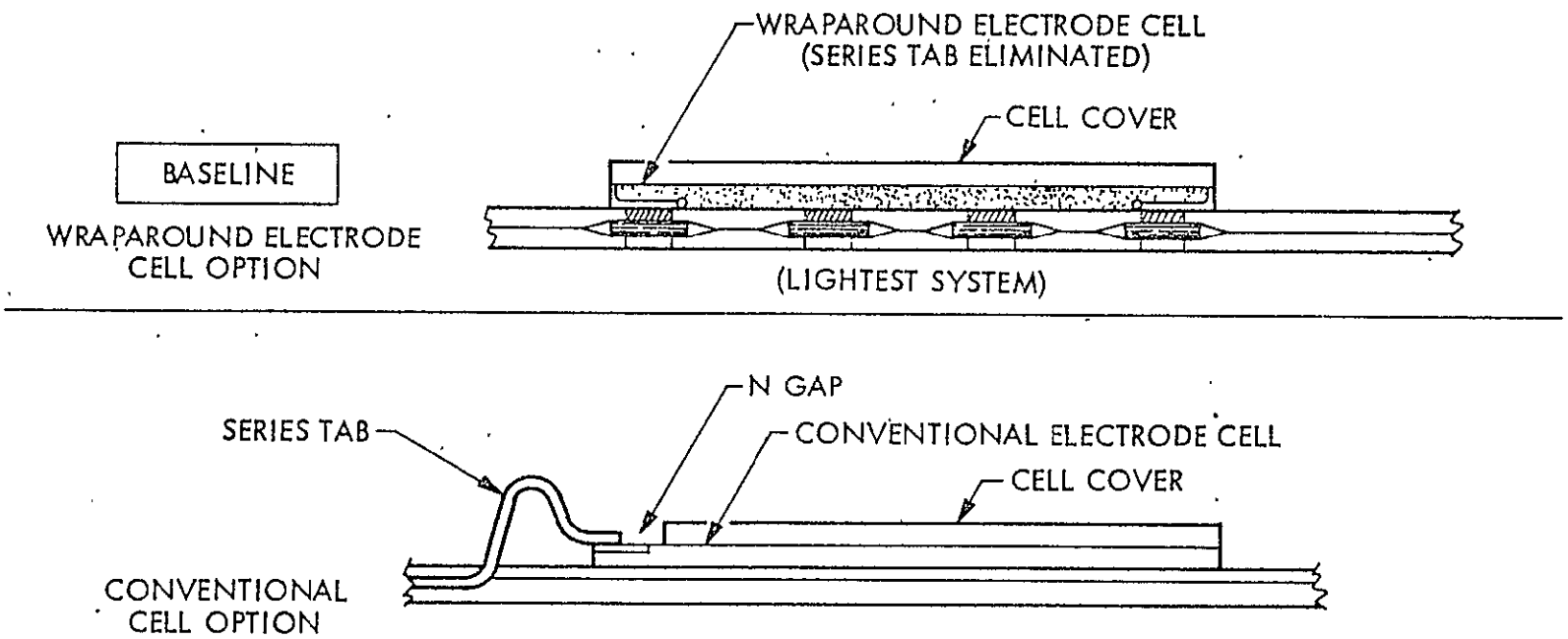

Figure 3-5 Integral Interconnect-Substrate Design

short dimension to form the full panel size, 76.2 x 401 cm. The solar cells in the electrical module will be electrically configured of cells in parallel by cells in series to give the desired voltage range for the PEP thermal environment. The electrical module and array panel configuration is shown in Figures 3-6 and 3-7. Since the panels are folded in half, when stored, along a line parallel to the long hinge lines, the interconnect system is designed to have only one location where a conductor crosses the fold line as indicated in Figure 3-7. The array harness connections are made at the outboard edge of the electrical modules, two per module.

3.2.7 Array Harness

The array harness is a flat cable conductor (FCC) assembly that is mounted on the back of the solar array wing blanket at the two long edges of the blanket. The harness assembly folds-up in the same manner as the array panels for retraction and storage. The folded harness stack height is different from that of the array blanket and, by placing the harness at the edge of the array, this difference in stack height is accommodated by appropriate relief in the containment box cover and floor. The folded solar cell area is kept free of local stresses when the harness is not behind the blanket. The thermal conditions of all the cells tend to be similar with the back of the substrate clear of the harness.

The harness design is a carryover from the SEP program where the harness conductors are aluminum to provide significant weight savings over copper. The FCC insulation is 1 mil thick Kapton and two sheets of Kapton film both with a 1 mil thickness of high temperature polyester adhesive are used to encapsulate the 3 mil thick aluminum conductors. The conductors vary in width from 7.62 mm for the longest length run down to 1.33 mm. The lower width limit is to facilitate the fabrication of joints to the electrical modules. The variation in conductor width provides a nearly constant voltage drop for each of the electrical modules regardless of the distance from the module to the base of the array.

3.2.8 Electrical Sizing Analysis

Figure 3-8 represents the performance characteristics, including 3% assembly losses, of a solar array panel configured 10 cells in parallel by 306 cells in series. The example shows that the power point for a 70°C panel occurs at 119 volts and 2.83 amps for 336.60 watts of output power per panel.

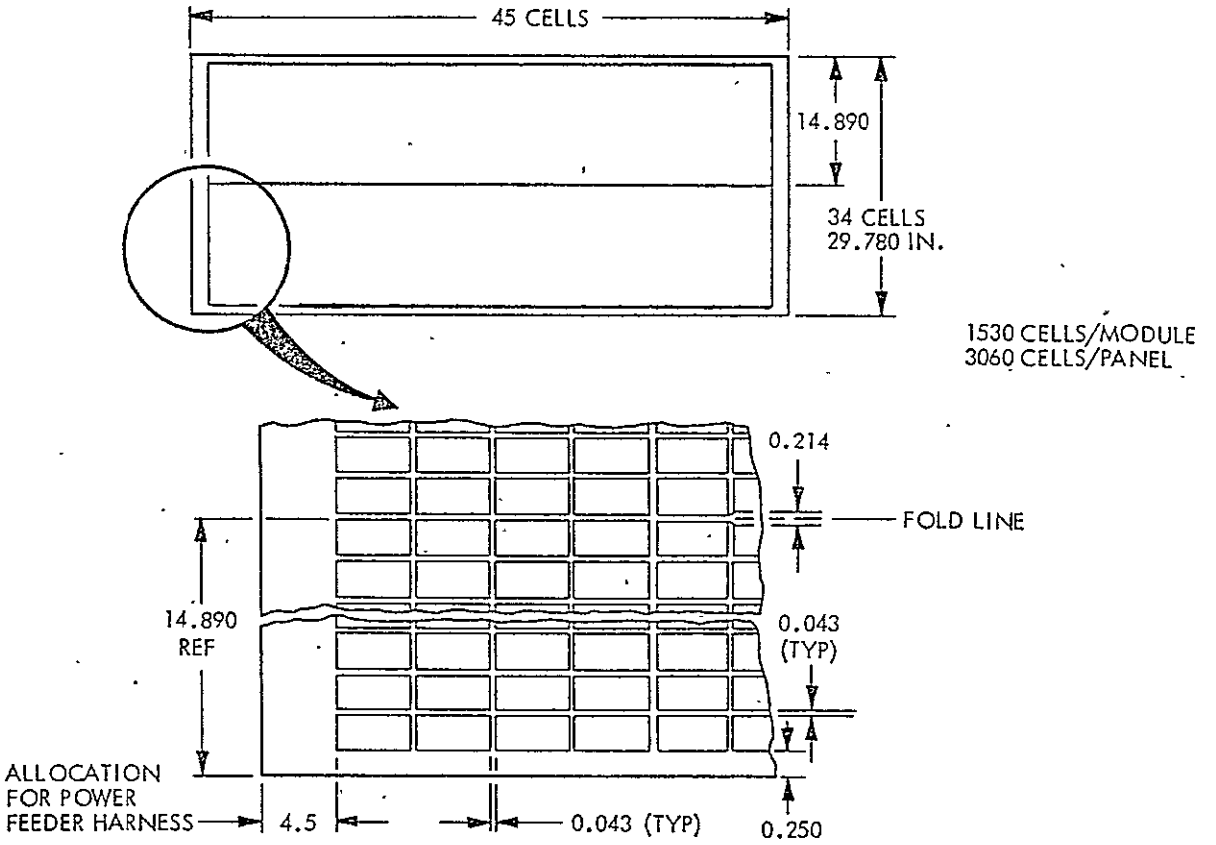

Figure 3-6 PEP Electrical Module

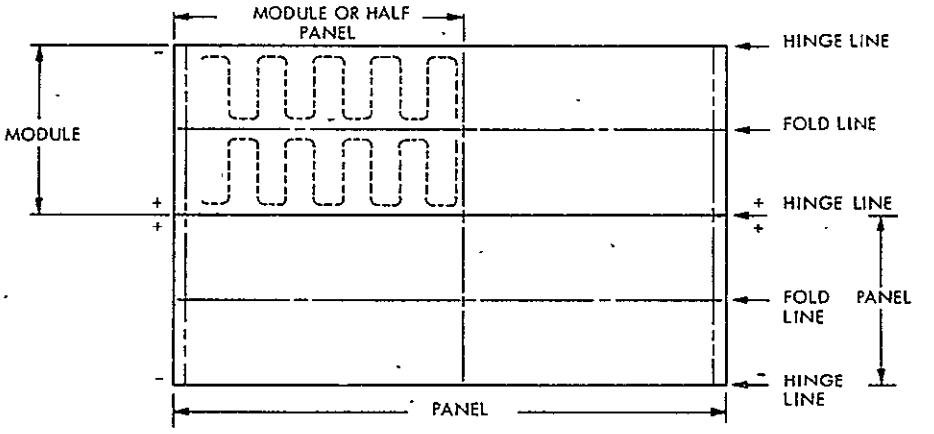

Figure 3-7 Array Panel Configuration

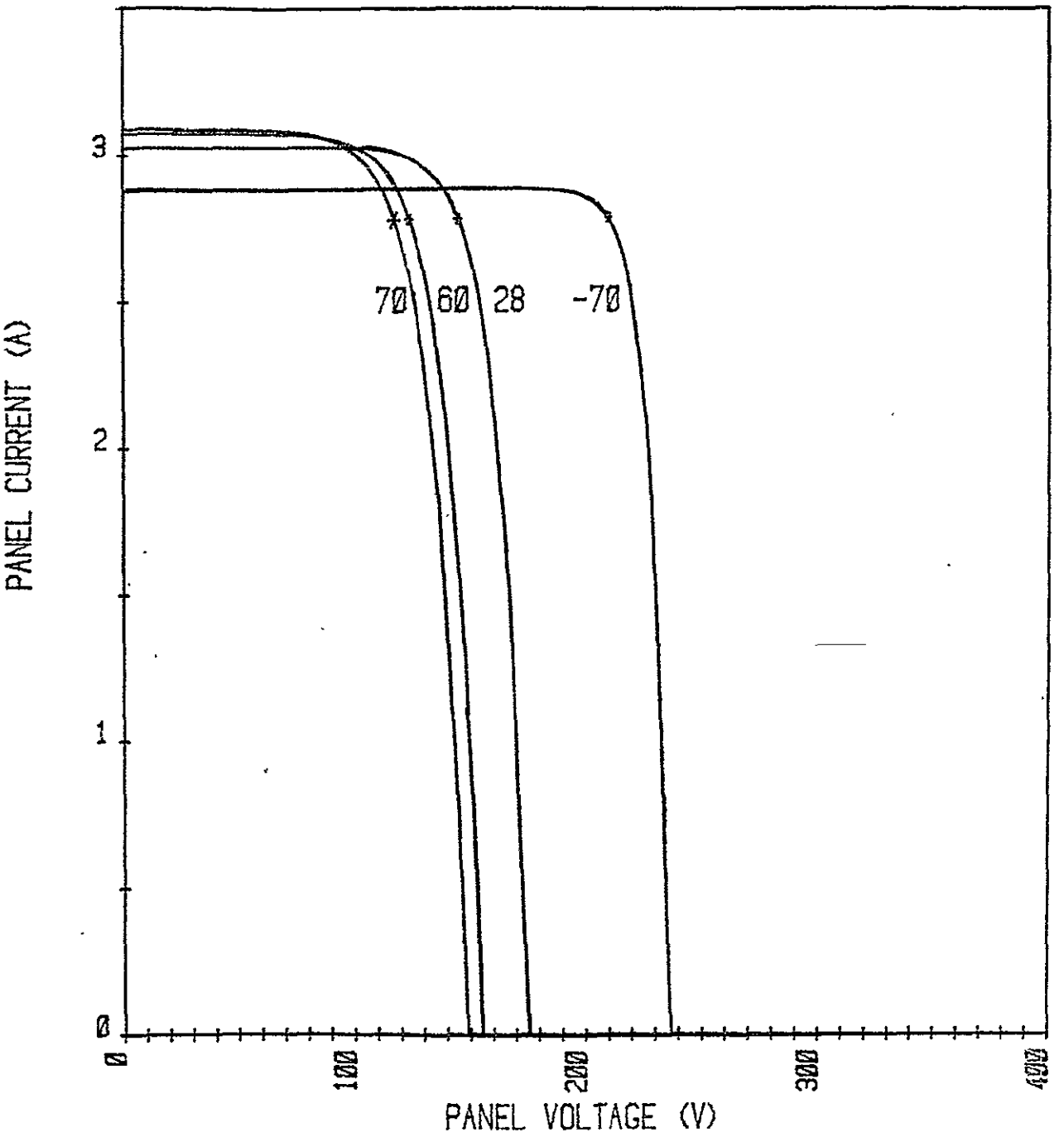

Figure 3-8 10 x 306 Cell Panel Performance

Figure 3-9 presents the performance characteristics, including 3% assembly losses, of a solar array panel configured 6 cells in parallel by 510 cells in series. This example shows that the power point for a 70°C panel occurs at 198 volts and 1.70 amps.

In calculating the E.O.L. electrical characteristics of the solar array the following environmentally induced losses should be accounted for.

Ultraviolet Radiation Micrometeoroid	combined	2%
Radiation at 235 NMI, 28° inclination		
$\Phi = .69 \times 10^{13}$ e/cm^2	P_{max}	1.5%
	V_p	(1%)

In addition, 3% power loss and 3% voltage drop will be contributed by the wire harness and a 0.5% power loss and a 1.2 volt voltage drop will be contributed by the electrical Modules Isolation Diodes.

Using Figure 3-8 or Figure 3-9 and the above loss factors the number of panels required to produce 30 kW of EOL power at 70°C would be calculated as follows:

$$\frac{30,000 \text{ Watts}}{336.60 \text{ watts } (.97)\ (.995)\ (.98)\ (.985)} = 95.7 \text{ panels}$$

In summary, the selected electrical baseline consisting of 96 electrical panels will meet the PEP array 30 kW End-Of-Life power requirement.

The main parameters to be considered in the correct selection of the parallel and series string for the PEP panels are: 1) periphery dimensions common to SEPS, 2) efficient use of allocated area (high packing factor) and 3) voltage range.

The existing SEPS panel configuration as shown in Figure 3-7 is 29.78 inches wide by approximately 157 inches wide. The SEPS cell spacing (.047 inches) provides a high packing factor and allows 90 cells to be placed length wise and 34 along its width for a total panel cell count of 3060. As shown in Table 3-4 there are three parallel by series configurations that approach the 120 volt requirement at 70°C. The parallel by series configuration selection for the PEP solar array is pending with any configuration easily achieved with the flexibility of the printed circuit approach.

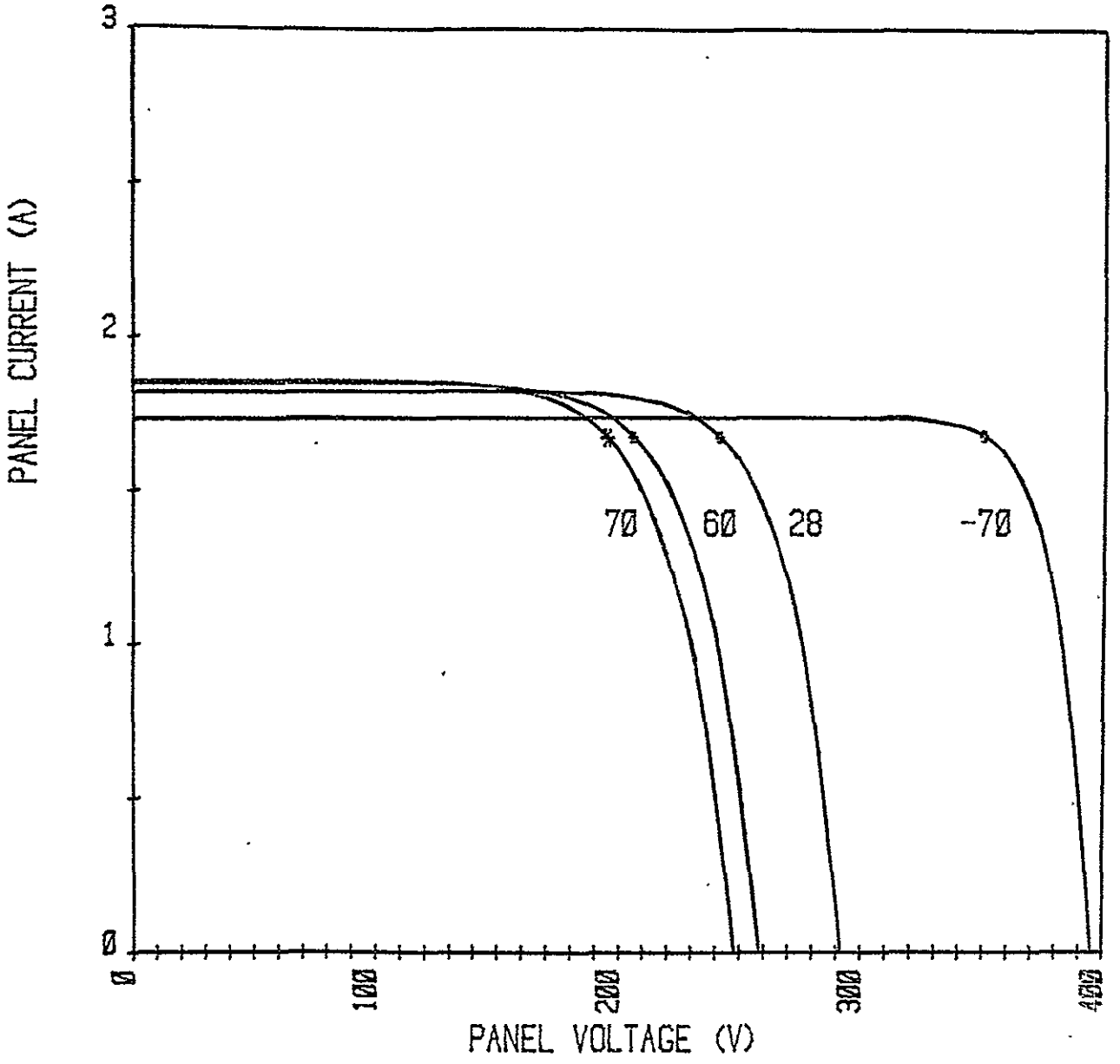

Figure 3-9 6 x 510 Cell Panel Performance

TABLE 3-4

PARALLEL BY SERIES CONFIGURATION OPTIONS (96 PANELS)

Cell Configuration	10 x 306 (SEP Configuration)		9 x 340		6 x 510	
Electrical Characteristics	Power at 70°C	BOL 31,187 watts EOL 30,105 watts	Power at 70°C	BOL 31,187 watts EOL 30,105 watts	Power at 70°C	BOL 31,187 watts EOL 30,105 watts
	Voltage at 70°C	BOL 114.2 volts EOL 111.9 volts	Voltage at 70°C	BOL 126.8 volts EOL 124.3 volts	Voltage at 70°C	BOL 190.9 volts EOL 187.0 volts

3.3 MECHANICAL DESIGN

The baseline mechanical design selected for the PEP array is adapted from the basic SEPS. Five of the eight major mechanical elements, however, are essentially identical in concept and design to the mechanical elements developed under the SEP Technology Program.

The PEP Solar Array is composed of the elements depicted in Figure 3-10 and itemized below

1) Blanket Assembly
2) Container Assembly
3) Box Cover Locking Mechanisms
4) Tensioning Mechanisms
5) Extension Mast
6) Canister to Cover Linkage
7) Canister Deployer
8) Support Structure

The first five elements comprise a basic array wing identical in concept to the SEP Solar Array wing which are integrated via elements 6 and 7 to form single units that are mechanically attached to the support structure (element 8). The preliminary weight estimates for the solar array elements are summarized in Table 3-5.

3.3.1 Blanket Assembly

The PEP Solar Array blanket assembly design discussed in Sections 3.2.3 through 3.2.7 is identical in design to the SEP blanket except for the number of panel assemblies. The PEP blanket consists of simply adding 7 panels to the existing 41 panel SEP blanket. The 48 PEP panel assemblies are folded into 96 half panels for stowage.

Each panel contains 3060 solar cell and cover assemblies welded to a copper interconnect system. For ascent and reentry phases of the PEP mission a form of cell protection from the environment is required. Several padding concepts were tested for slip resistance and vibration survival. Slip resistance data were then used to determine the level of preload necessary to eliminate slippage of the

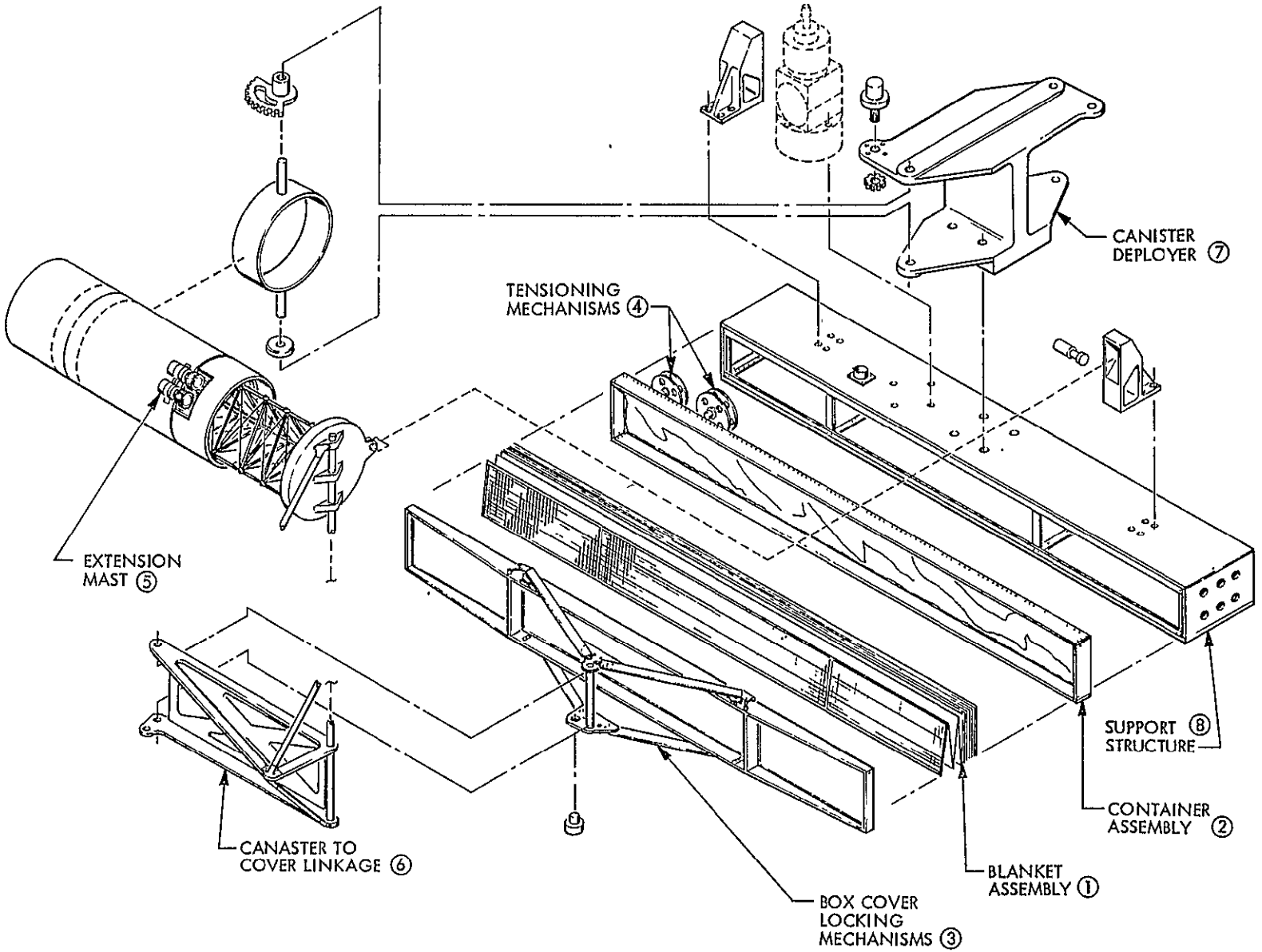

Figure 3-10 Solar Array Elements

TABLE 3-5

PEP SOLAR ARRAY WEIGHT SUMMARY

Element Number	Component Tree	Estimated Weight (KG)	No. Per System	Weight/ SA System (KG)
1	Blanket Assembly	151.04	2	302.08
	Upper Leader	.14		
	Upper Attach Bar	.22		
	Bottom Tension Dist. Bar	.91		
	Lower Leader	.17		
	Substrate W/Pad-W/Stiffening	28.04		
	Solar Cells	57.83		
	Cover Adhesive	6.86		
	Coverslide	43.90		
	Hinge	3.26		
	Hinge Pin	.17		
	Interconnect Harness	9.54		
2	Container Assembly	9.29	2	18.58
	Skin	6.53		
	Honeycomb Core	1.28		
	Pad	.35		
	Perimeter Shield	1.13		
3	Box Cover Locking Mechanism	11.83	2	23.66
	Honeycomb Panel	8.89		
	Preload Distribution Structure	2.94		
4	Tensioning Mechanisms	1.899	4	7.60
	Guide Wire Mechanism			
	Wire	.400		
	Negator	.671		
	Wire Reel	.164		
	Negator Hub	.097		
	Negator Reel	.078		
	Shaft	.038		
	Washers	.010		
	Panel/Wire Retainer	.008		

TABLE 3-5 (continued)

Element Number	Component Tree	Estimated Weight (KG)	No. Per System	Weight/ SA System (KG)
4 (cont.)	Full Tension Mechanism			
	Wire	.001		
	Negator	.185		
	Wire Reel	.018		
	Negator Hub	.060		
	Negator Reel	.098		
	Shaft	.064		
	Washers	.007		
5	Extension Mast	56.69	2	113.38
	Canister	23.83		
	Mast Element	32.86		
6	Canister to Cover Linkage	5.89	2	11.78
	Support Brace	2.30		
	Cap	2.26		
	Preload Lever Arm	1.29		
	Pivot Pins	.04		
7	Canister Deployer	19.15	1	19.15
	Yoke	13.61		
	Canister Ring	2.27		
	Motors	3.12		
	Gear Segment	.15		
8	Support Structure	49.79	1	49.79
	Skin	12.66		
	Bulkhead	9.33		
	Longeron	21.00		
	Support Fitting	1.33		
	Canister Latches	4.65		
	Motor	.82		
	Miscellaneous	9.59	1	9.59
	Thermal Control	5.52		
	Misc. Nuts & Bolts	1.80		
	Wire Harness & Connectors	2.27		

ESTIMATED WEIGHT	555.61
ESTIMATED WEIGHT WITH CONTINGENCY	611.17

stowed blanket during the ascent phases. The padding concept selected for the SEPS baseline and proposed for the PEP Solar Array is shown in Figure 3-11. The criss-cross padding alternates between adjacent panel halves so that, when they are folded in the stowed position, the pad patterns cross each other providing cell separation. The padding should be rigid enough to support preload not allowing compression to the cell level and yet compress a sufficient amount to produce depressions in the mating surfaces. The depressions will develop a slip resistance higher than the friction coefficients of the mating materials. The SEP slip resistance tests indicated that the criss-cross padding required the least preload and, therefore, structure weight to launch the array container in any orientation.

Stiffening of the panels insures fold up in zero-gravity and has varied in concept from early SEP studies through the zero-gravity flight testing. The SEP baseline stiffening concept is shown in Figure 3-12. It provides stiffening along the fold and hinge-lines and at the guide wire positions. The stiffener elements near the wire harnesses were removed because sufficient support was given by the harness. The elements between the guide wires were removed because they are not directed sufficiently during folding process and may actually delay the proper folding direction if an impulse occurs just at the right moment to deflect the panel toward the back side. The guide wires, on the other hand, will assure proper direction. Although the height of the stiffeners is limited to the cell/coverslide height due to stacking limitations, the stiffener element width capabilities have been increased from .064 to .13 inches along the hinge and fold areas and from 0.064 to 0.3 inches at the guide wires. Each fold line is thermally set into a crease for proper fold direction. The stiffeners along the crease are also butted for the same reason. Additional SEP testing to be performed may influence the SEP stiffener design and any refinements will be carried over to the PEP design since their stiffener requirements are identical.

3.3.2 Container Assembly

The array blankets must be supported in the folded condition during ascent and reentry phases of the PEP mission to assure its survival for satisfactory performance. A

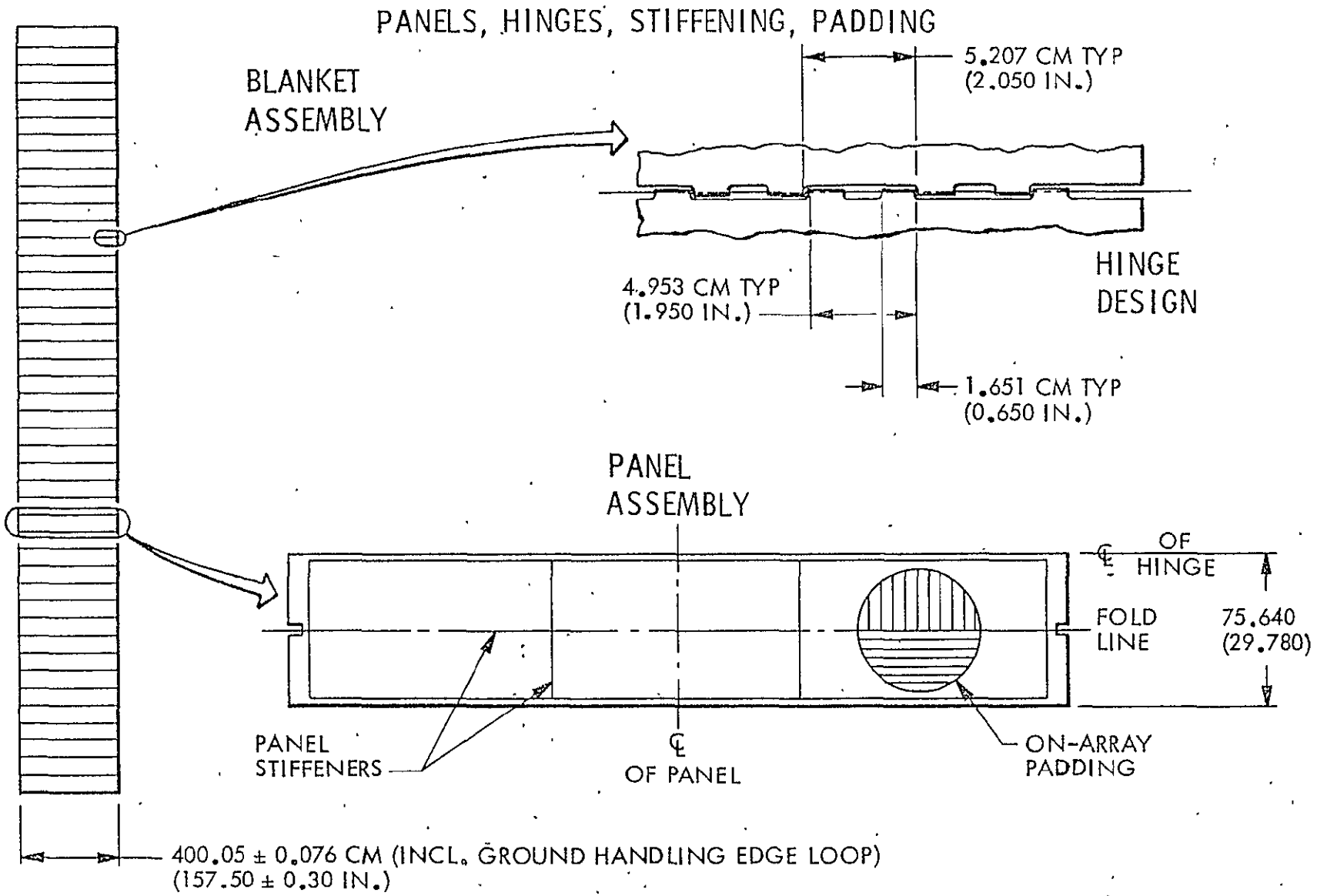

Figure 3-11 Proposed PEP Solar Array Blanket Design

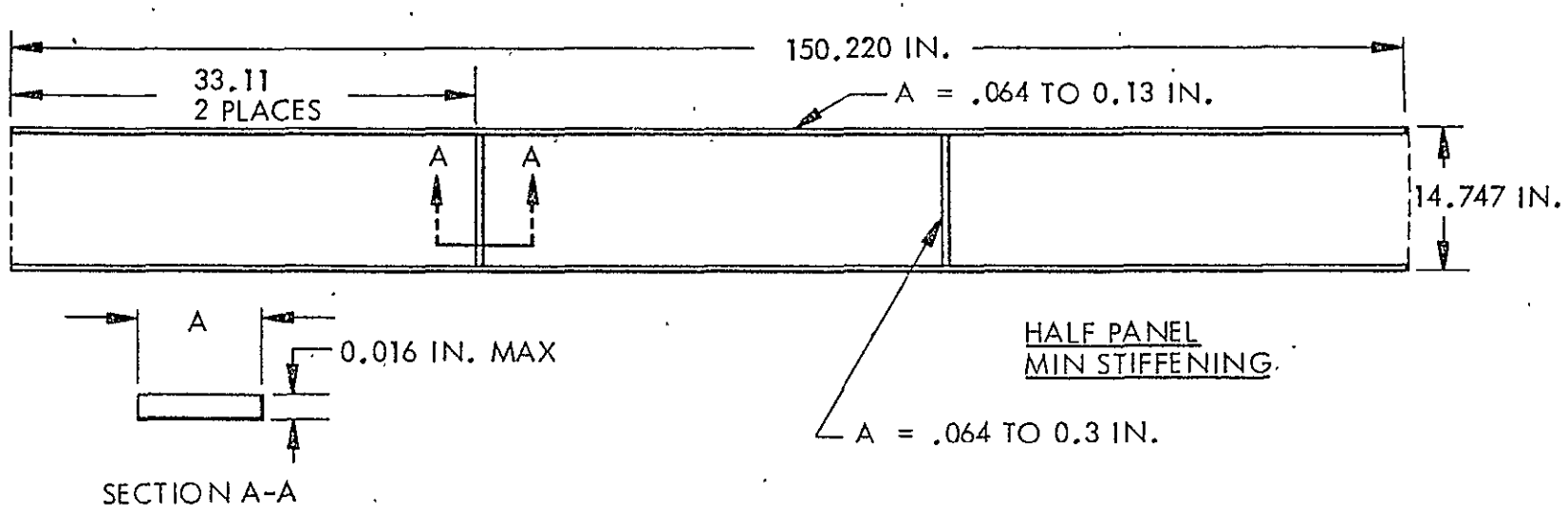

Figure 3-12 Array Panel Stiffening

preload of 1.03 N/cm^2 (1.5 psi) average is created over the folded blanket between the box cover and the container floor. This force is created by the mast during retraction. It is transferred from the mast through the mast tip to cover linkage to four locking levers. This pressure is reacted by a sufficiently stiff structure to allow no more than a 20 to 25% load variation over its surface area. The honeycomb cover and array containment box provide an equal and opposite reaction capability in stiffness to react this pre-load force. It must also support the tension mechanisms and interface with the spacecraft. The floor of the container is a 2.54 cm (1.00 in.) thick honeycomb panel with aluminum skins and aluminum core. The blanket side is faced with polyurethane foam like the cover for cell protection with the blanket stowed. The guide wire and full tension mechanisms are mounted on the underside of this honeycomb panel. The central section of the container is rectangular with aluminum skins and extrusions.

The perimeter of the honeycomb floor is a shield for large contaminant protection during ground operations with the stowed array wing. One end of the shield is removable for attachment of supports for ground extension of the wing.

The basic PEP container differs from the SEP only in its material usage. The SEP containment tray design utilizes graphite epoxy to minimize weight. The PEP design will utilize aluminum in an effort to minimize cost.

3.3.3 Box Cover Locking Levers

The locking lever design used on the SEP Solar Array is presently planned to be evaluated for usage on the PEP. The addition of the rotating canister so the basic SEP design and its associated complexity warrants a more in depth analysis as to compatibility than can be accomplished under this assessment contract.

The SEP Solar Array locking levers shown in Figure 3-13 utilize graphite-epoxy in their construction while the planned structural material for the PEP locking levers will be aluminum. The main function of the locking levers is that of transmitting the mast force into the containment box and cover which provides the preload pressure which was determined necessary for vibration survival.

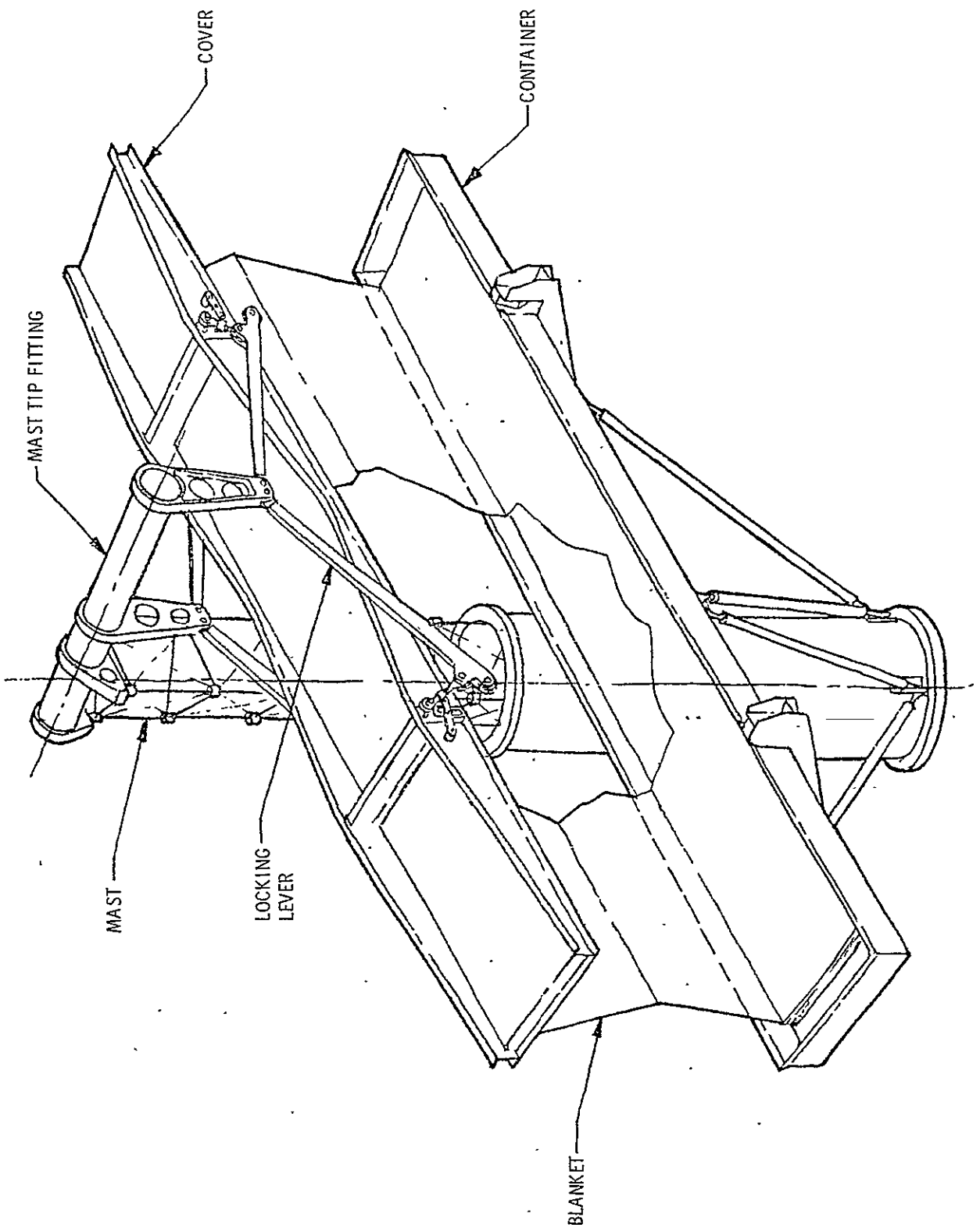

Figure 3-13 SEP Locking Levers

3.3.4 Tensioning Mechanisms

The PEP blanket tension and guide cable systems are all negator powered. They differ from the SEP only in the amount of cable travel and force required. There are 2 pairs of mechanisms, 2 guide, and 2 bottom tension. Each guide cable mechanism provides a 4.4 N (1 lb.) force to a cable which passes through an eyelet at each hinge line in the foldable blanket. The bottom negators power a central cable reel which is appropriately sized based on the length of cable necessary to guide the panels to their fully deployed position. The negator spring lengths and the two negator drum diameters are sized to provide sufficient tension and revolutions to the cable take-up reel. The shafts for each reel end drum are directly attached into the containment box honeycomb floor to minimize the system weight. Inserts are tooled into the floor to provide parallelism to the mechanism shafts. Solid film lubricants are used throughout to minimize friction within the assembly.

The blanket tension mechanisms provide tension to the blanket through a tension distribution system (see Figure 3-14) which distributes the two local loads over the blanket width. The local loads from the mechanism are introduced to a tube through a fitting. The loads from the tube are then transferred to a blanket hinge line by 38 spring assemblies. The spring rates of the assemblies are sufficiently low such that straightness tolerances in the blanket and tube, and tube deflections will not represent large tension variations across the blanket. In the stowed position, the tube is guided to rest on a stop within the container by the tension mechanism cable as shown in Figure 3-15. The tension mechanism uses the same principles, construction, and materials as the guide wire mechanism. The reels and drums will be appropriately sized for the forces and lengths involved to meet the $\geq .04$ Hz requirement and/or preclude mast/blanket contact.

The SEP system utilizes a third tensioning mechanism which allowed the blanket to be tensioned at a partially extended position. The PEP system, since no intermediate tensioned position is required, will not require this and some weight reduction and reliability will be realized.

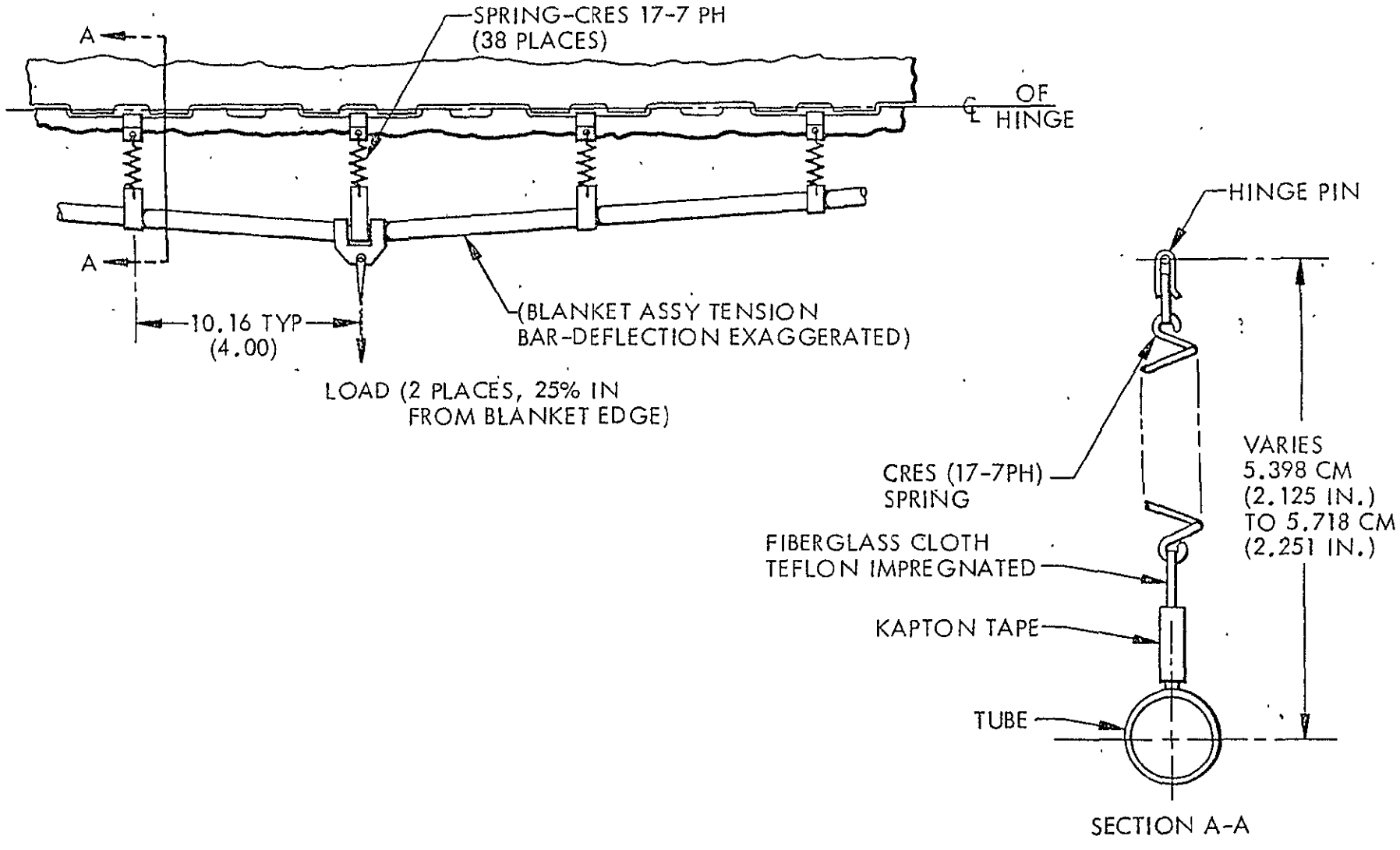

Figure 3-14 Blanket Tensioning

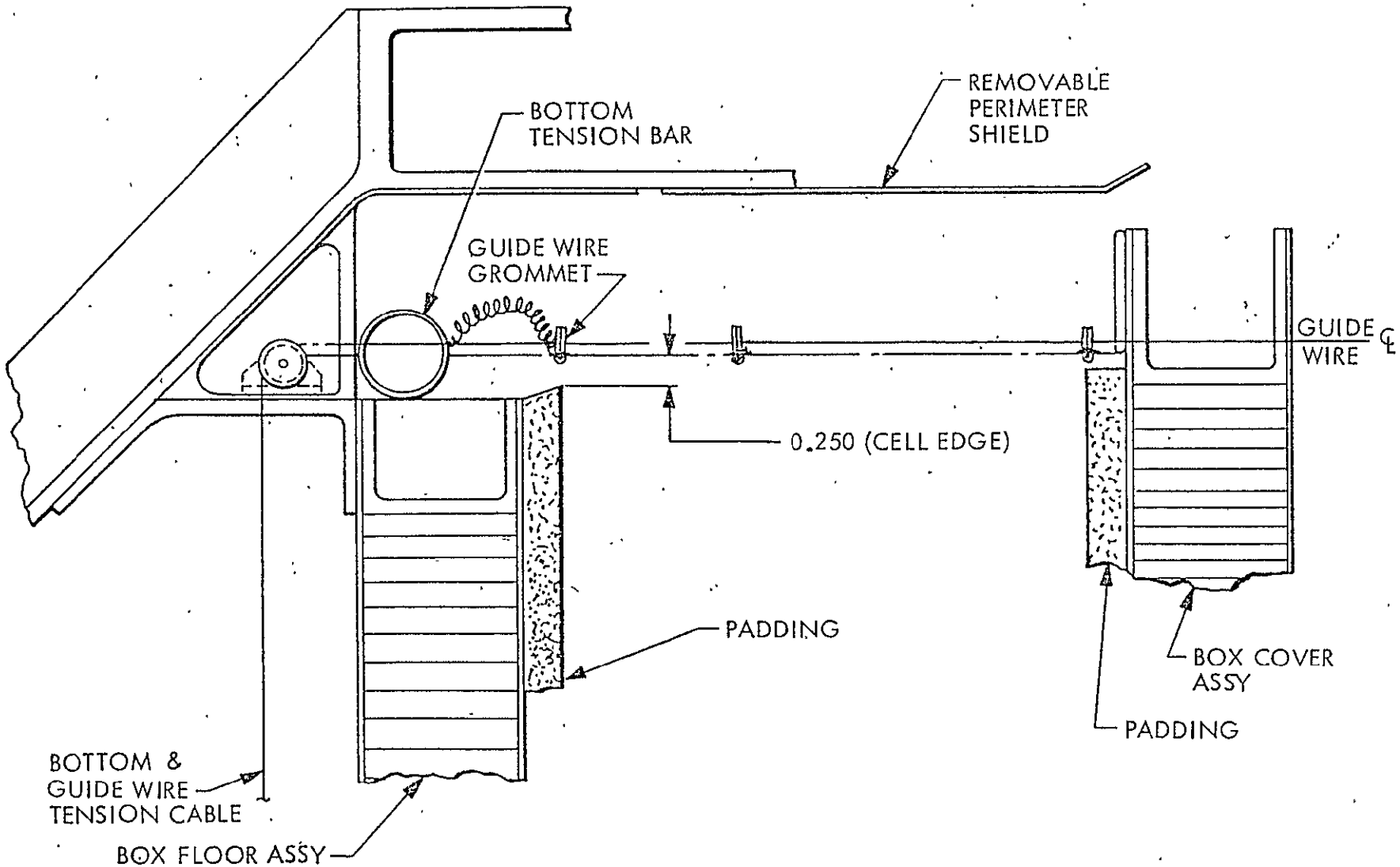

Figure 3-15 Blanket and Tension Bar Stowage

3.3.5 Extension Mast

The continuous coilable longeron mast was selected for SEP based on its minimum weight for the SEP application. The mast developed for SEP is illustrated in Figure 3-16 and summarized in Table 3-6.

The SEP mast is deficient in many areas for use on the PEP Solar Array. Primarily, the SEP mast was sized for a deployed natural frequency of .04 Hz and minimal weight. The PEP mast must be sized for a minimum bending strength capability of 150 ft-lbs. Additionally, the PEP mast must be designed for high reliability through its 5 year multi-mission/multi-extension and retraction life cycle.

The mast canister must also be redesigned to accommodate the loads induced by cantilevering it from its base off the deployer.

Potential mast deficiencies and questions associated with the 5 year life and multiple extension/retraction cycle requirement include:

Extension Motors

- Redundancy required for reliability?
- Brush material wear rate
- Bearing and gear lubricant evaporation rate

Longeron and Batten Material

- Fatigue at high and low temp through multiple coiling cycles

The mast meeting the PEP requirements is shown in Figure 3-17. Although larger than the SEP mast there is no major technology required to scale-up this mast.

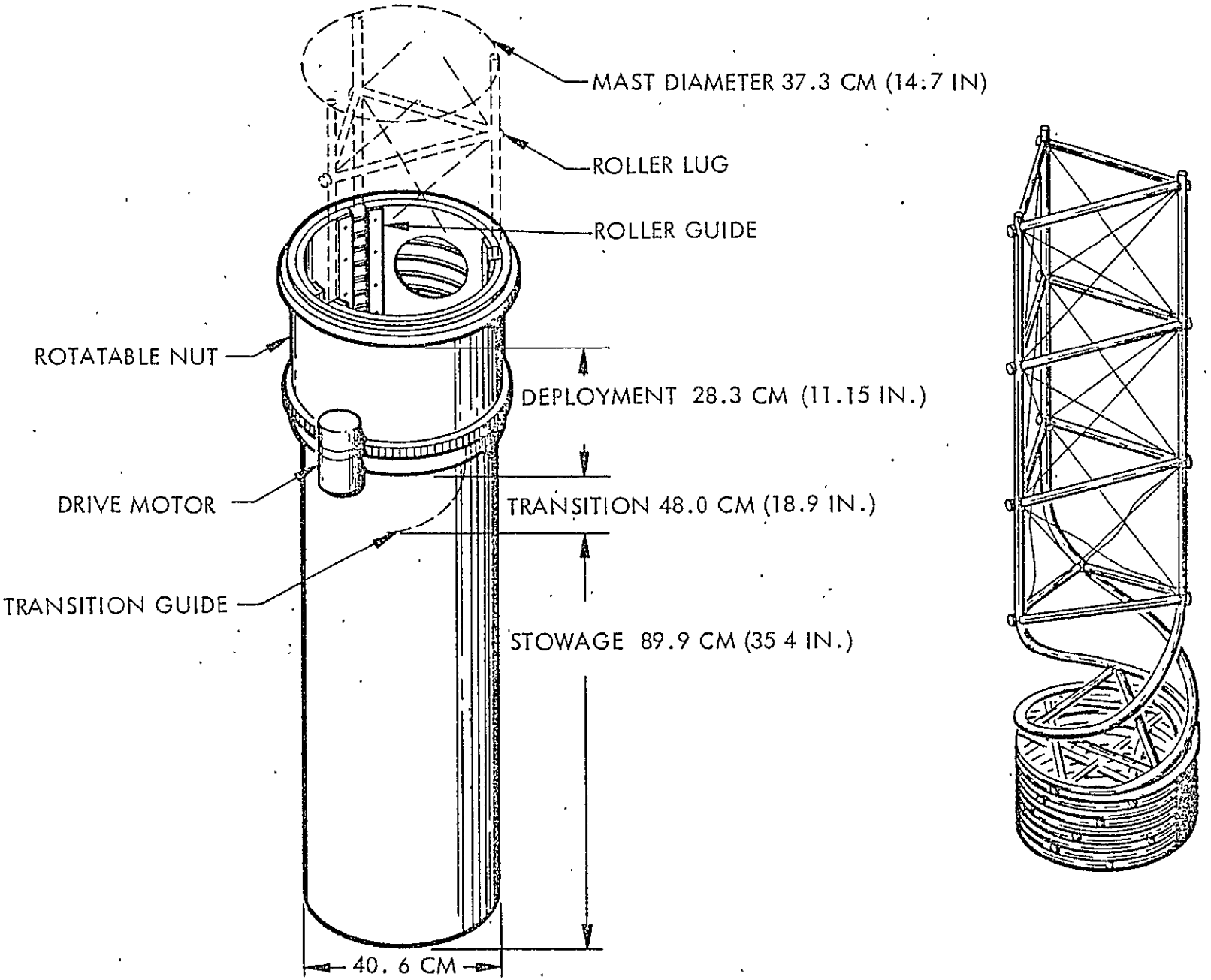

Figure 3-16 SEP Solar Array Extension Mast

TABLE 3-6

SEP EXTENSION MAST DESIGN

MAST ELEMENT DATA

Mast Diameter: 37.3 cm (14.7 in.)

Mast Mass: 18.8 kg (41.4 lb)

Longerons:

Cross section - 0.553 x 0.572 cm (0.218 x 0.225 in.), rectangular with corners rounded to 0.030 in. radius

Material - S-glass/polyimide composite using 20-end glass roving/PMR 15 polyimide resin

Battens:

Cross section - 0.457 x 0.457 cm (0.18 x 0.18 in.), square with corners rounded to 0.030 in. radius

Material - Same as longerons

Diagonals: 3/64 in diameter, 3 x 7 strand, stainless steel cable

Bay Length: 23.9 cm (9.0 in.)

Mechanical Properties:

Bending stiffness	- 62.8 kN-m^2 (21.96 x 10^6 lb-in^2)
Bending strength	- 164.4 m-N (1456.3 in-lb), minimum valve associated with one longeron in compression
Shearing stiffness	- 87.2 kN (19,620 lbs)
Shearing strength	- 134.8N (30.33 lb)
Torsional stiffness	- 1.433 kN-m^2 (5.08 x 10^5 lb-in^2)
Torsional strength	- 970.7N (218.4 lb)

TABLE 3-6 (CONTINUED)

DEPLOYMENT CANISTER DATA

Canister Height: 24 cm (61 in.)

Canister Diameter: 40.6 cm (16 in.)

Canister Mass: 15.5 kg (34.08 lb)

Extension Motors: Two ea. 27 vdc, TRW/Globe, 102A175-8.
Maximum rate torque - 0.0507 m-kg (4.39 in-lb), 1.4 amp.
Maximum intermittent torque - 0.102 m-kg (8.79 in-lb) 3.0 amp.
Stall torque - 0.254 m-kg (21.97 in-lb) 11 amp.
Operating temp. - 232°C max. TBD min.

Canister Materials: Principally aluminum (2024-T4 and 6061-T6), deployment nut has aluminum threads inside fiberglass/epoxy shell.

Dissimilar materials in contact:

a. Stainless steel Kaydon bearings (2 ea.), 40.64 cm (16 in), i.e., mounted in aluminum ring. Thrust load per bearing is one-half maximum tension or compression in mast. Radial load is minimal.

b. DuPont Vespel pinion gears drive 2024-T4 aluminum ring gear on deployment nut. Tooth pressure is 84.4N (19 lb) at stall torque and 23.3N (5.25 lb) at 533.3N (120 lb) mast force.

c. Steel bearings in aluminum mast base turntable. Maximum thrust load is 22.2N (5 lb); minimal radial load.

Lubrication System: Ball Brothers "Vac Kote" or equivalent (e.g. Micro Seal) Aluminum mast rollers rotate on aluminum pivots (axles) and bear on Al deployment nut threads.

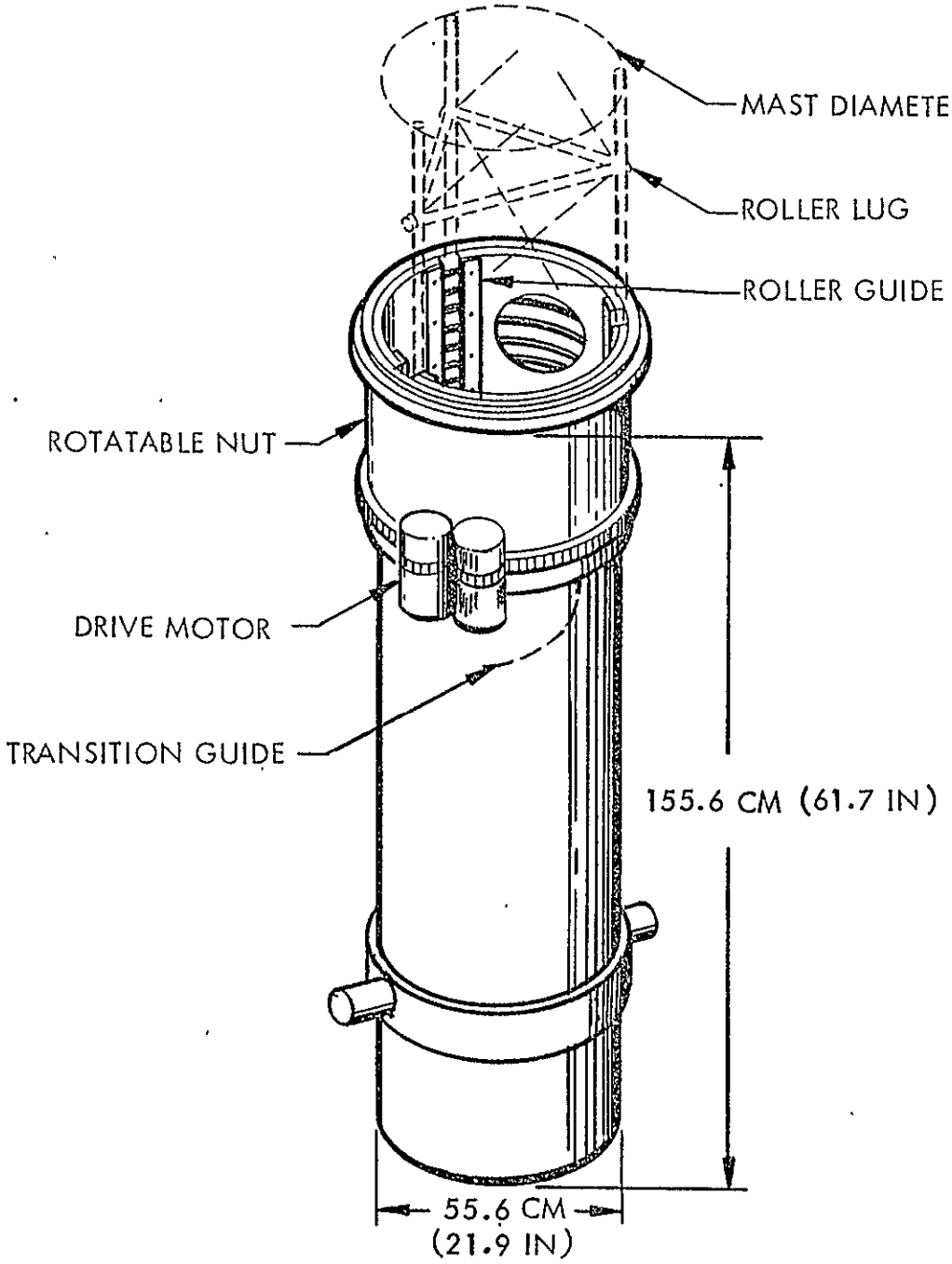

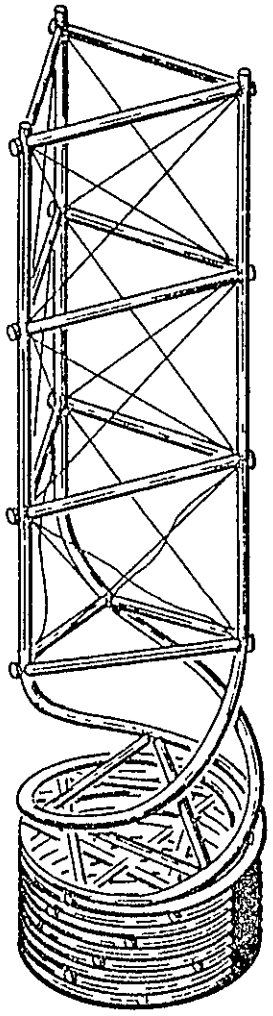

Figure 3-17 PEP Extension Mast

3.3.6 Canister to Cover Linkage

The cover linkage mechanism allows the canister to rotate 90° relative to the box cover for compact stowage within the Orbiter during its ascent and reentry phases. The incorporation of this capability is the only major deviation from the basic SEP mechanical design.

Figure 3-18 shows the preliminary design for the linkage mechanism.

The linkage consists of two levers structurally tied together with coaxially aligned bearings on each end. The cover end of the linkage employs a redundant electrically actuated pin indexing mechanism to fix the linkage to the cover after rotation to the pre-extension position. Power is provided to the solenoids by way of additional flat conductor cables in the array harness which are then routed up the box locking levers to the solenoids.

3.3.7 Canister Deployer

The deployer mechanism supports the mast canister for the ascent and reentry phases of the Orbiter mission, positions the canister for mast extension, and restows the canister back to its original launch position. The canister deployer includes a hinge assembly that interfaces the canister to the support structure, and a rotational drive system. The rotational drive system (Figure 3-19) uses an electric motor drive with redundant motors. The primary motor drives a gear segment that is attached to the canister which rotates the canister to its deployed position and provides the necessary force to essentially lock the canister to the deployer hinge assembly in the deployed position.

3.3.8 Support Structure

The support structure interfaces the deployers and container assemblies to the Orbiter's trunnion latching structure. The conceptual design for the support consists of a rectangular cross sectional beam stiffened with truss structure. Two sets of electrically activated canister tip latching mechanisms are attached to the support structure and provide canister tip caging during ascent and reentry. The canister latching mechanisms are shown in Figure 3-20. The holddown pins on the canisters are released from the

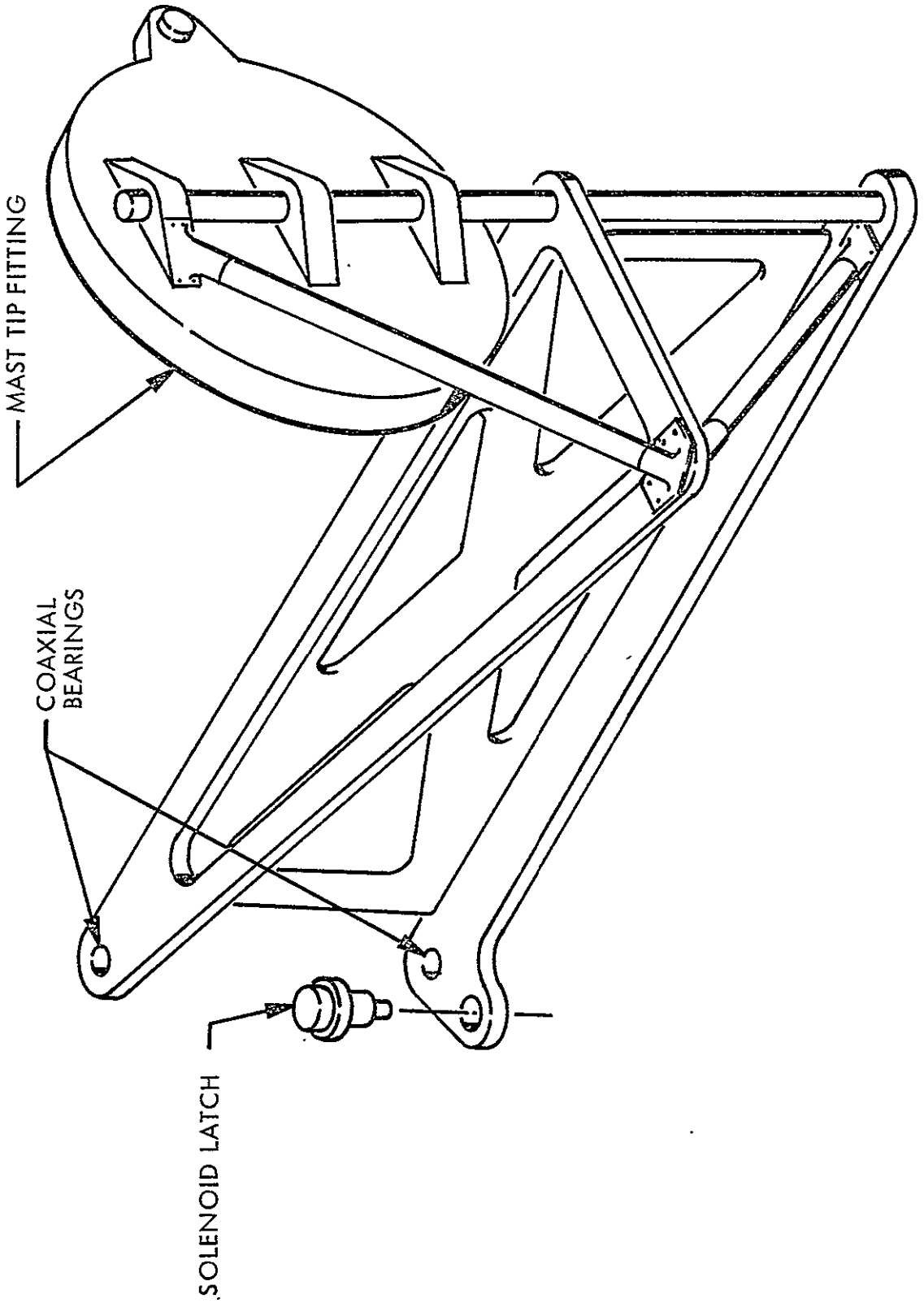

Figure 3-18 Linkage Mechanism

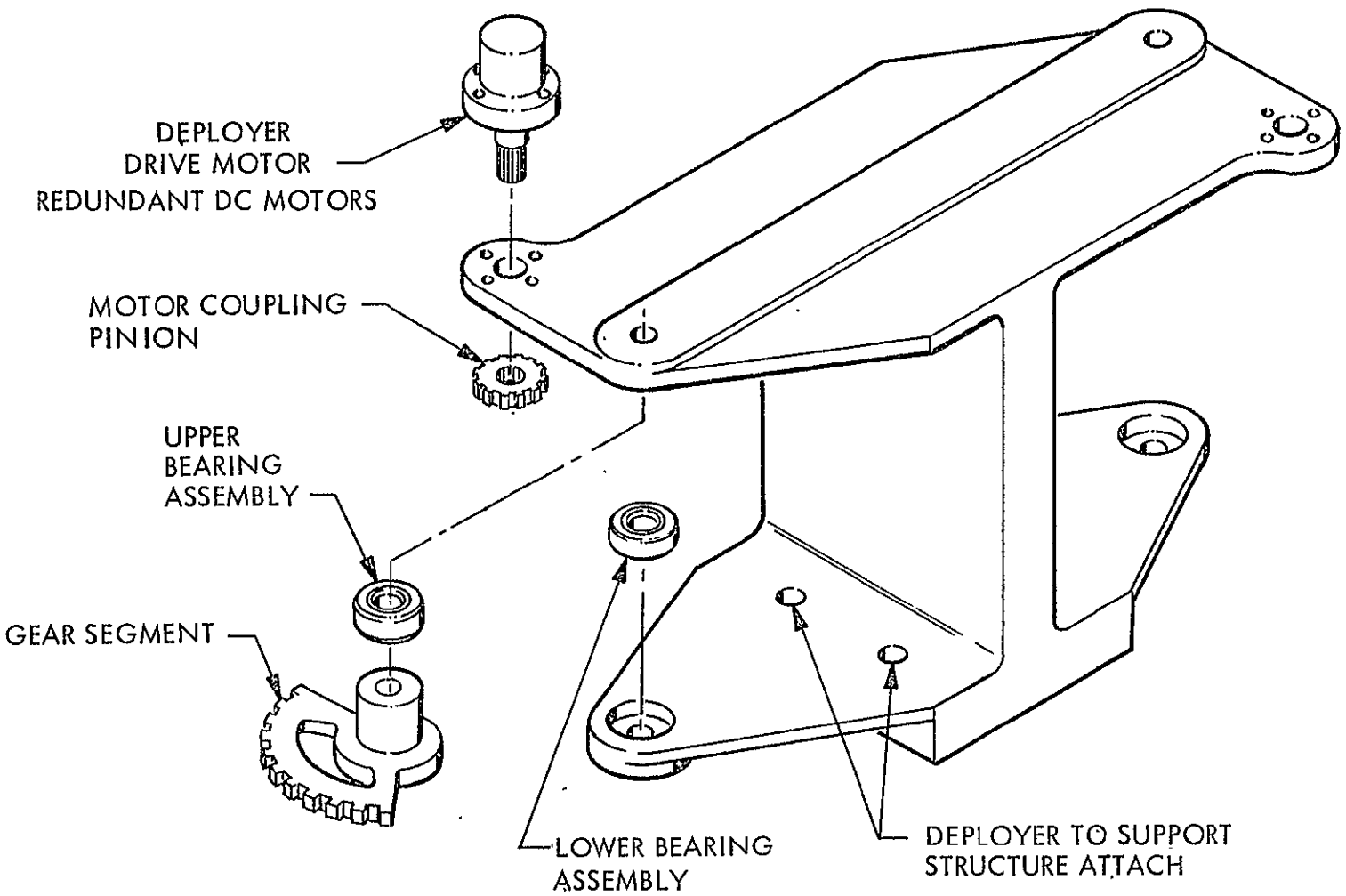

Figure 3-19 Canister Deployer Drive

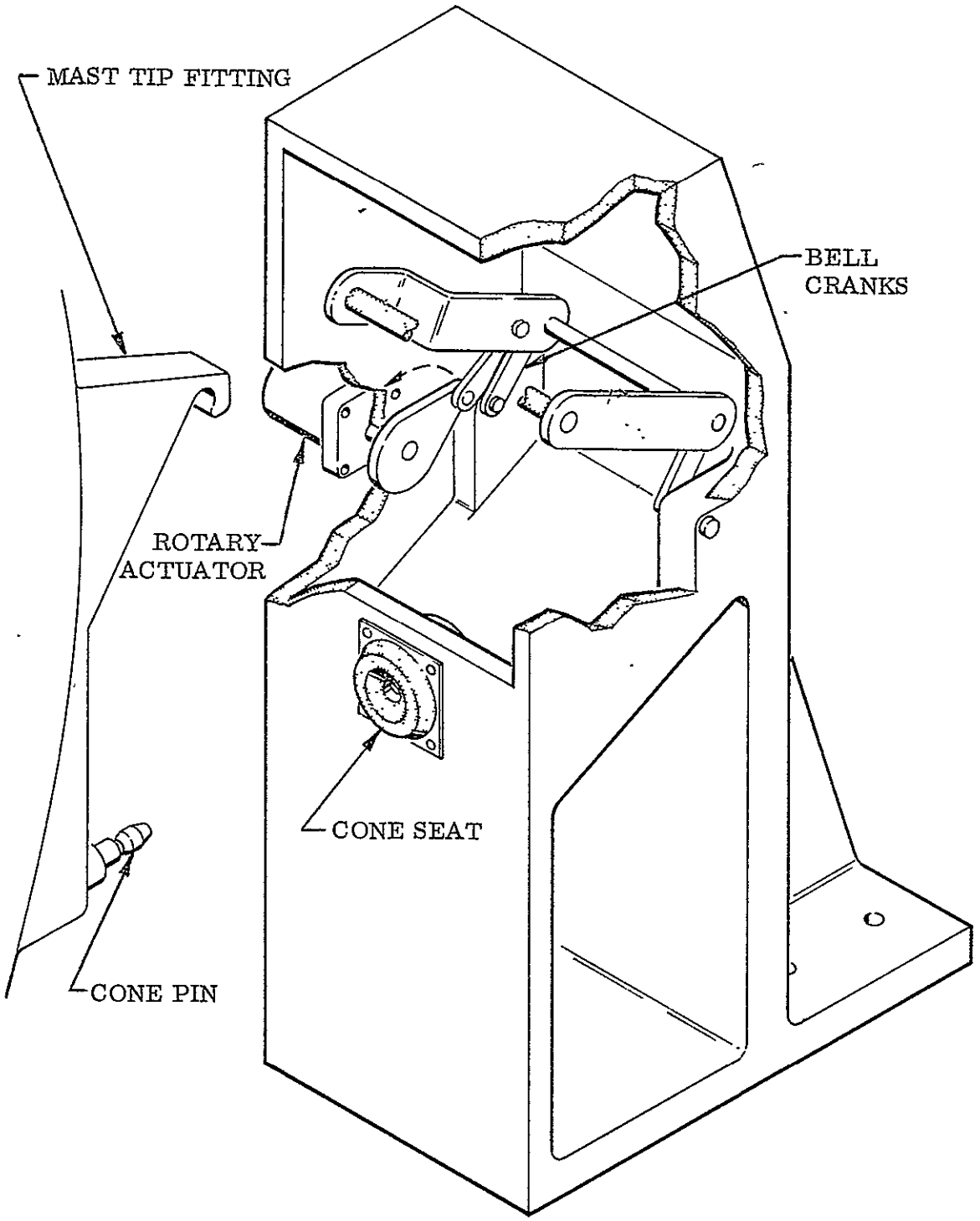

Figure 3-20 Canister Latching Mechanism

latches when the rotary actuators are activated. The rotary actuators are electrically redundant and provide the necessary force to rotate the bell cranks and preload conical pins on the tip fitting into seats on the support structure. The bell crank on the output of the rotary actuator travels to the over-center position of the links, and also actuates electrical switches at each end of travel to provide signals for both the latched and unlatched condition. The latch hooks react only X-X loads, while the mast tip fitting is pinned to the support structure to react both Y-Y and Z-Z loads.

4.0 DESIGN SUPPORT STUDIES

This section presents the results of analyses performed to support the array design effort.

4.1 DYNAMIC ANALYSIS

This section presents the details of parametric investigations of the dynamic properties for various designs of the PEP Solar Array wing.

Discussion

Initially, a parametric study was performed to assess geometric and loading variation effects on the physical characteristics of the PEP Solar Array wing. MDAC specified particular wing power levels, load cases, and desired frequencies which they wanted analyzed. LMSC then came up with a power level/panel number/blanket density matrix (Table 4-1).

Nine geometric configurations were analyzed with three values of power and three values of blanket density. The two static load cases MDAC specified are shown in Table 4-2, for which bending moments were attributed to an external moment, a moment due to an axial force times a prescribed eccentricity, and a moment due to a transverse force, one-fourth of which was applied at the boom tip. These three possible moments were then combined to give three distinct loading conditions. The critical moment was then specified as 1.5 times the maximum of the distinct moments. The critical bending moments for the two load cases are shown in Tables 4-3 and 4-4.

The mast EI's required to sustain these max. critical bending moments were calculated and used in a Fortran Eigensolver program to calculate the systems first two natural frequencies. The results of the frequency analysis are graphically presented for the two load cases in Figures 4-1 and 4-2.

TABLE 4-1

POWER LEVEL/CONFIGURATION TABLE

(kW)	0.4 lb/ft^2	0.25 lb/ft^2	0.1 lb/ft^2	0.4 lb/ft^2	0.25 lb/ft^2	0.1 lb/ft^2
Power Level	No. Panels			Boom Length (inches)		
9	30	32	39	894.0	954.0	1102.8
15	50	54	65	1490.4	1609.2	1936.8
18	60	64	78	1788.0	1908.0	2205.6

TABLE 4-2

MDAC LOAD CASES

		LOAD	CASE 1	CASE 2
	A	Bending Moment in-lb	2160	2520
*	B	Axial Force - lbs	6	3
**	C	Lateral Force - lbs	2	5
		2nd Mode Frequency	.08 Hz	.2 Hz

* Bending moment due to axial force is the force x moment arm of 21 inch

** Bending moment due to lateral force is the force x 0.25 x L; where L is the mast length in inches, given in Table 4-1.

Designate the separate moments as M_A, M_B, and M_C respectively.

Calculate:

$$M_1 = |M_A| + |M_B|$$

$$M_2 = |.7 * M_A| + |M_B| + |.7 * M_C|$$

$$M_3 = M_B + M_C$$

$$M_{CR} = 1.5 * \text{Max}\,(M_1, M_2, M_3)$$

TABLE 4-3

CRITICAL BENDING MOMENTS - CASE 1

(kW)		0.4 lb/ft^2	0.25 lb/ft^2	0.1 lb/ft^2
9	M_1 =	2286.	2286.	2286.
	M_2 =	1951.	1972.	2024.
	M_3 =	573.	603.	677.
	M_{CR} =	3429.	3429.	3429.
15	M_1 =	2286.	2286.	2286.
	M_2 =	2160.	2202.	2316.
	M_3 =	871.	931.	1094.
	M_{CR} =	3429.	3429.	3474.
18	M_1 =	2286.	2286.	2286.
	M_2 =	2264.	2306.	2410.
	M_3 =	1020.	1080.	1229.
	M_{CR} =	3429.	3459.	3615.

TABLE 4-4

CRITICAL BENDING MOMENTS - CASE 2

(kW)		0.4 lb/ft^2	0.25 lb/ft^2	0.1 lb/ft^2
9	M_1 =	2583.	2583.	2583.
	M_2 =	2610.	2662.	2792.
	M_3 =	1181.	1256.	1442.
	M_{CR} =	3915.	3993.	4188.
15	M_1 =	2583.	2583.	2583.
	M_2 =	3131.	3235.	3522.
	M_3 =	1926.	2075.	2484.
	M_{CR} =	4697.	4853.	5283.
18	M_1 =	2583.	2583.	2583.
	M_2 =	3392.	3497.	3757.
	M_3 =	2298.	2448.	2820.
	M_{CR} =	5088.	5246.	5636.

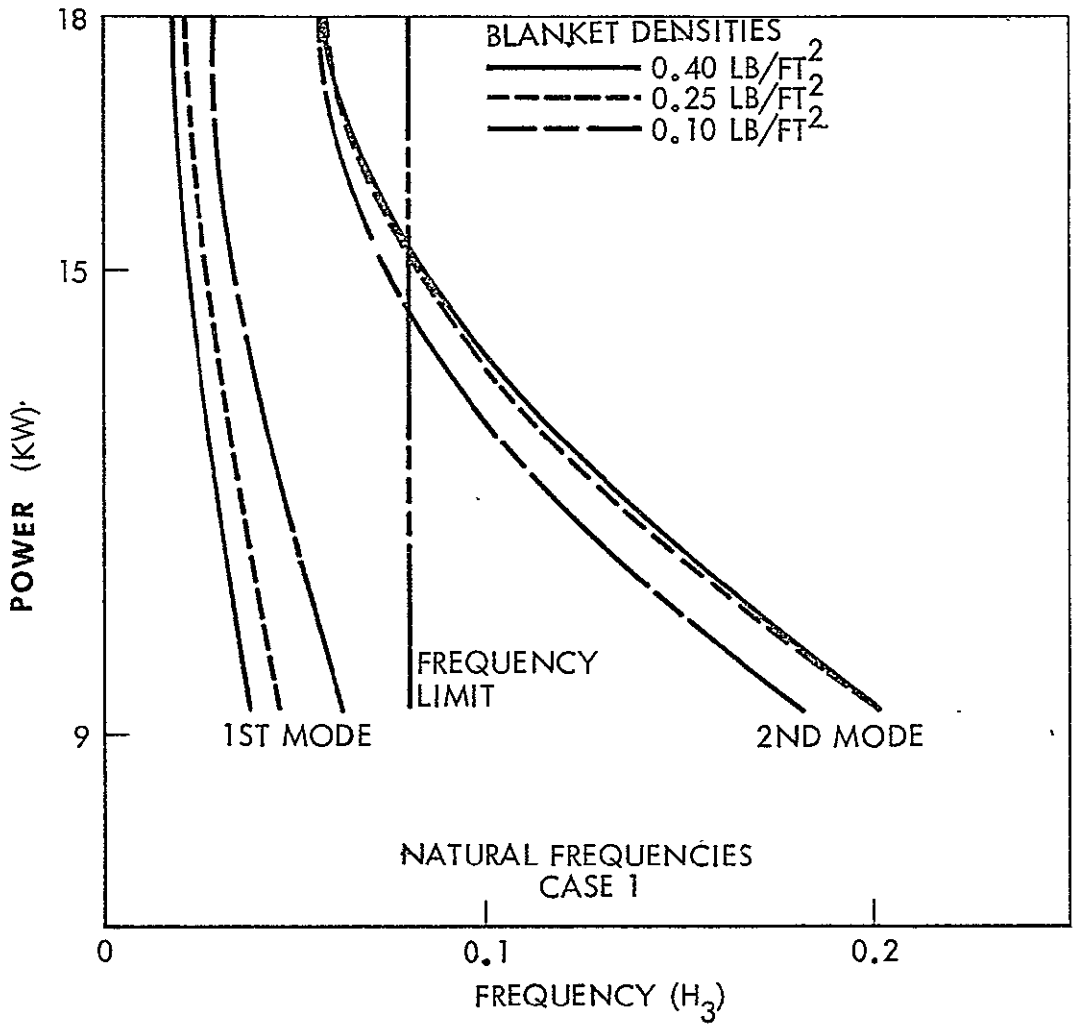

Figure 4-1 Natural Frequencies - Case 1

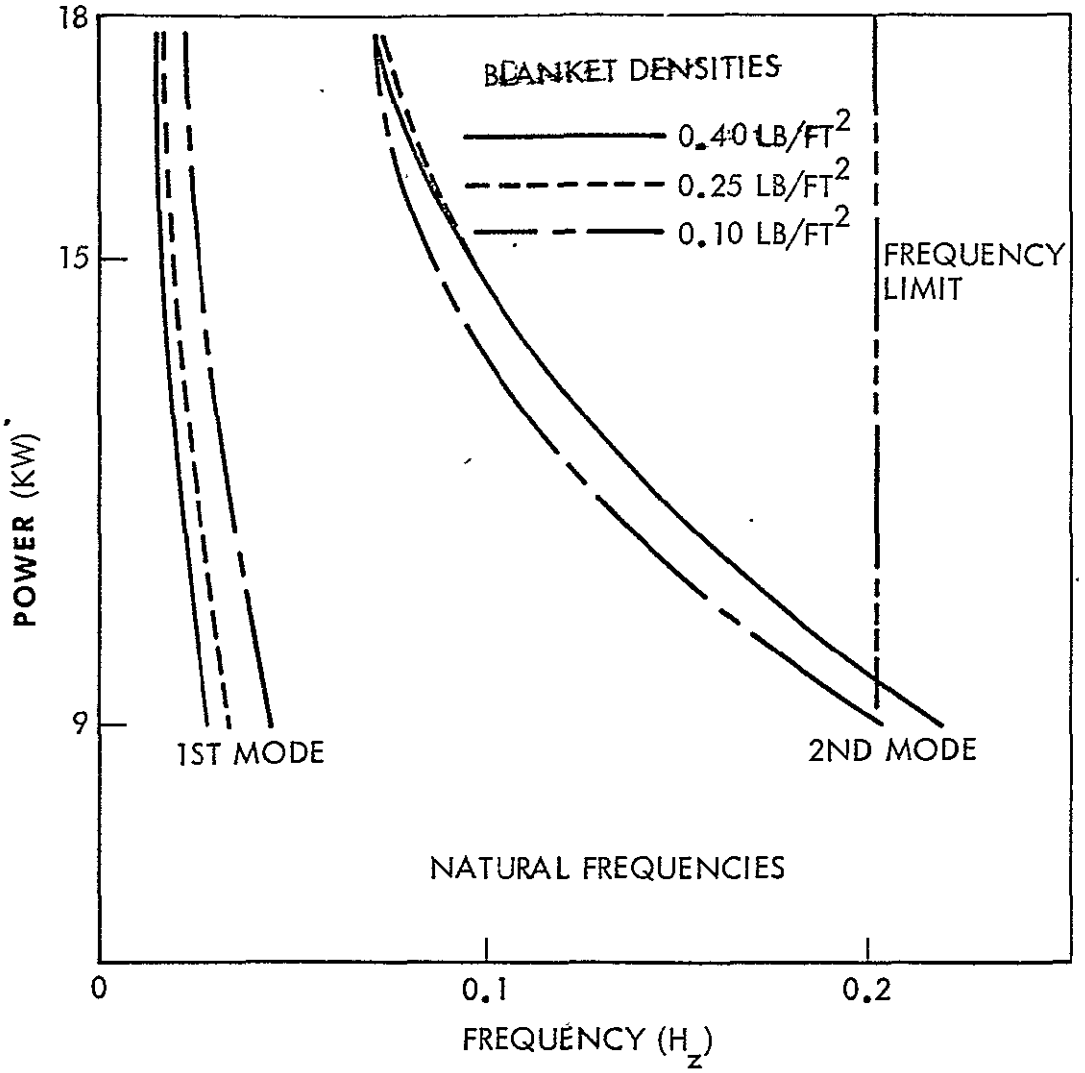

Figure 4-2 Natural Frequencies - Case 2

At the request of MDAC a parametric study was performed to determine the first symmetric mode and the first antisymmetric mode frequencies of a symmetric (split sheet) pair of solar array blankets.

By considering the first cantilever mode for a single array, the symmetric overall mode would be represented by in-phase motion of the two cantilever modes.

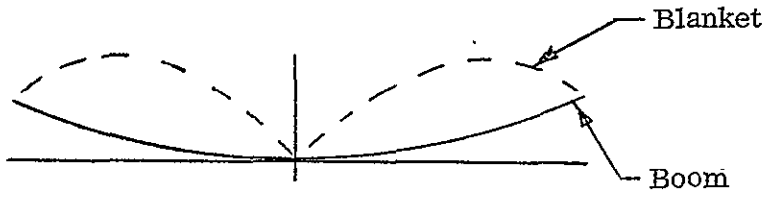

Such an overall mode shape would produce a shearing reaction at the origin and no resultant bending moment. By considering these two cantilever modes out of phase

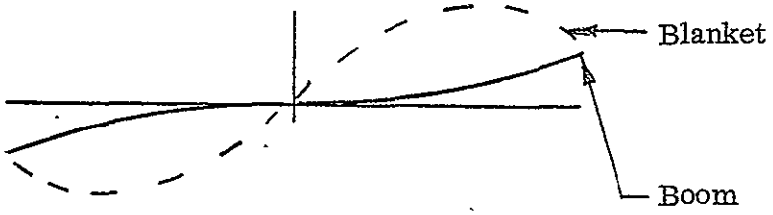

a resultant external moment would be required at the origin but no resultant shear. The frequencies of the in-phase and out-of-phase motions would be equal.

In addition to bending in which motion was normal to the plane of the undeflected blanket, transverse bending was also requested. The relative mode shape for a single cantilever array would be of the form:

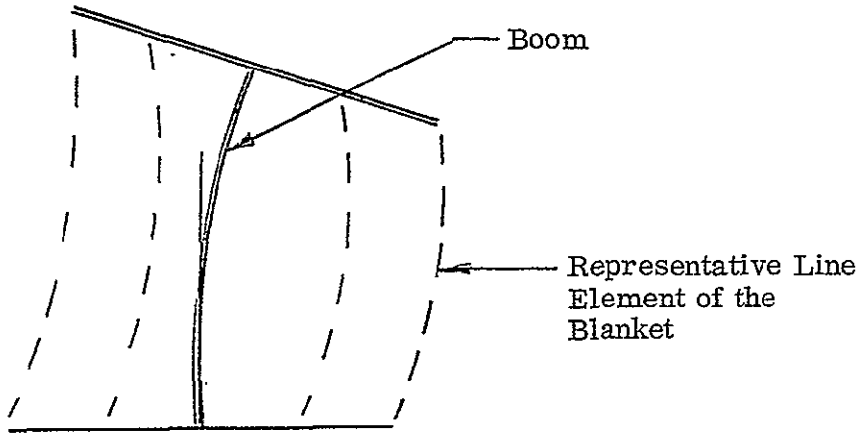

Again, symmetric and antisymmetric combinations of these cantilever modes would give the desired first and second overall mode shapes of equal frequency.

The transverse bending will have a somewhat higher frequency than the normal bending due to slight changes in preload due to rotation of the rigid member attached to the end of the boom.

This present work has been accomplished with a closed-form eigensolution where eccentricity of the blanket attachment to the end of the boom and possible coupling with other mode forms have been disregarded.

The basic loads material properties and geometry used in this analysis were:

Boom length	1535 inch
Width	158 inch
Thickness	.003 inch
Blanket weight	350 lbs
End weight	40 lbs
Blanket tension	10 lbs
$E_{blanket}$	700,000 lb/in^2

Formulas used for calculating the boom geometric and elastic properties were taken from the Able Engineering Company deployable boom literature (Appendix B).

Table 4-5 presents the geometric and frequency characteristics of systems where the masts are sized for 100, 200 and 300 ft-lb bending capability.

The mode shapes graphically displayed in Figures 4-3 and 4-4 for normal and transverse bending show a significant reduction in boom amplitude for the transverse bending case. However, the rather small shift in frequency can be attributed to the fact that the blanket is the principal mass element and there is only a slight reduction in its half wavelength if the sine curve is extrapolated to a zero displacement value.

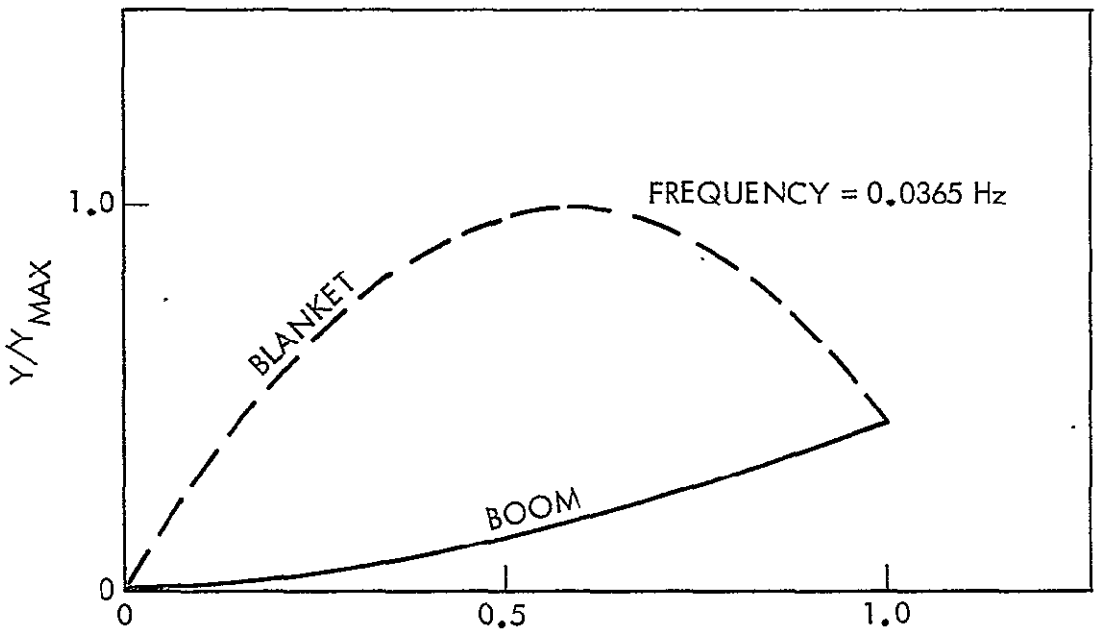

Figure 4-3 Cantilever Mode

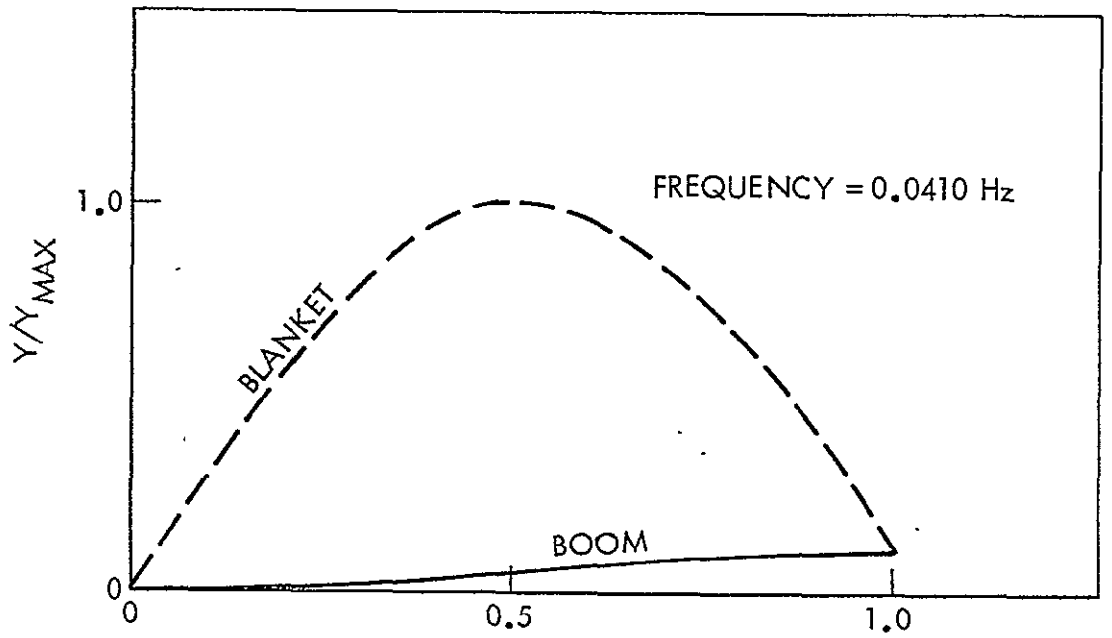

Figure 4-4 Cantilever Mode

TABLE 4-5

GEOMETRIC AND FREQUENCY CHARACTERISTICS

Moment ft-lb	R inch	Boom EI lb-in^2	Boom Weight lb	Frequency Hz*
100	7.52	2.540E7	41.4	.0289
200	9.47	6.400E7	65.7	.0365
300	10.84	1.099E8	86.1	.0390

* These frequencies apply to modes normal to the plane of the blanket and transverse modes

A second parametric study was performed but with varying blanket tensions of 2, 4, 6, 8, 10 and 12 lbs with the moment requirement of 100, 200 and 300 multiplied by 1.5 factor to determine mast EI and weight.

Table 4-6 presents the boom properties that meet the above requirements.

The system constants used in the model for this analysis are summarized below.

Length	1535 inch
Width	158 inch
Density	0.25 lb/ft^2
Blanket Weight	0.25 x 1535. x 158./144. = 421 lb/side
End Weight	60 lb - Case 1, 120 lbs - Case 2

The resulting calculated frequencies for the out-of-plane bending are shown in Tables 4-7 and 4-8 .

TABLE 4-6

BOOM PROPERTIES

Moment ft-lb	Boom Radius Inch	Boom EI * $lb\text{-}in^2$	Boom Weight Lb
100	8.605	4.36103E7	54.2
200	10.342	1.09906E8	86.1
300	12.411	1.88718E8	112.8

*Boom EI required for 1.5 load factor

TABLE 4-7

FREQUENCY OUT-OF-PLANE BENDING - CASE 1

Moment ft-lb	Preload					
	2 lb	4 lb	6 lb	8 lb	10 lb	12 lb
100	.0118	.0160	.0187	.0207	.0222	.0233
200	.0120	.0168	.0202	.0230	.0253	.0272
300	.0121	.0170	.0206	.0236	.0261	.0283

TABLE 4-8

FREQUENCY OUT-OF-PLANE BENDING - CASE 2

Moment ft-lb	Preload					
	2 lb	4 lb	6 lb	8 lb	10 lb	12 lb
200	.0120	.0168	.0202	.0229	.0252	.0271

Subsequent analyses were performed on base shape type responses to determine boom loads and blanket displacements relative to the boom for varying types of input accelerations.

Response analyses were run to calculate boom base moments and structural deflections for 4 types of base input accelerations: step translation, step rotation, spike translation and spike rotation.

A continuous model for out of plane bending of the solar array was developed. The solar array panel was modeled as a uniform string under tension, and the supporting boom was represented by a uniform straight beam under a compressive preload. Initial curvature of the boom, and the offset of the boom from the panel were neglected, reducing the problem to one having only one spatial coordinate. Figure 4-5 is a diagram of this model, and lists the equations of motion for the system.

The first 20 cantilever mode shapes and frequencies were generated for the PEP array model using the 100 ft-lb boom and a preload of 5 lbs. Plots of the mode shapes are shown in Appendix C.

Although the actual force applied by the Shuttle would be a series of square pulses from its thrusters, the solar arrays would experience these transients as filtered by the dynamics of the vehicle. For the purpose of this study, however, idealized step and spike base accelerations were applied directly to the base of the array wing model. Because of the low frequencies associated with the array wings, the application of a long series of square pulses results in the same response as that of the application of a step force (of lower magnitude). Thus, for preliminary purposes, the application of a step forcing function adequately represents response to a long series of thruster pulses in the same direction. Likewise, the application of a single pulse may be represented by the application of a pure impulse (delta function) resulting in a step velocity change in the system. These approximations are valid so long as the duration of any single pulse is much shorter than the period of the highest mode used in the analysis.

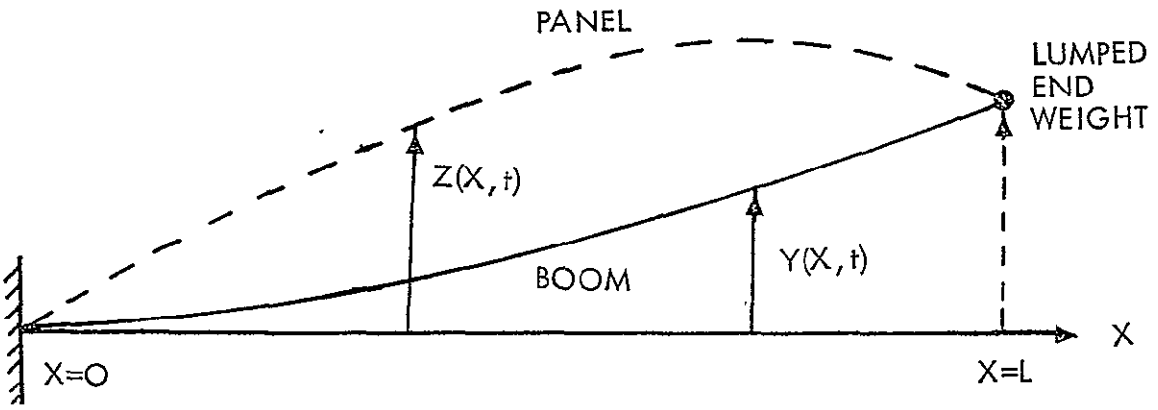

EQUATIONS OF MOTION:

$$\text{BOOM:} \quad (EI)\frac{\partial^4 Y}{\partial X^4} + \frac{\partial^2 Y}{\partial X^2} + \left(\frac{W_{BM}}{gL}\right)\frac{\partial^2 Y}{\partial t^2} = 0$$

$$\text{PANEL:} \quad -P\frac{\partial^2 Z}{\partial X^2} + \left(\frac{W_P}{gL}\right)\frac{\partial^2 Z}{\partial t^2} = 0$$

WHERE:

P	=	PRELOAD
EI	=	BOOM STIFFNESS
W_{EM}	=	BOOM WEIGHT
W_P	=	PANEL WEIGHT
g	=	GRAVITATIONAL CONST.
t	=	TIME

Figure 4-5 Dynamics Model

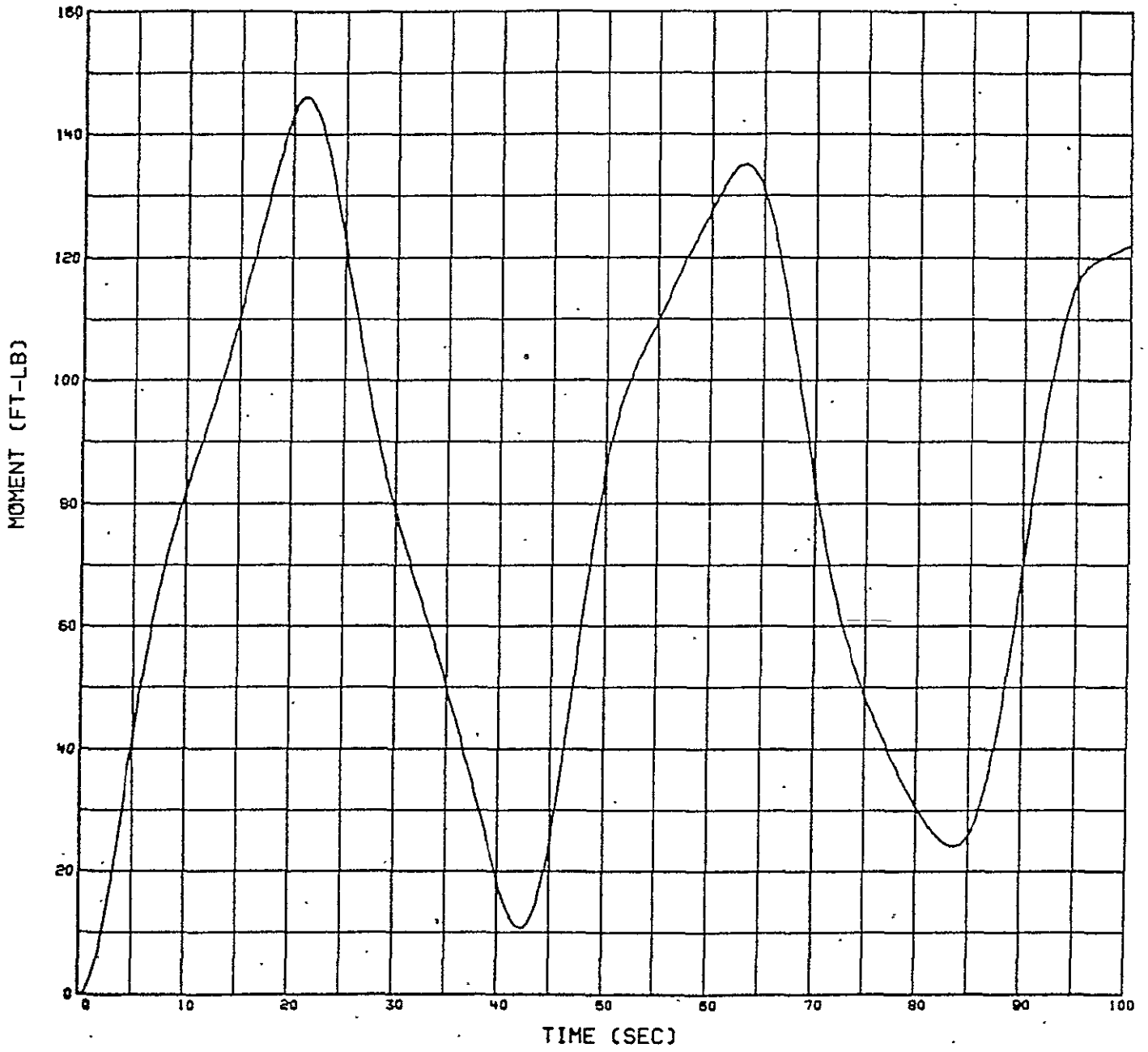

Figure 4-6 Base Reaction Moment - Step Translation Input

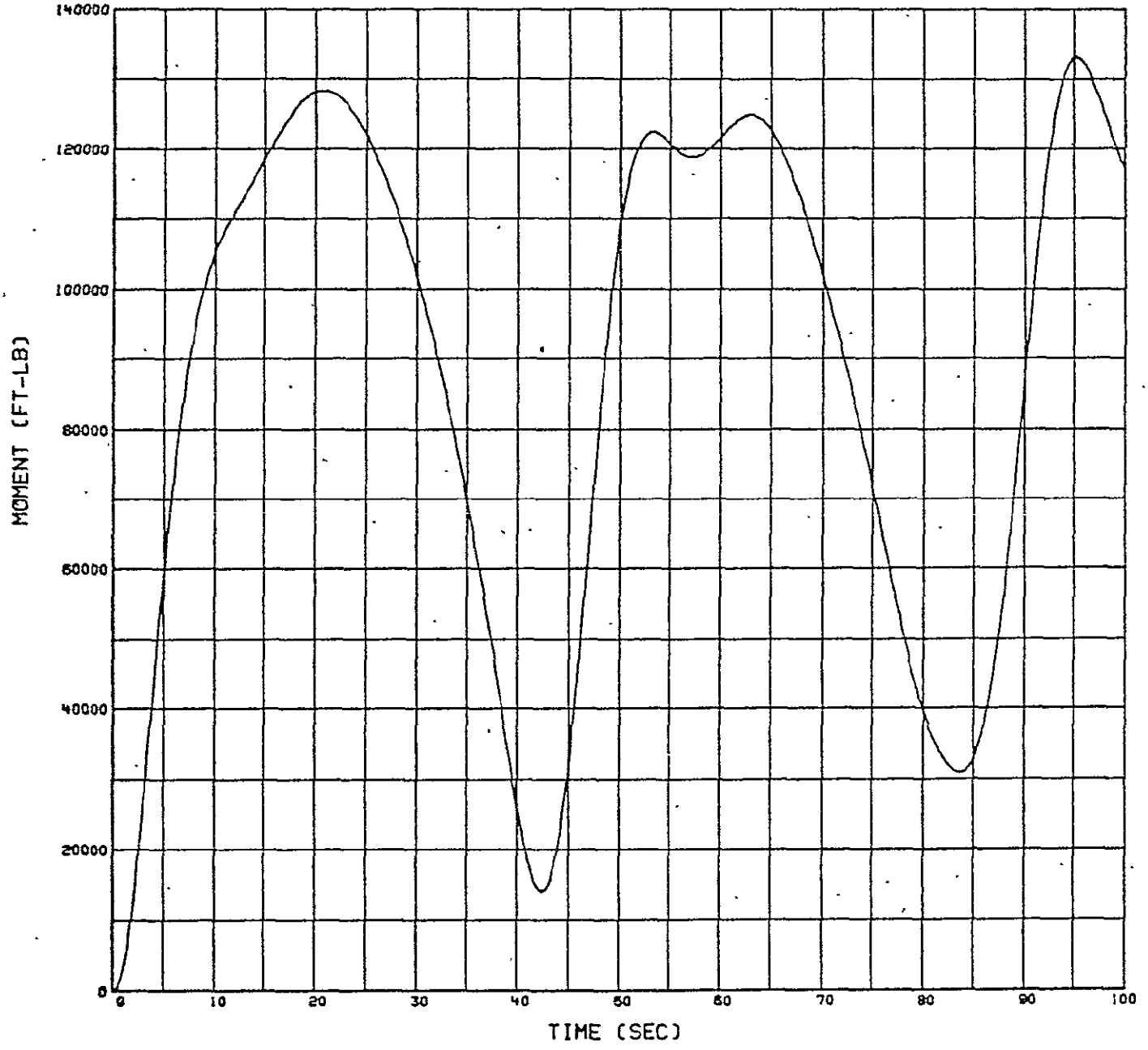

Figure 4-7 Base Reaction Moment - Step Rotational Input

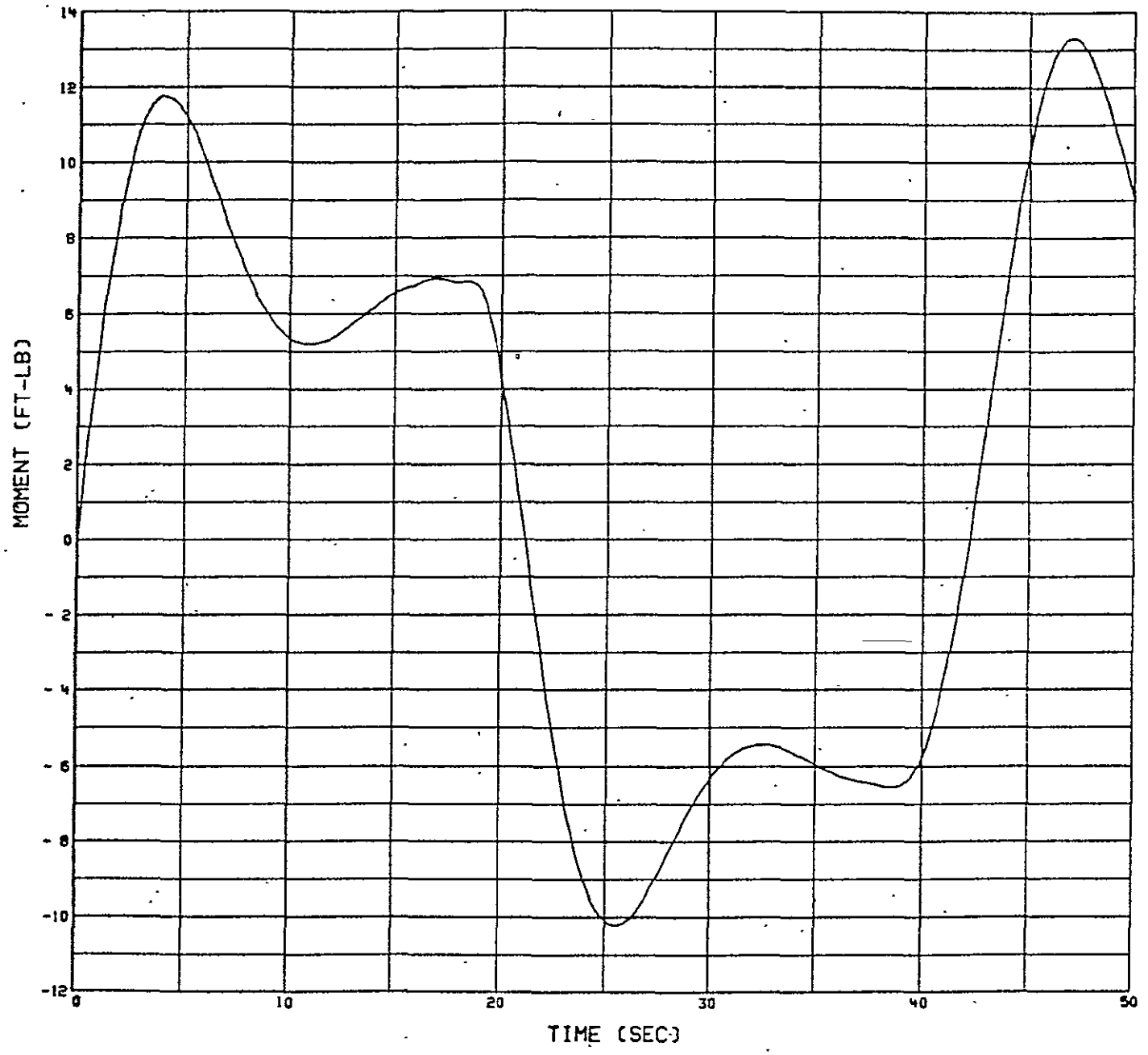

Figure 4-8 Base Reaction Moment - Spike Translational Input

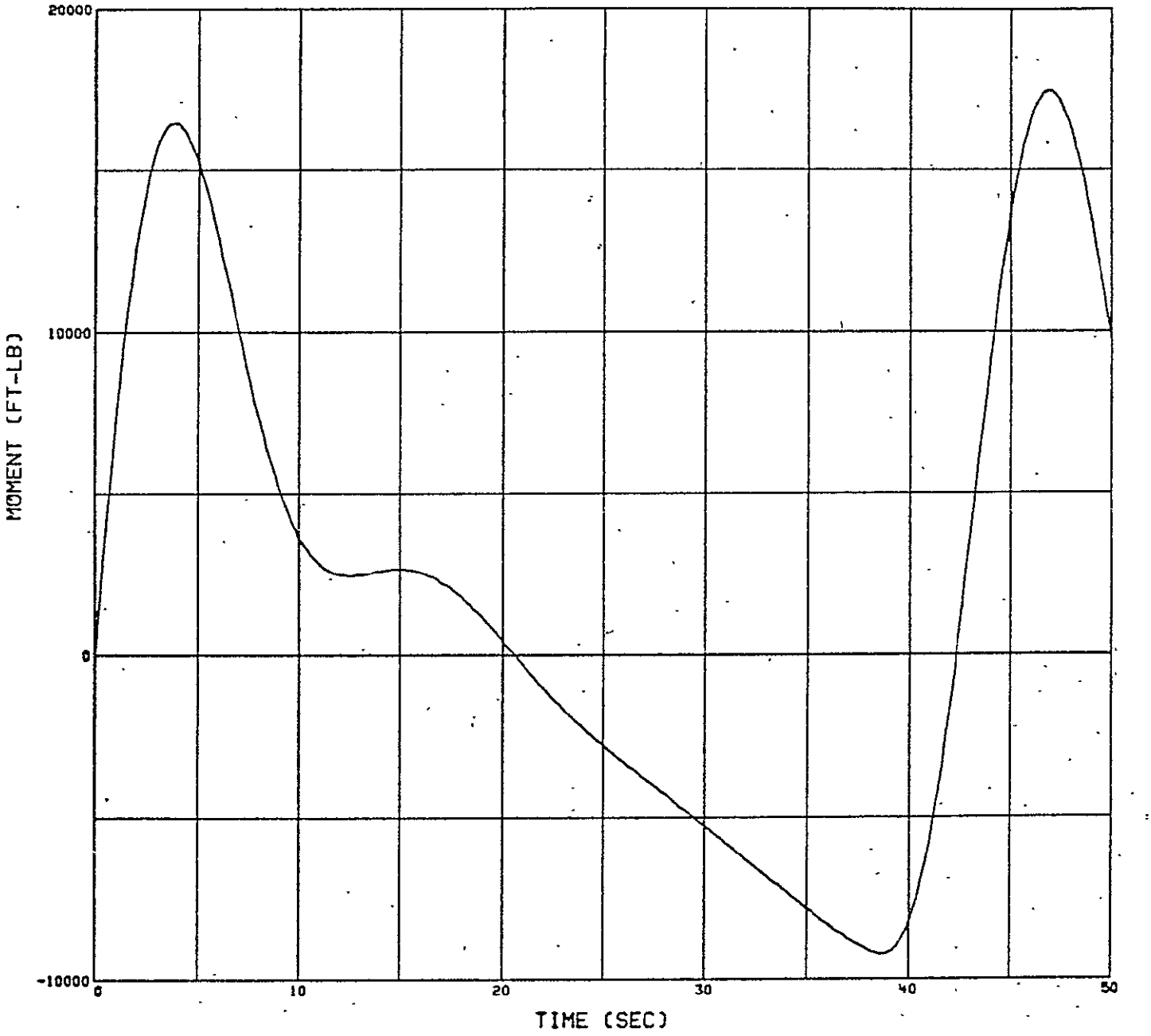

Figure 4-9 Base Reaction Moment - Spike Rotational Input

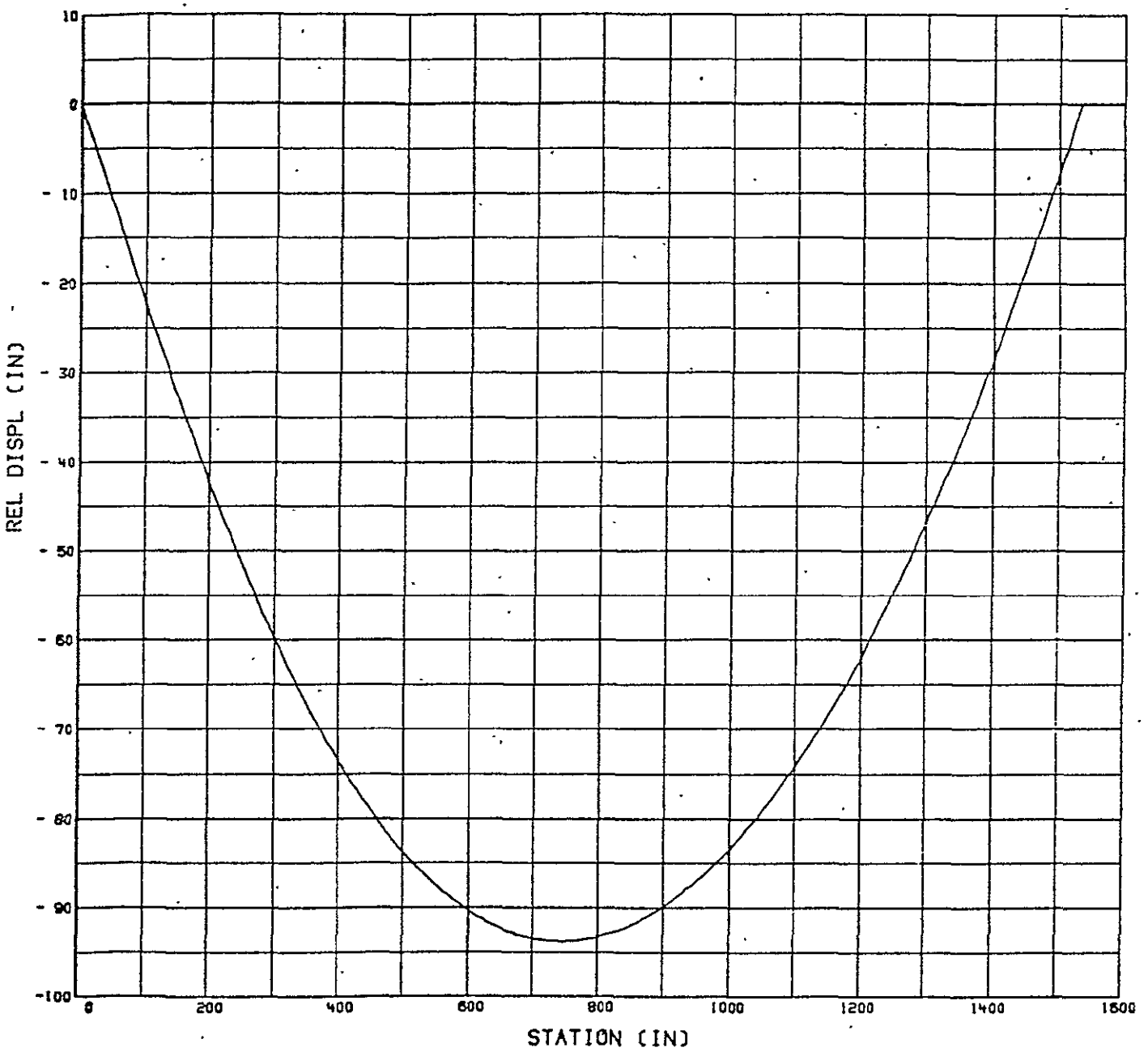

Figure 4-10 Relative Displacement Case 1

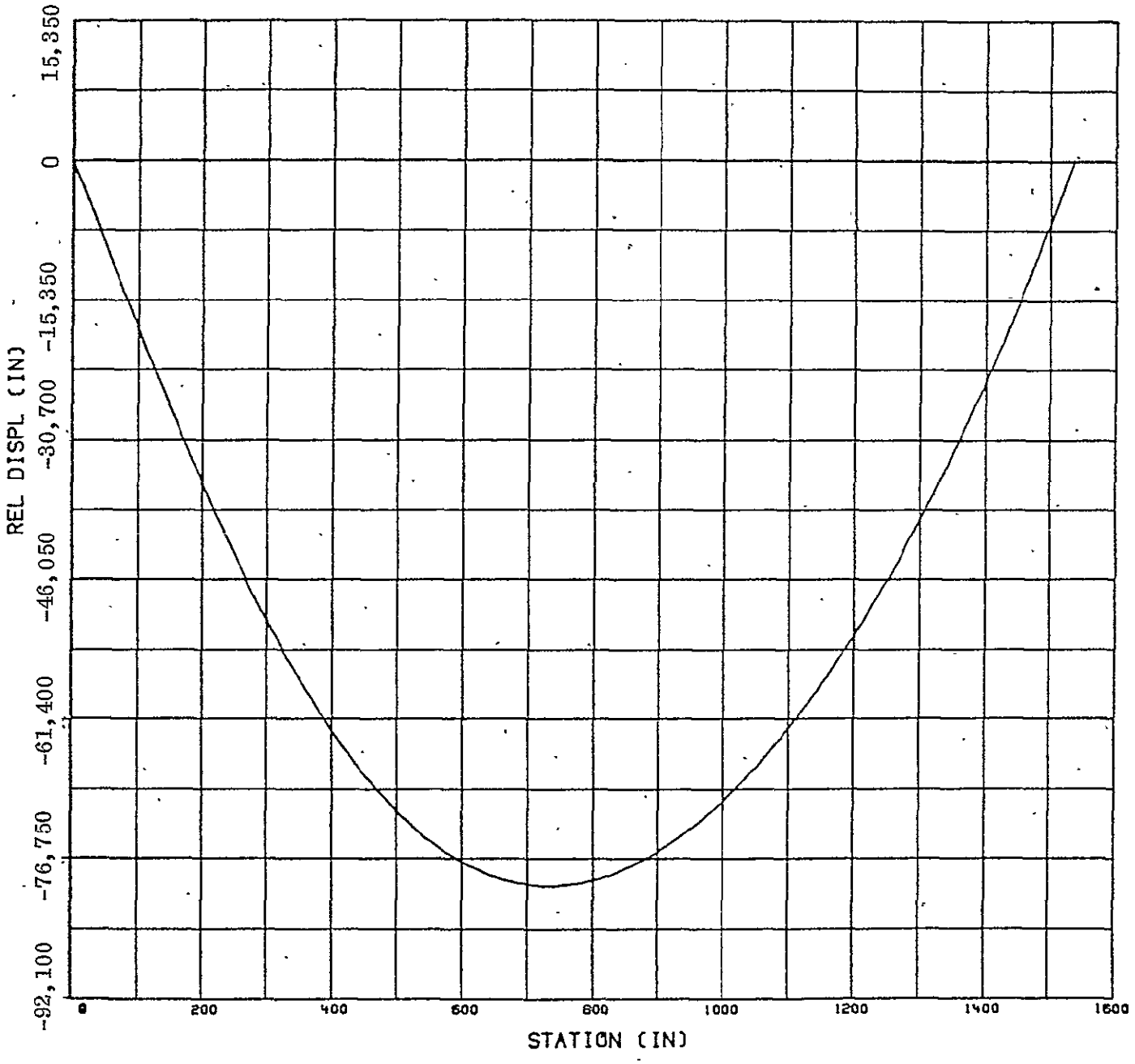

Figure 4-11 Relative Displacement Case 2

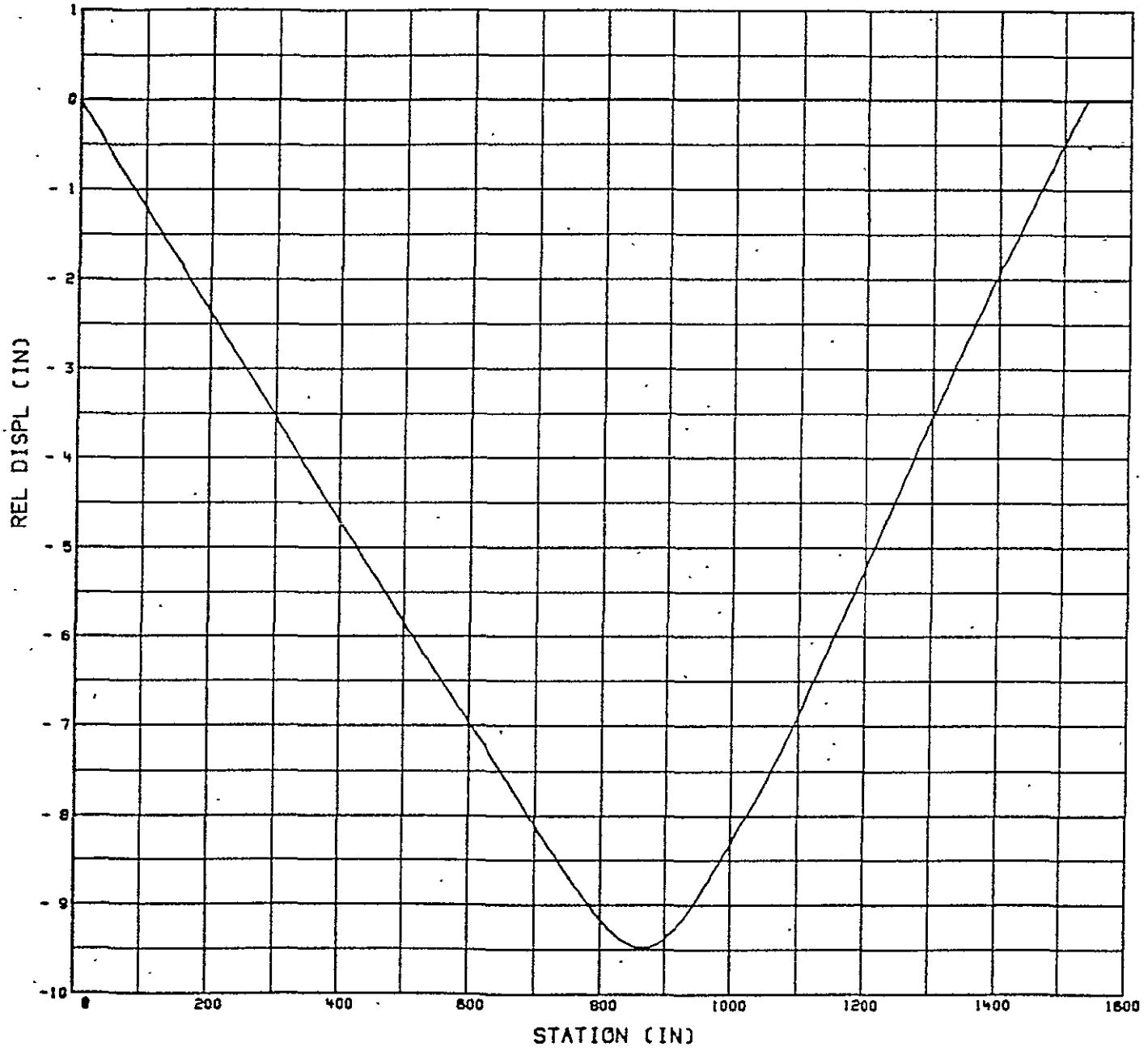

Figure 4-12 Relative Displacement Case 3

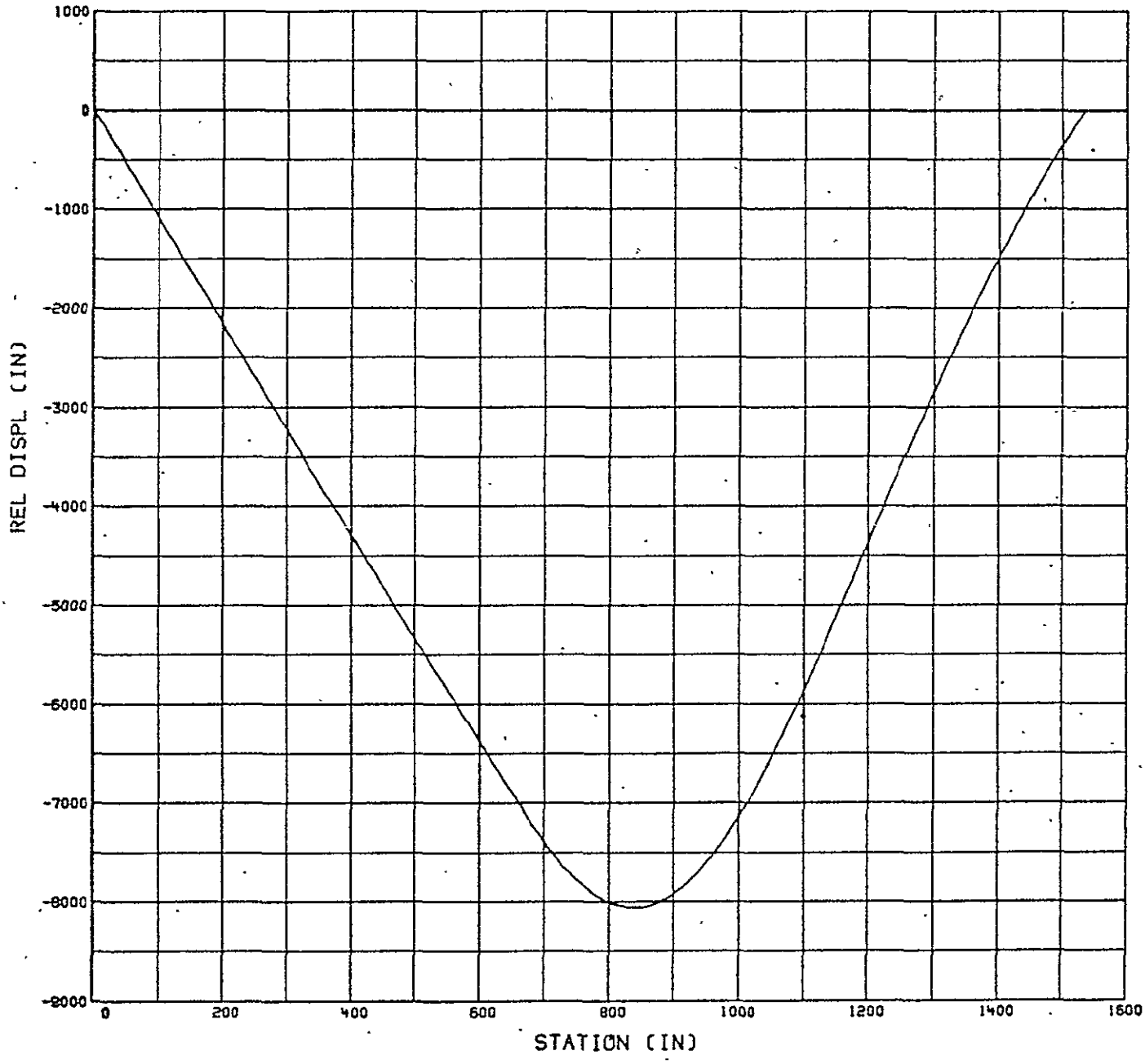

Figure 4-13 Relative Displacement Case 4

In the response calculations, the modal damping was set at 1% for all 20 modes ($\zeta = .01$). The time step used in the integration was 0.2 seconds, which is 1/10 the period of the highest modal frequency. Structural displacements of the boom and panel, and the resultant base moment, were calculated at each time step. The base moment was calculated using the modal displacement method. Although it is not as accurate as modal acceleration, the latter method requires calculation of accelerations of the structure and since (for two of these cases) the reference frame is accelerating, the problem is no longer linear with respect to input. The 4 response cases are summarized in Table 4-9.

TABLE 4-9

SUMMARY OF RESPONSES FOR UNITARY INPUT VALUES

Case No.	Input		Max Base Moment (ft-lb)	Max Tip Deflection (in)	Max Rel Deflection (in)
	Type	Magnitude			
1	Step-trans.	1 in/sec^2	146.	31.7	93.8
2	Step-rotat.	1 rad/sec^2	133,000	28,836	79708.
3	Spike-trans.	1 in/sec*	13.	2.87	9.48
4	Spike-rotat.	1 rad/sec*	17460.	2002.	8061.

*Impulse input used, resulting in velocity step changes shown

Time histories of the base reaction moment are plotted for the 4 cases in Figures 4-6 through 4-9, for the unitary values of input shown in Table 4-9. Figures 4-10 through 4-13 are plots of the boom and panel displacements for each of these four cases. Since boom to panel contact is highly undesirable due to the fragile nature of the solar cells, the input values were calculated which would preclude contact. The distance from the blanket to the mast is approximately 7 inches in the mast's undeflected mode. This preliminary analysis was linear, so the results of the four cases were scaled down so that the maximum relative displacement (panel-to-boom) was 7.0 inches. These scaled results are shown in Table 4-10.

TABLE 4-10

SCALED RESPONSE RESULTS

Case No.	Input		Max Base Moment (ft-lb)	Max Tip Deflection (in)	Max Rel Deflection (in)
	Type	Magnitude			
1	Step-trans.	.0747 in/sec^2	10.8	2.35	7.0
2	Step-rotat.	8.782 x 10^{-5} rad/sec^2	11.7	2.52	7.0
3	Spike-trans.	.738 in/sec*	9.76	2.12	7.0
4	Spike-rotat.	8.676^{-4} rad/sec*	15.17	1.737	7.0

*Impulse input transient used, resulting in velocity step changes shown

In summary, it appears from preliminary analysis that if the mast were sized to meet the frequency requirement of $\leq .02$ Hz, the blanket would contact the mast.

In an effort to assess the effect of increasing blanket preload to preclude mast/blanket contact a decision was made to look at a mast sized for 300 ft-lbs with a 1.5 load factor and parametrically plot the systems natural frequency and relative mast to blanket deflections as a function of blanket preload. Figure 4-14 graphically displays the mast to blanket relative displacements for a uniform acceleration input of one inch/sec/sec. Figure 4-15 displays the mast to blanket relative displacements for an angular acceleration at the array's base of 1/1535 rad/sec/sec.

The results of these preliminary analyses indicated that a low array wing natural frequency and the preclusion of blanket to boom contact are obtainable by controlling the mast EI and blanket tension relationship.

As indicated in Figure 4-16 blanket tensions in the 50 to 100 lb region which greatly minimize the blanket to mast relative deflections, exhibit array wing frequencies in the .07 Hz region.

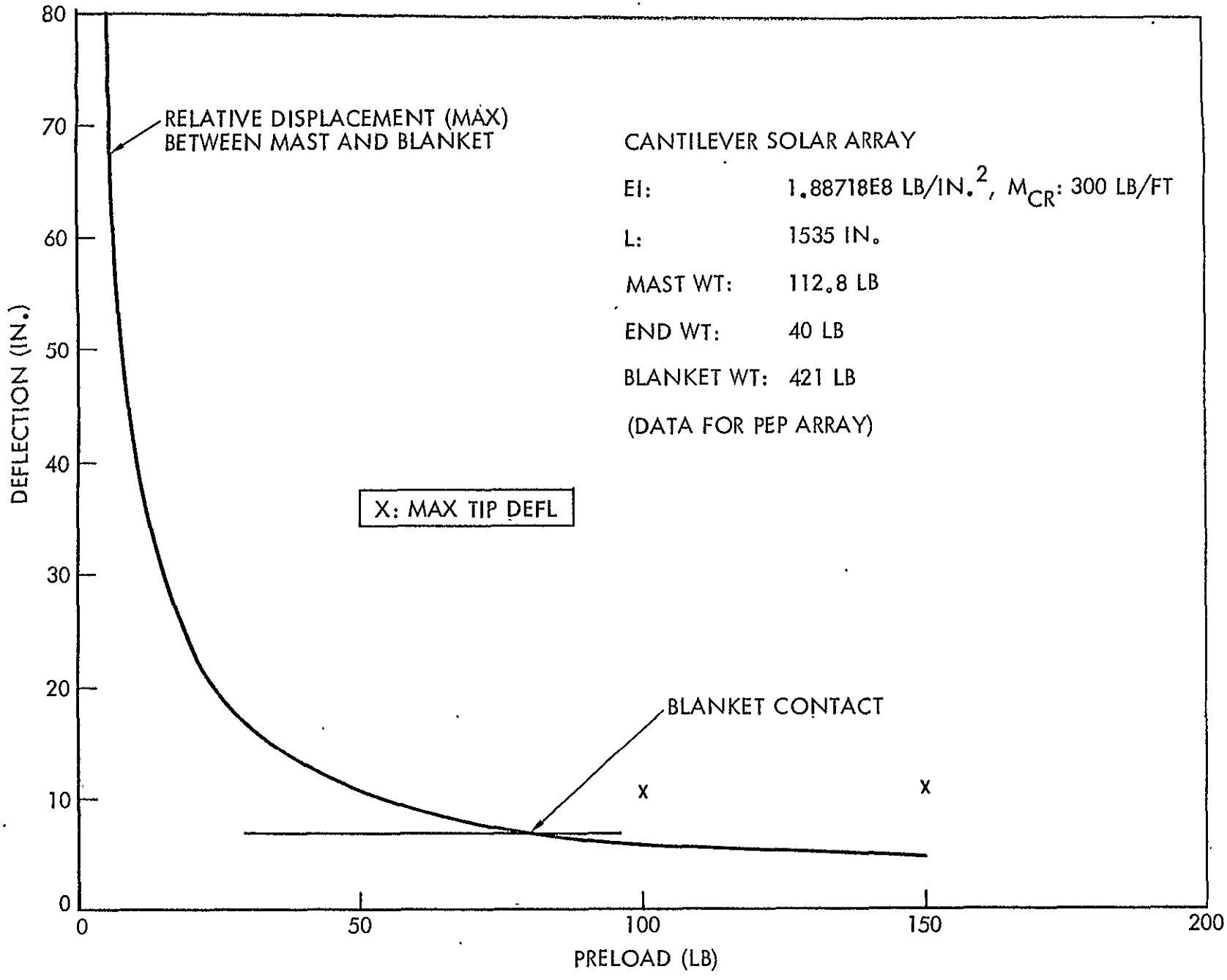

Figure 4-14 Lateral Deflection vs Blanket Preload

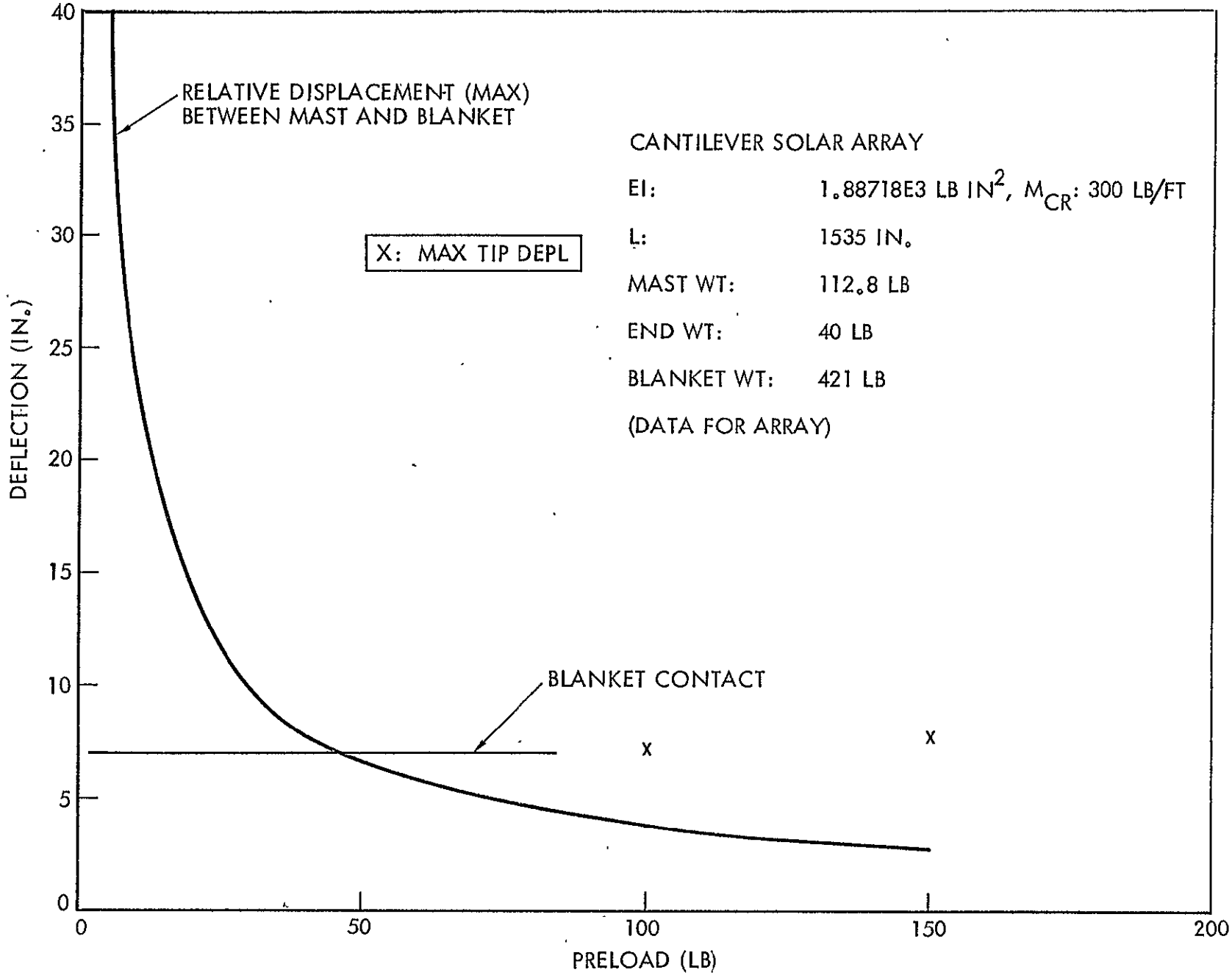

Figure 4-15 Lateral Deflection vs Blanket Preload

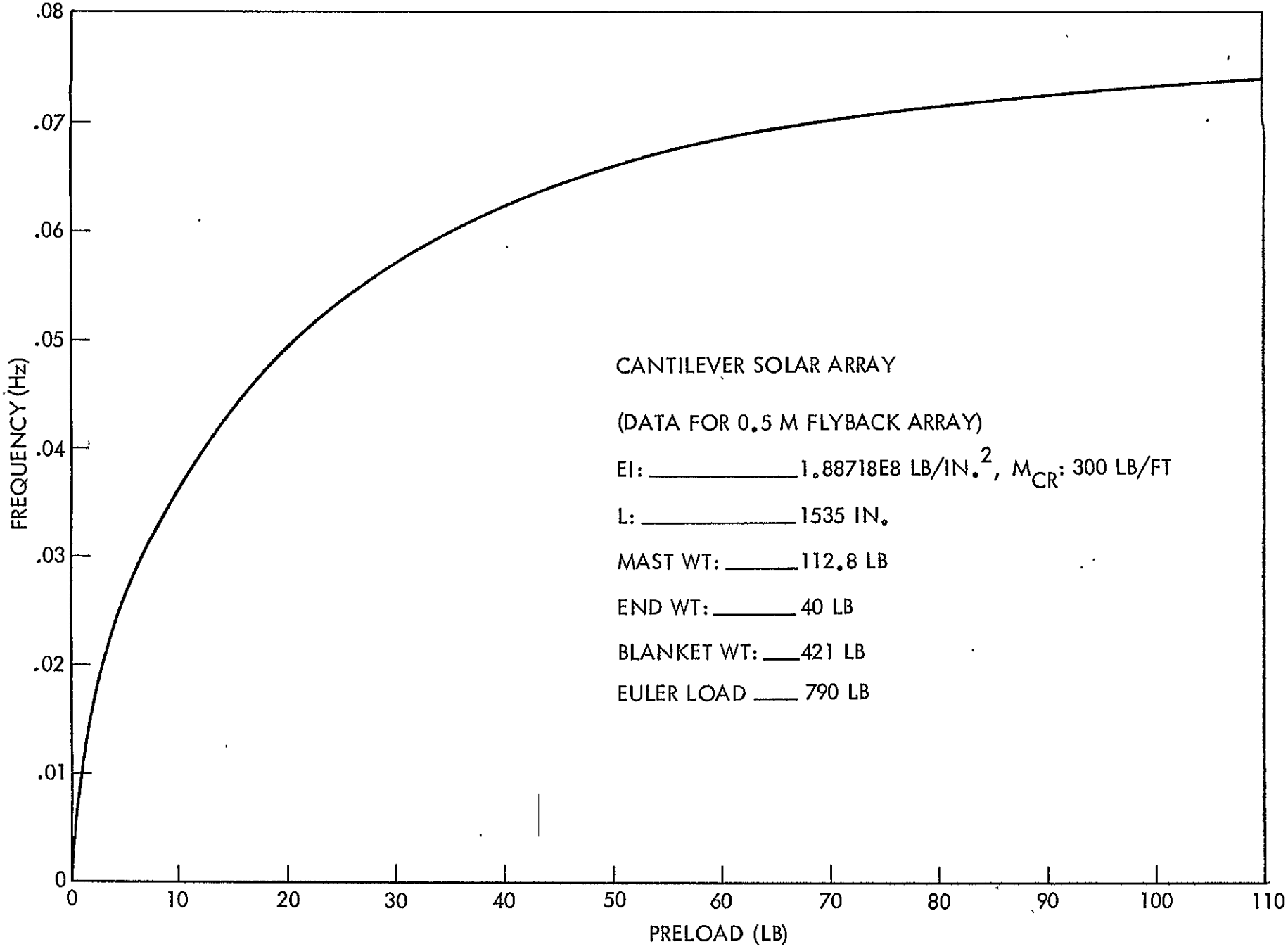

Figure 4-16 Fundamental Frequency vs Blanket Preload

4.2 THERMAL ANALYSIS

This section presents the results of thermal analyses performed in support of the PEP Solar Array. Several cases with differing orbit Beta angles were analyzed to assess the effect of cell temperature and efficiency as a function of time in orbit.

Discussion

In this analysis flexible solar arrays of the type proposed for the PEP Solar Array were analyzed for a typical 235 nautical mile equatorial earth orbit (see Figure 4-17). Since cell efficiency is a function of cell temperature and cell temperature is a function of orbit inclination, studies were initiated to relate Beta angle as a function of orbit performance.

Cell efficiency was programmed into the analysis as 12.8% at 28°C decreasing by .000585 for each 1°C rise in cell temperature.

The optical properties of the cell assemblies and Kapton were modeled as shown below:

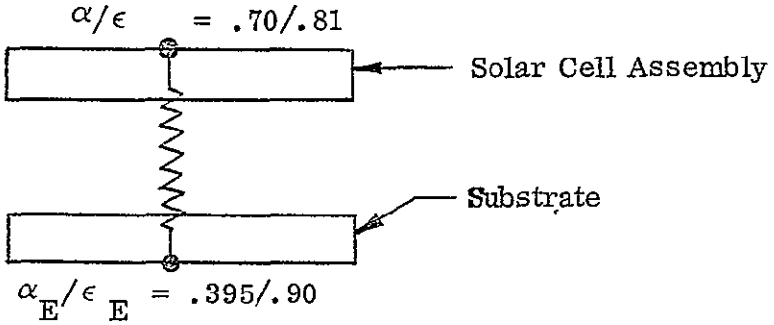

Table 4-11 presents the cell's predicted maximum and minimum orbital temperatures for various Beta angles.

Figures 4-18 through 4-21 show the predicted cell temperature for Beta angles of 0, 30, 60 and 90 degrees as a function of orbit time.

Figures 4-22 through 4-25 show the predicted power output of a cell for the four Beta angles as a function of orbit time.

FIRST ORBIT	MID SHADOW TIME	1398 SEC
	SUBSOLAR TIME	4194 SEC
SECOND ORBIT	MID SHADOW TIME	6991 SEC
	SUBSOLAR TIME	9787 SEC

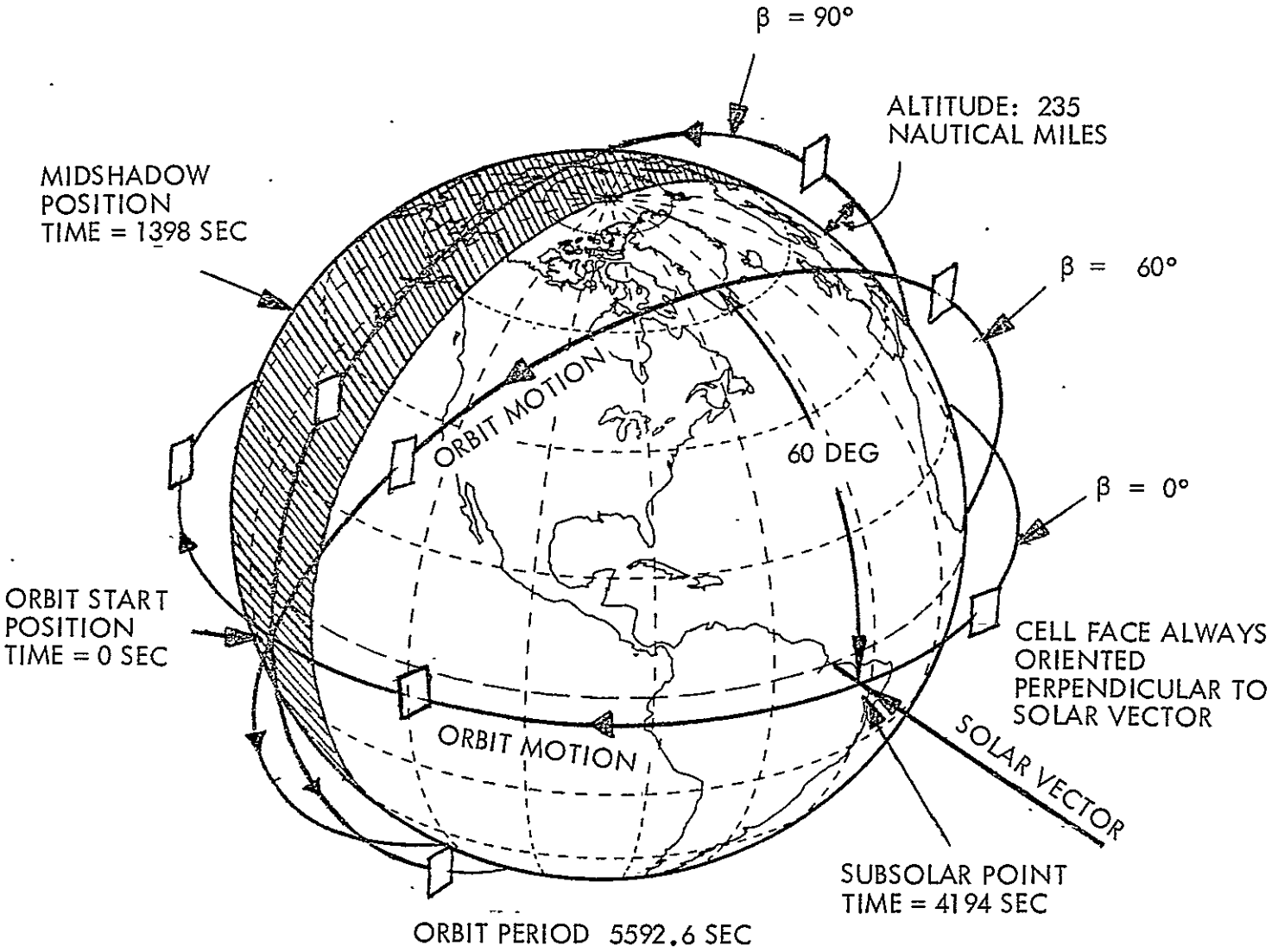

FIRST ORBIT	ENTER SHADOW	EXIT SHADOW	% TIME IN SUN
β = 0	320 SEC	2476 SEC	61.45
β = +60	695 SEC	2101 SEC	74.85
β = +90	–	–	100.00

Figure 4-17 Equatorial Orbits

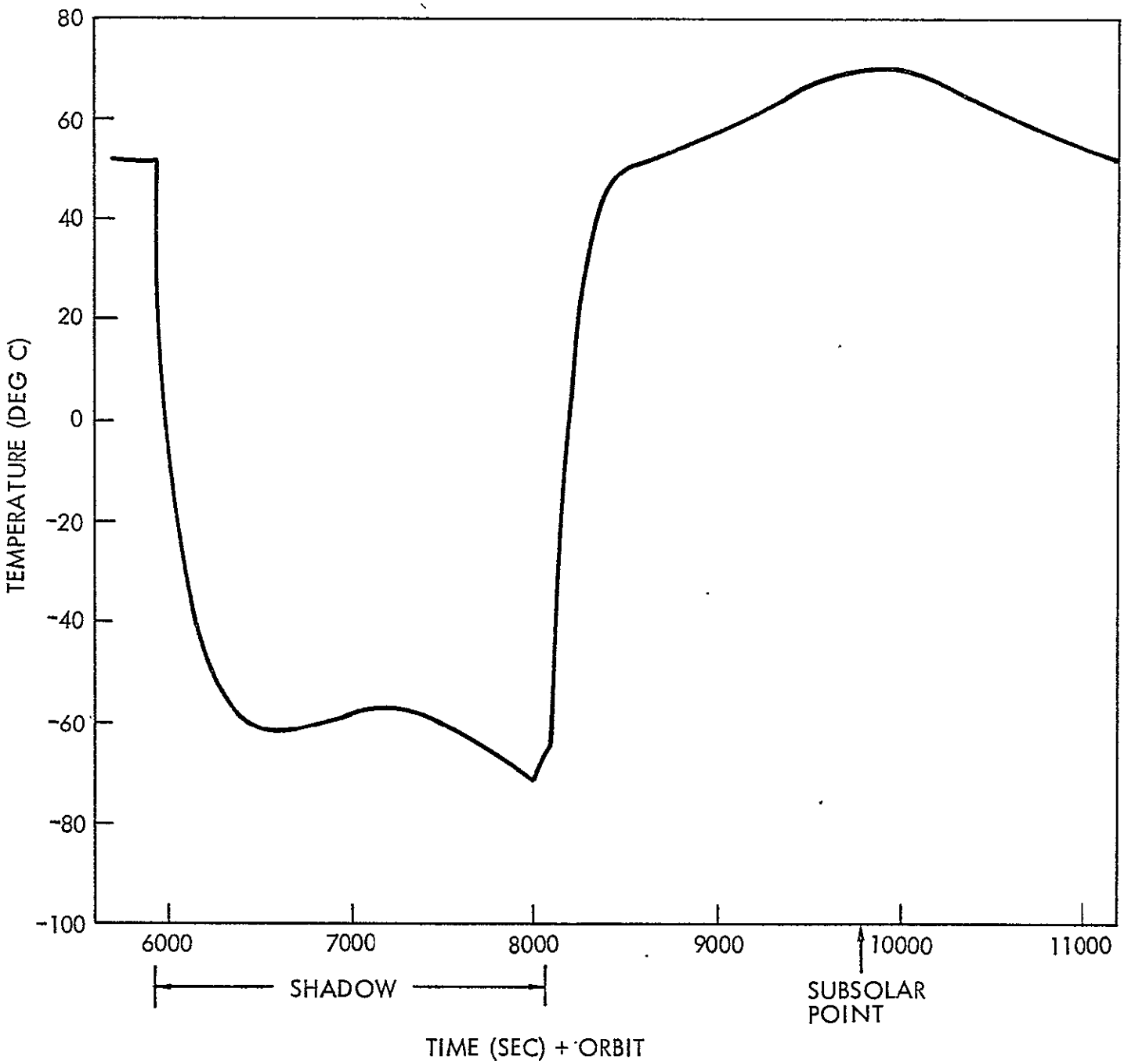

Figure 4-18 Solar Cell Temperature Beta = 0°

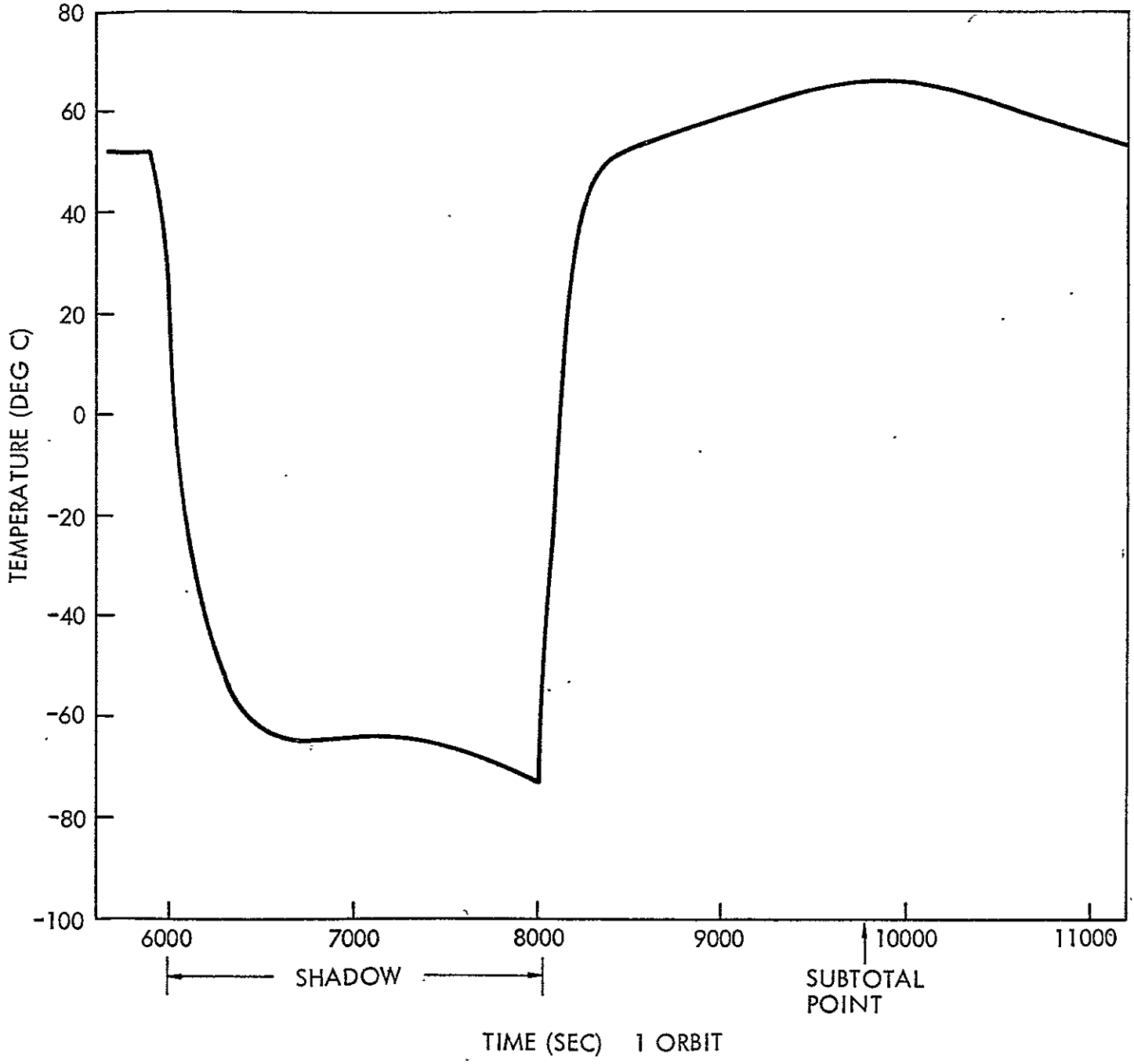

Figure 4-19 Solar Cell Temperature Beta 30°

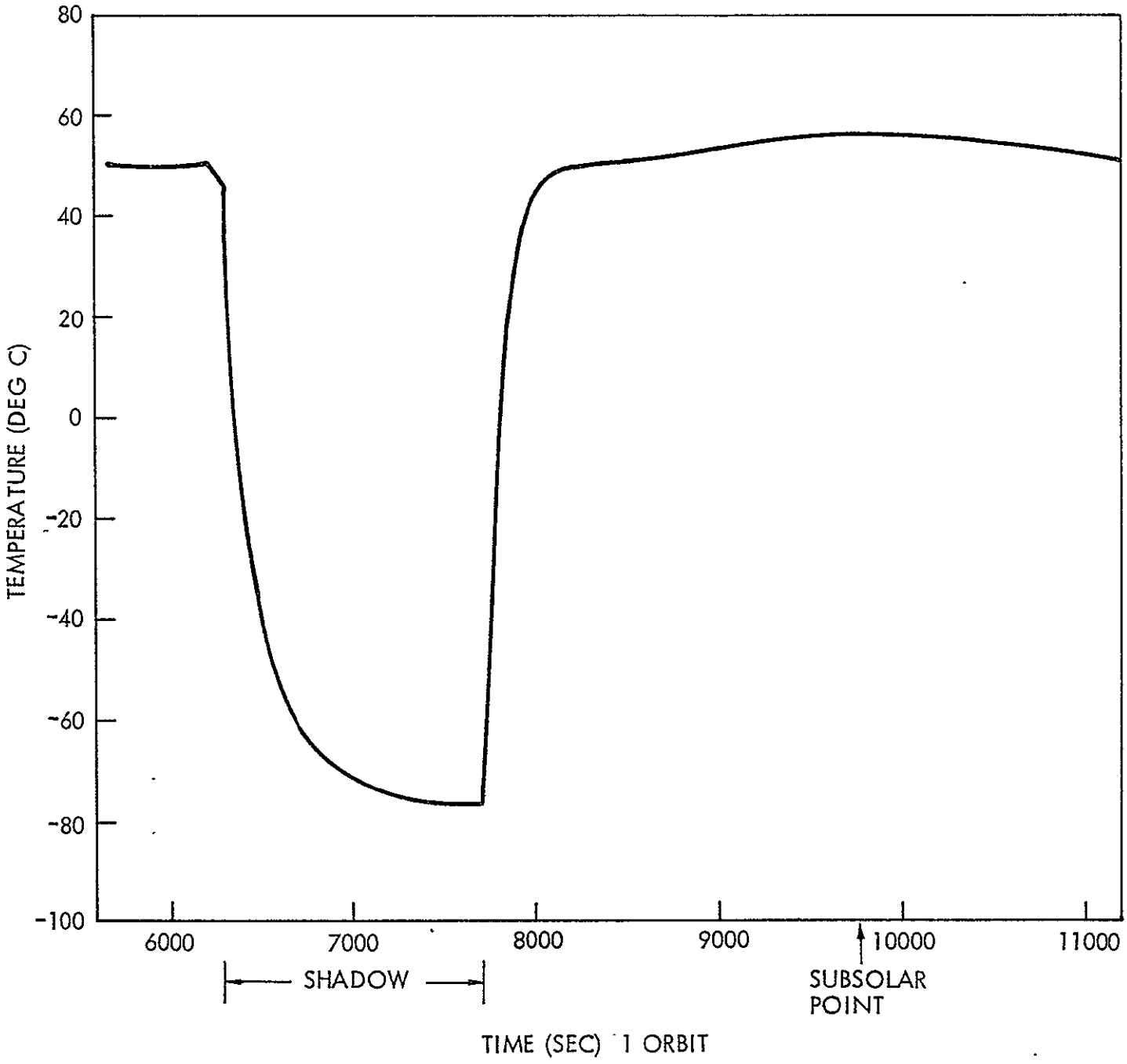

Figure 4-20 Solar Cell Temperature Beta 60°

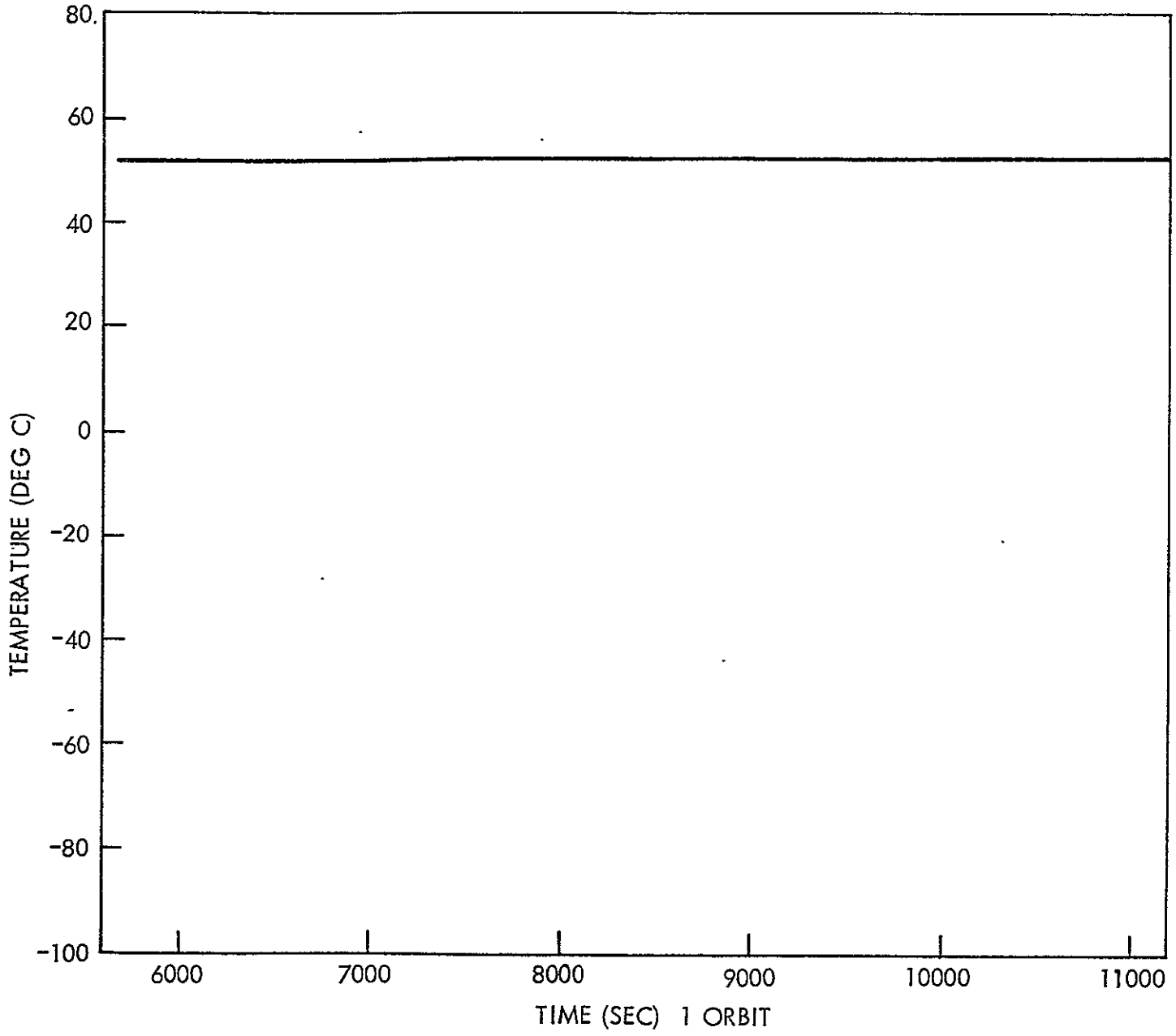

Figure 4-21 Solar Cell Temperature Beta 90°

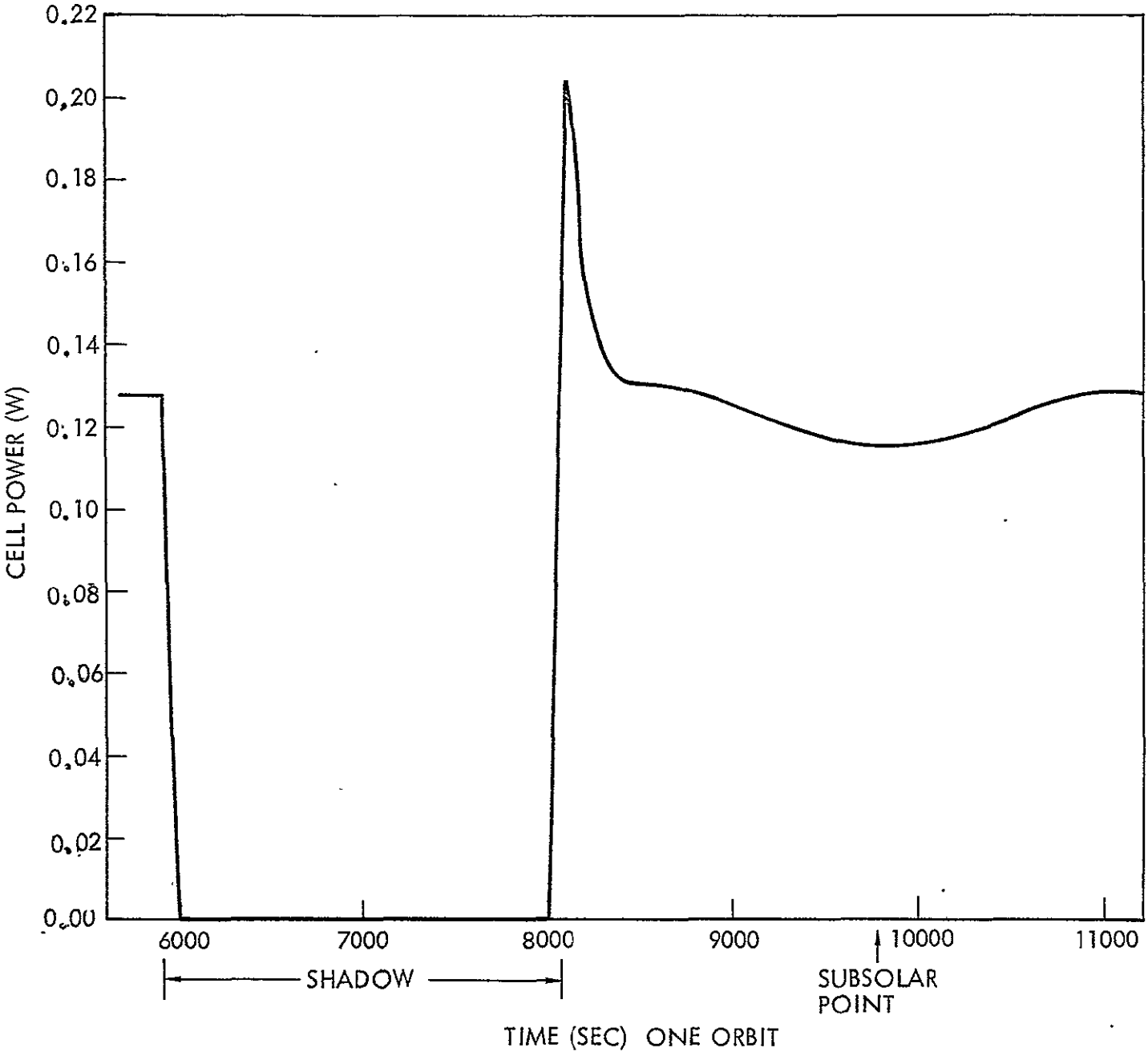

Figure 4-22 Power/Cell Beta = 0°

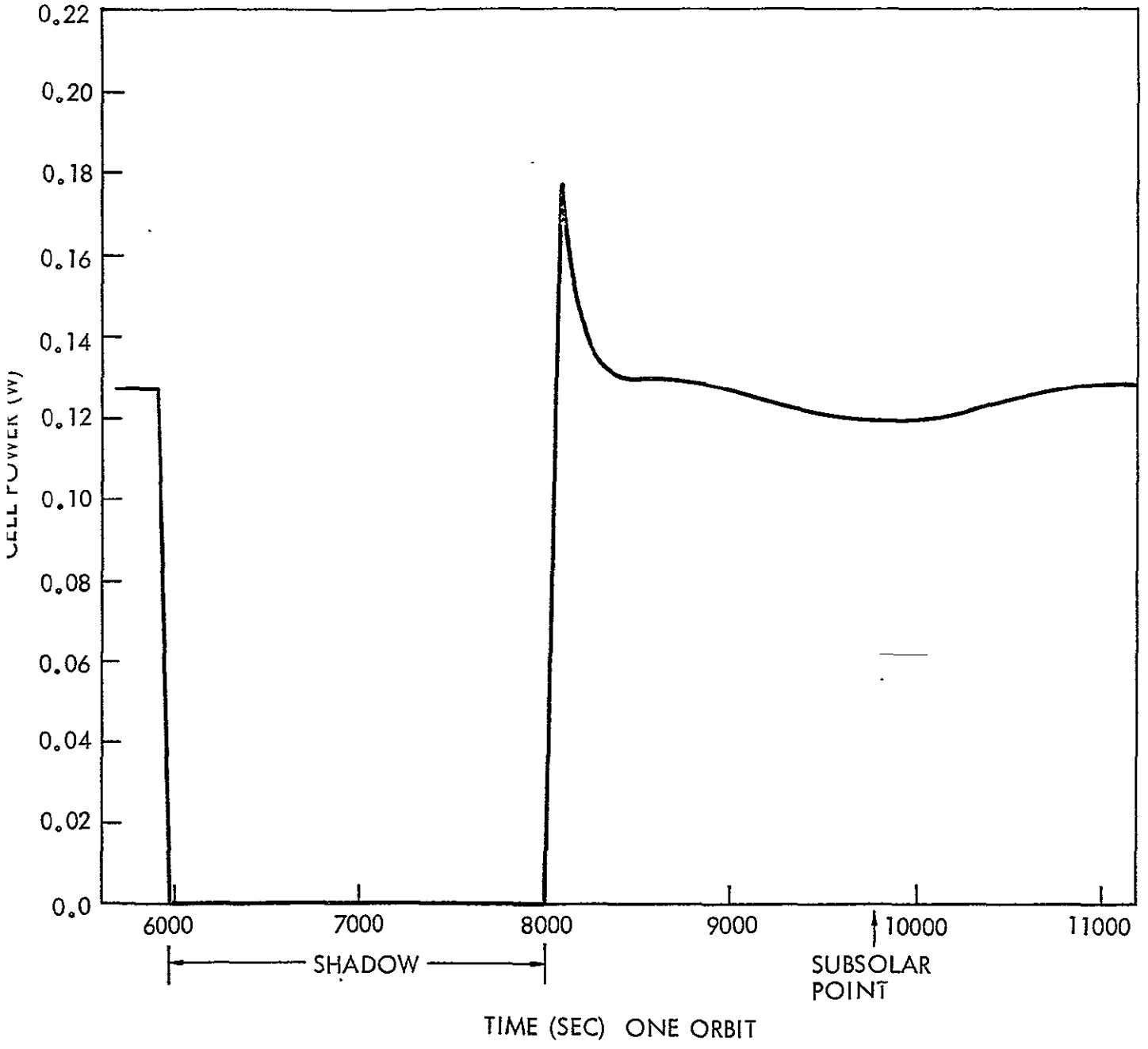

Figure 4-23 Power/Cell Beta = 30°

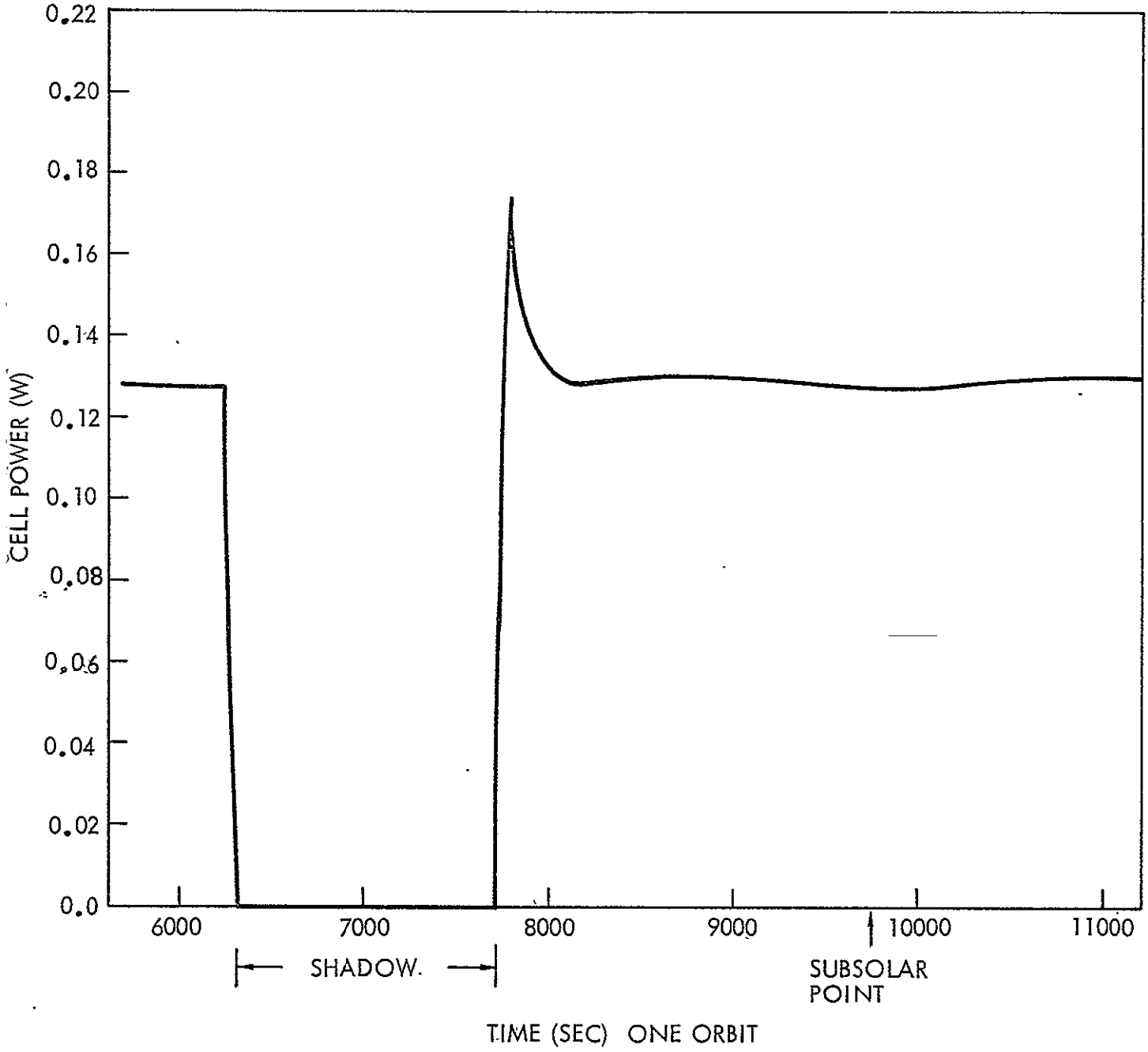

Figure 4-24 Power/Cell Beta = 60°

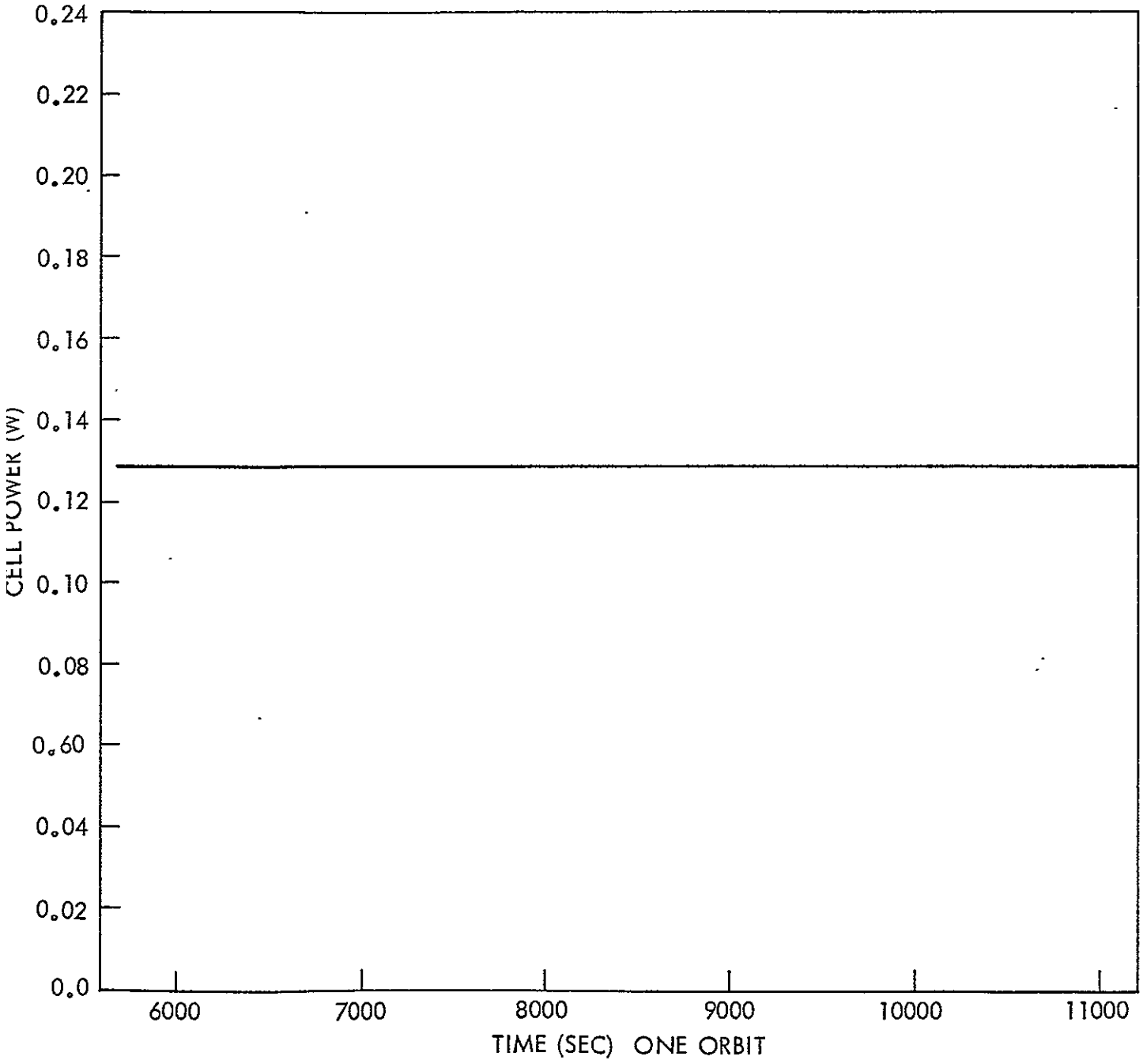

Figure 4-25 Power/Cell Beta = 90°

TABLE 4-11

TEMPERATURE DATA SUMMARY

Orbit Beta Angle	Cell Maximum Temp °C	Cell Minimum Temp °C
$\beta = 0°$	+ 70.4	- 71.0
$\beta = 30$	+ 65.1	- 74.2
$\beta = 60$	+ 57.4	-75.8
$\beta = 90$	+ 52.0	+ 52

Substrate optical property variations and cell electrical conversion degradation resulting from environmental effects were not considered in this analysis and could raise the cells EOL operating temperature and hence lower its output. (See Section 4.4).

The predicted on orbit maximum cell temperature of 70.4°C which resulted from this preliminary thermal analysis was used in the electrical sizing analysis. (Section 3.2.8).

4.3 RELIABILITY ANALYSIS

This section presents the results of a preliminary reliability analysis for the PEP Solar Array. The results of the analysis are compared with the goal of R = .999 per cycle for the array's extension and retraction sequence.

Discussion

The mechanical system consists of the following mechanical or electro-mechanical items:

a. Canister latching and unlatching mechanisms
b. Canister deployer drive motors
c. Extension/retraction mast drive motors

d. Mast rotating nut bearings and gear system (mast canister)
e. Truss bay batten/diagonal/longeron joints and rollers
f. Guide wire tensioning system
g. Full tensioning system

The mechanical system reliability block diagram is shown in Figure 4-26. The mast rotating nut rotates three revolutions per bay. There are 122 bays for 3 x 122 = 366 revolutions per extension and 366 revolutions per retraction. The approximate gear ratio between the rotating nut ring gear and the motor spur gear will be 16:1 for 16 x 732 = 11712 revs of the motor spur gear for an extension/retraction cycle.

The deployer motor rotates ≈400 revolutions per a deploy/stow cycle. The gear ratio between the rotating deployer and the deployer drive motor is ≈ 50:1.

The failure rates used for all mast components are shown in Table 4-12.

The reliability of the deployer latching mechanism is

$$R = (e^{-.5 \times 10^{-5}}) \times (e^{-1.17 \times 10^{-8} \times .5}) \times (e^{-1.17 \times 10^{-8} \times 400})$$

$$R = \underline{.99999}$$

The deployer motor has the following reliability

$$R = e^{-.995 \times 10^{-9} \times 400}$$

$$R = \underline{.99999}$$

The extension mast drive motor has the following reliability

$$R = e^{-.995 \times 10^{-9} \times 11712}$$

$$R = \underline{.99998}$$

The reliability of the mast canister is

$$R = (e^{-5.04 \times 10^{-10} \times 732}) \times (e^{-1.17 \times 10^{-8} \times 732}) \times (e^{-1.17 \times 10^{-8} \times 11712})$$

$$R = \underline{.99985}$$

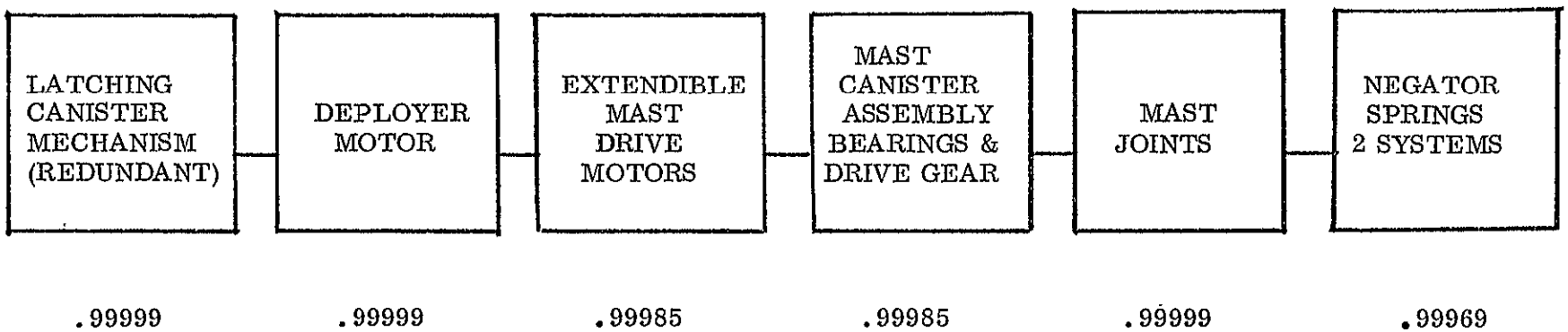

R = .99936 One Wing

R = .99872 Total System (Two Wings)

Figure 4-26 Mechanical System Reliability Block Diagram

TABLE 4-12

DEPLOY/EXTENSION/RETRACTION SYSTEM FAILURE RATES

DEVICE	FAILURE RATE	SOURCE
TORQUE MOTOR	0.995×10^{-9}/REV	BBRC* (FLIGHT DATA)
RING GEARS	1.17×10^{-8}/REV	BBRC (GROUND TEST)
BEARINGS	5.04×10^{-10}/REV	BBRC (FLIGHT DATA)
MAST JOINTS	0.5×10^{-6}/ACT	ESTIMATE
LATCHES	$.5 \times 10^{-5}$/ACT	ESTIMATE

*Ball Brothers Research Corp.

The mast joint reliability is

$$R = e^{-.5 \times 10^{-6} \times 2}$$

$$R = .99999$$

The reliability of the PEP Solar Array System (.99872) does not meet the design goal of .999 per deployment cycle and requires the incorporation of redundant elements. The reliability analysis accomplished to date is of sufficient depth to recommend specific design modifications which would enhance the array's extension/retraction performance reliability.

As shown in Figure 4-26 the negator springs exhibit the lowest reliability due to the large number of revolutions of the five negator motors required to store the tensioned cable on the take up reel as displayed in Figure 4-27. The incorporation of redundant bearings on the negator motors would be recommended as a design modification to raise the PEP Solar Array's reliability to the .999/cycle requirement.

The addition of redundant deployer drive motors, redundant canister bearings and redundant mast drive motors, although they are not required to meet the per cycle reliability requirement are recommended due to the multi-deployment mission requirement of the PEP Solar Array.

It is LMSC's desire to minimize the ground refurbishment effort to accomplish a substantial program cost savings. Figure 4-28 represents the reliability block diagram of a PEP Solar Array system that has redundant mechanical elements incorporated into the design which will enhance the system's overall reliability, minimize mid-mission refurbishment and reduce the systems per mission cost.

Figure 4-29 presents the reliability predictions per cycle for a PEP solar array system with non-redundant and redundant mechanical elements.

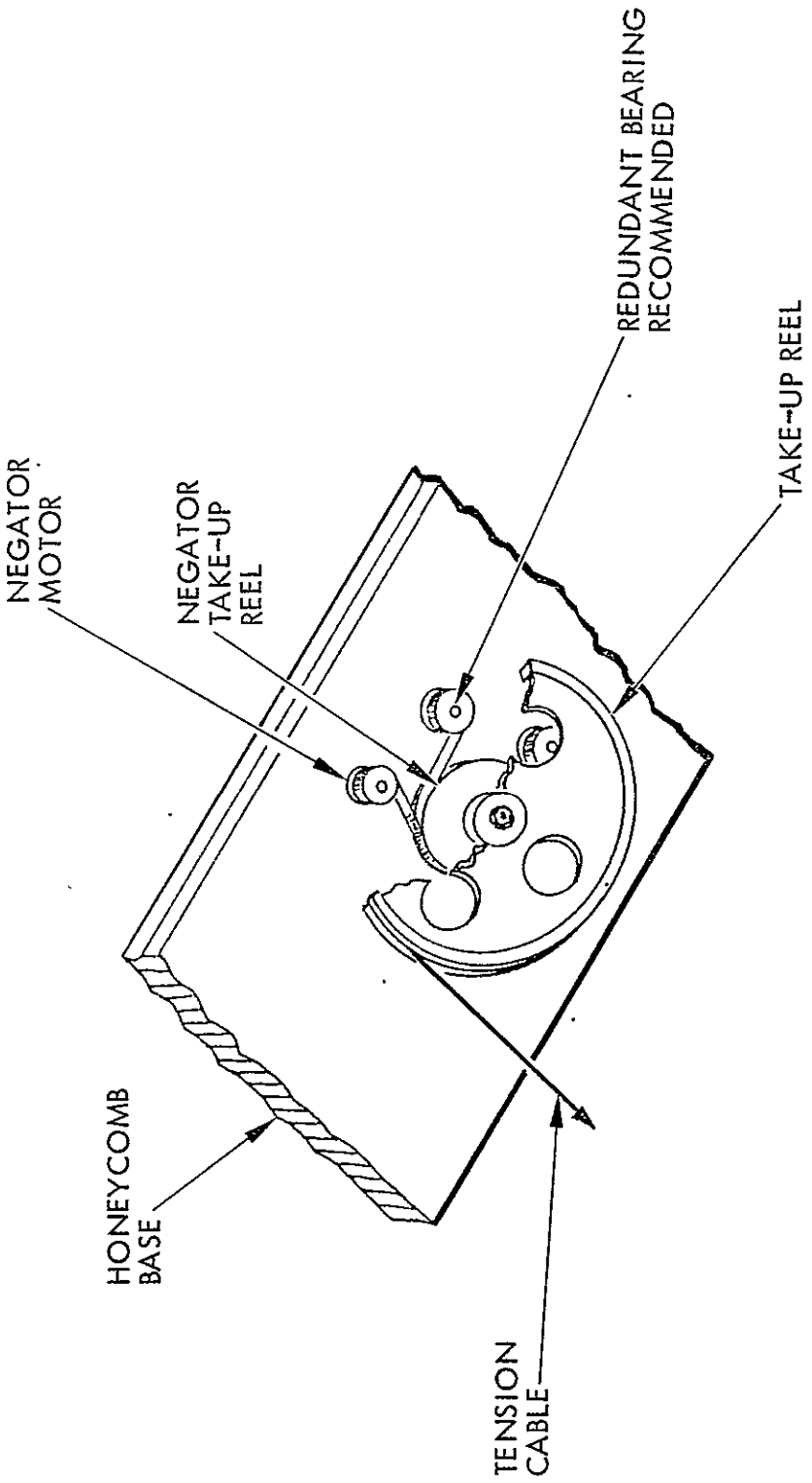

Figure 4-27 Negator Motor

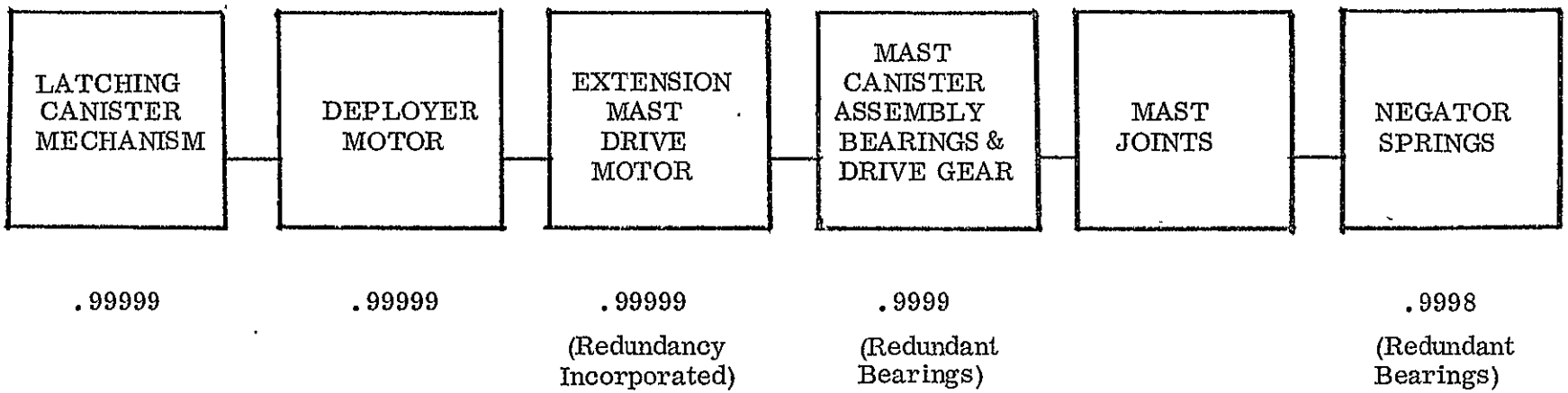

R = .99967 One Wing Per Cycle

R = .99934 Total System (Two Wings) Per Cycle

Figure 4-28 Reliability Block Diagram (Redundant Elements)

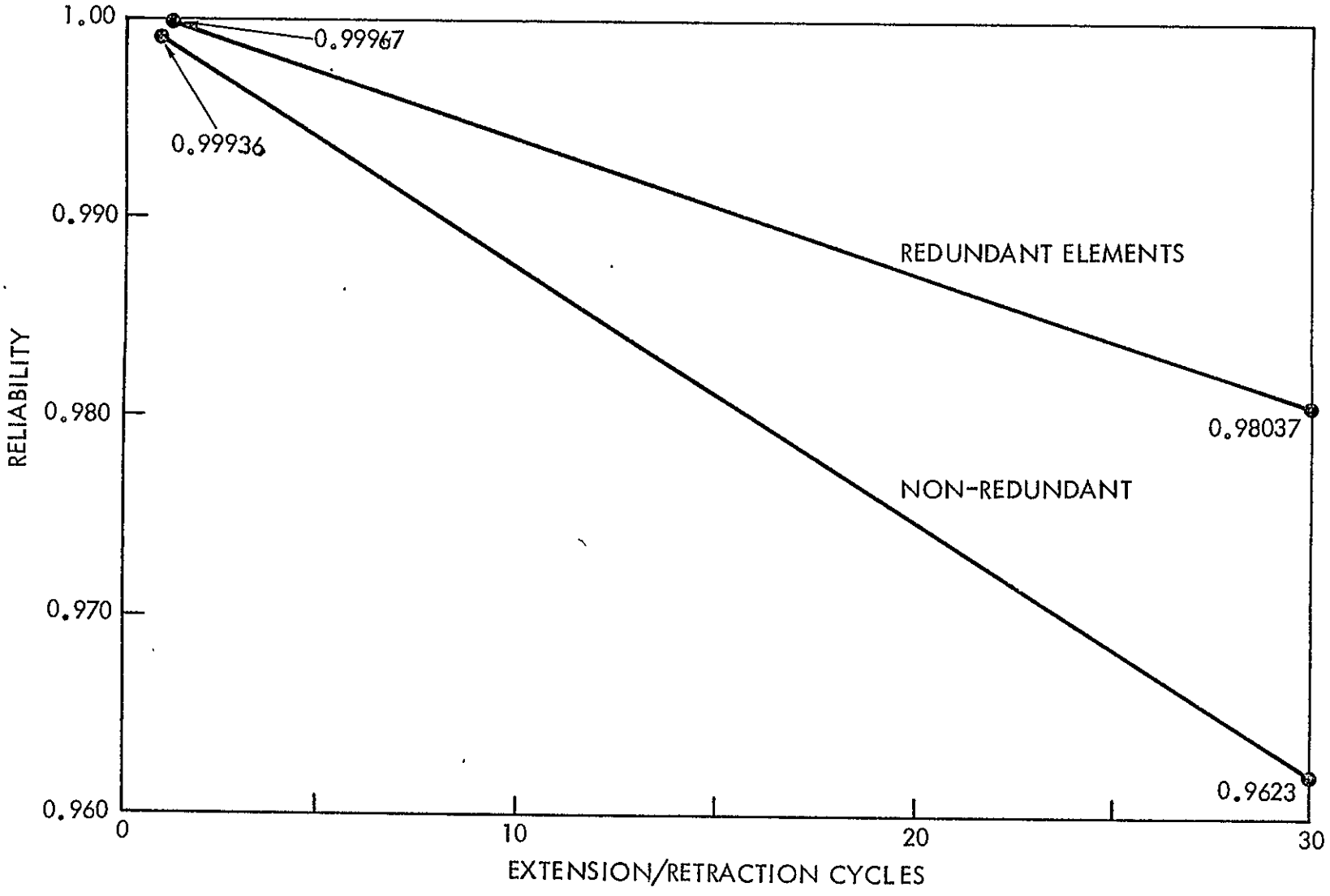

Figure 4-29 Reliability Per Extension/Retraction

4.4 CONTAMINATION CONSIDERATIONS

The degradation of blanket assembly performance resulting from the accumulation of contamination deposits on the cover slide is a concern for the PEP solar arrays. In the shuttle-induced environments the contamination sources are the plumes from the Reaction Control System (RCS), the vernier control system VCS, and the outgassing products from payloads and shuttle surfaces. The main concern of this study is the contamination-caused degradation of the solar cells optical properties. Since the most detrimental condensable is the Nitrate Salts of Monomethylhydrazine (MMH-Nitrate) from the N_2O_4 - MMH RCS and VCS plumes (Refs. 8 and 9), attention is concentrated on estimating the quantity of this substance produced during orbiter maneuvers. The VCS thrusters, as compared to RCS thrusters, are much smaller in thrust (25 lb versus 870 lb), fewer in number (6 versus 38), and their contribution to surface contamination should be much smaller. The potentially critical source of MMH-Nitrate is the RCS thrusters. Other exhaust products and outgassed products have vapor pressures too high to be of concern at the solar cells surface temperature. The RCS modules are shown in Figure 4-30 (Ref. 3).

MMH-Nitrate is formed as a result of incomplete combustion at low chamber temperatures. It is most prolifically produced during pulsing and other transient events, such as startup and shutdown (Refs. 8 and 9). MMH-Nitrate is the principal compound of the wall film in the thruster. The usual mechanism for MMH-Nitrate dispersal into the plume is by wall shear and the resulting efflux is generally composed of large droplets and liquid mass mostly concentrated in the outer portion of the plume. A small amount of the wall film component is dragged along the plume surface due to shear and mixed with the plume flow a few exit radii downstream.

The mass fraction of the MMH-Nitrate can be considered to be 1.2% in the boundary layer, though the amount varies with different thrusters. To estimate the contamination effect it is assumed that the mass fraction of MMH-HNO_3 (the predominant nitrate compound) particles is 0.1% in the total plume efflux, and that all the MMH-HNO_3 impinging on a surface is deposited on the surface. The mass fluxes versus the

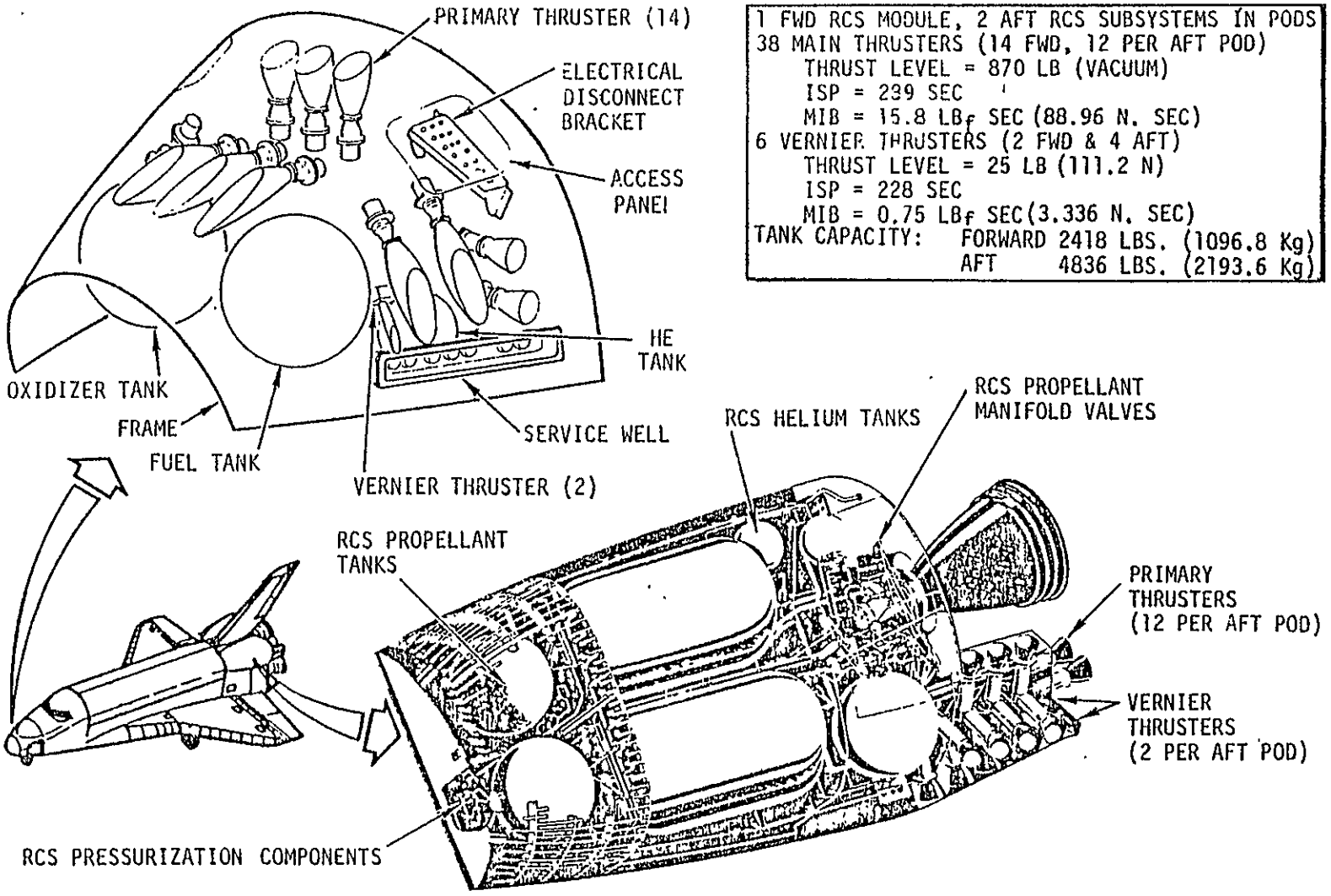

Figure 4-30 Orbiter Reaction Control Subsystem (Reprinted from Reference 3)

distances from the RCS thruster are given in Table 4-13 (Ref. 7). The change of solar absorptance of the glass cover slide surfaces due to MMH-HNO_3 deposit is given in Figure 4-31 (Ref. 7).

TABLE 4-13

MMH-HNO_3 MASS FLUXES ALONG ORBITER RCS PLUME CENTER LINE

DISTANCE, FT.	MASS FLUX OF MMH-HNO_3, G/CM^2 - SEC
25	1.66×10^{-6}
50	4.15×10^{-7}
100	1.04×10^{-7}
500	4.15×10^{-9}
1000	1.04×10^{-9}
2000	2.55×10^{-10}
3000	1.15×10^{-10}

Mass Fraction of MMH-HNO_3 = 0.1% Assumed

The change of emissivity of the coverslide surface due to MMH-HNO_3 deposit was also measured as shown in Figure 4-32.

Comparing Figures 4-31 and 4-32, it is seen that the degradation of solar absorptivity due to MMH-HNO_3 deposition is at approximately the same rate as that of surface emissivity. If the mass fraction of MMH-HNO_3 is conservatively assumed to be 1% in the plume, as the level in the boundary layer region, it takes about 900 seconds of cumulative transient operation at the distance of 25 feet to build up a 0.015 G/cm^2 layer. The buildup would increase the coverslides α by .01 and decrease its ϵ by .01 and hence alter its operating temperature. Perhaps a more detrimental effect would be the coverslide's transmission degradation caused by these buildups.

Any changes to the blanket assemblies performance characteristics caused by contamination deposits were not addressed in this study.

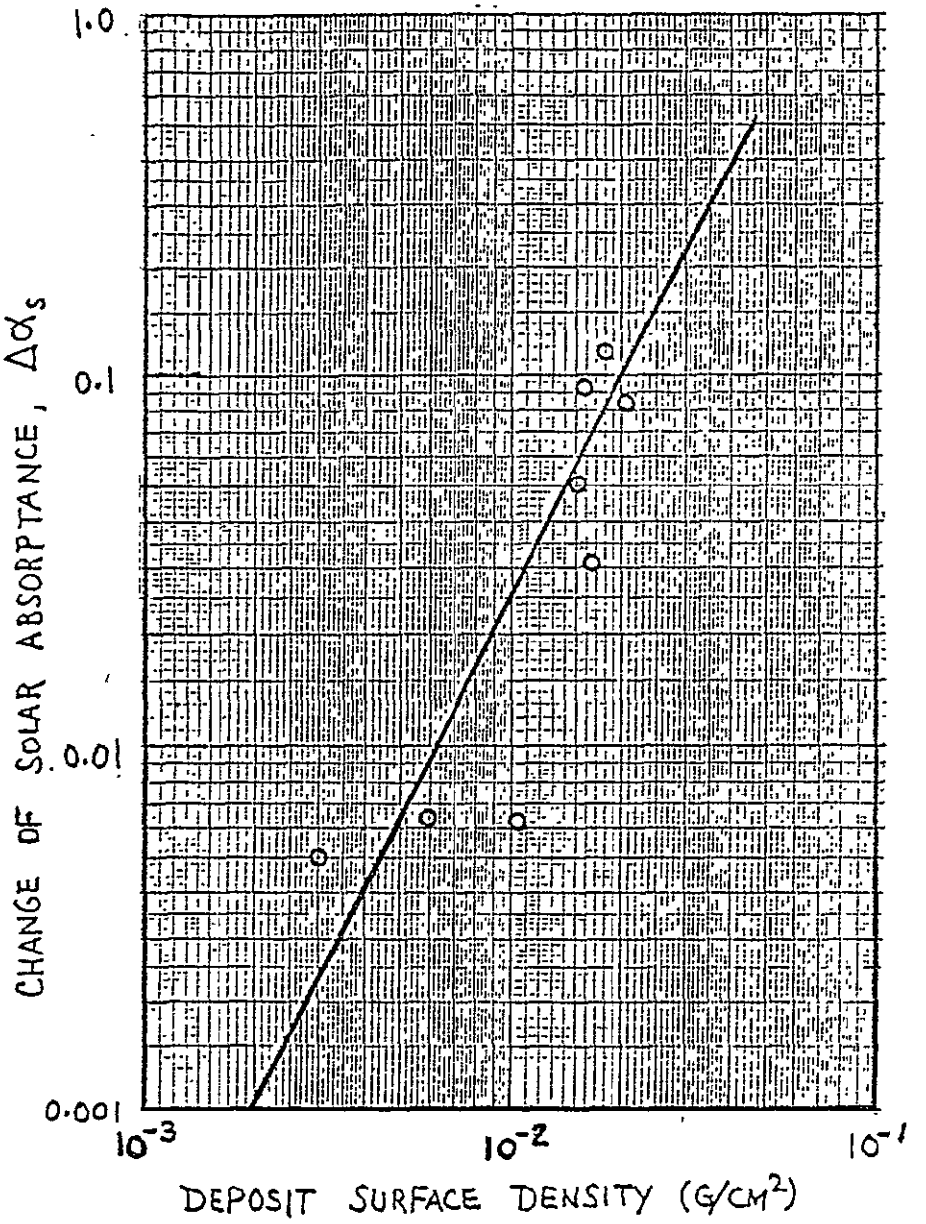

Figure 4-31 Change of Solar Absorptance of Glass Coverslide Surface Due to MMH-HNO_3 Deposit (Reprinted from Reference [7])

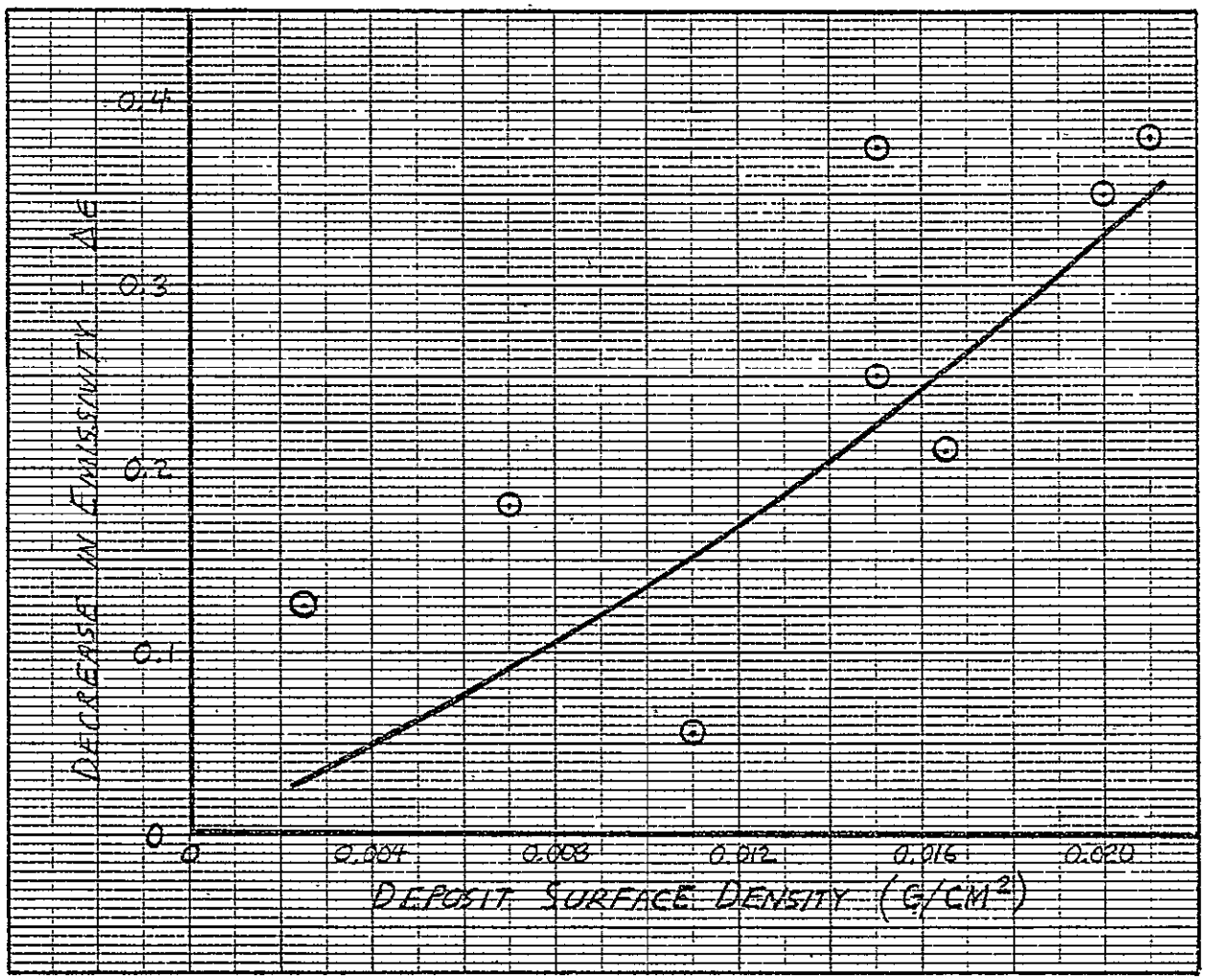

Figure 4-32 Change of Emissivity of Glass Coverslide Surface Due to MMH-HNO_3 Deposit

5.0 SUMMARY DISCUSSION OF MODIFICATION RECOMMENDATIONS

The following section summarizes LMSC's recommendations for modifications to the basic SEPS design for adaption into a PEP capable Solar Array system.

5.1 CONFIGURATION RECOMMENDATION

The advantages of a compact solar array bridged between the Orbiter (longeron bridges), while using a minimum of Orbiter length, leads us to choose Configuration 3 of this study (discussed in Section 3.1 of this report and Appendix A) as the Strawman approach. This concept has basically been verified by analysis performed by MDAC (References 4 and 5).

The modifications required to the basic SEPS design to accommodate this configuration are all structural in nature and present moderate risk and cost increases.

The additional mechanical elements required represent standard mechanism technology and, as shown in Figure 4-26, detract little from the PEP Solar Array's overall reliability.

Since the incorporation of the canister rotating and latching mechanism represents the only usage of mechanical elements not previously qualified or slated for qualification testing on the SEP program, we recommend the fabrication and demonstration testing of these elements as part of the next phase of this contract.

5.2 ELECTRICAL MODIFICATION RECOMMENDATION

Inherent to the power increase requirement from the 12.5 kW/wing (planetary) system to 15.3 kW/wing (Low Earth Orbit) comes an increase in solar array panels per wing from 41 to 48. Due to time phasing and the associated technology advancement from the SEPS to PEP program an increase in state-of-the-art cell efficiency from 11.4% to 12.8% is realized for sizing of both SEP and PEP Solar Array Systems.

Table 3-3 presents the differences between the SEP solar cell and the solar cell recommended for usage on the PEP Solar Array. The usage of the High Efficiency Hybrid solar cell provides for a lighter weight system with relatively no increase in technical risk over the conventional SEP cell.

The basic substrate, array harness, panel size, interconnect method, welding technology and assembly techniques can be identical between the SEP and PEP Solar Arrays.

5.3 MECHANICAL MODIFICATION RECOMMENDATION

The mechanical modifications and additions required to the SEP Solar Array are summarized by element in the following sections.

5.3.1 Blanket Assembly Modifications

Modification

1) Increase number of panels from 41 panels/wing to 48 panels/wing to achieve increase in power requirement. Material, hinge and fold lines, panel stiffening, padding, panel cell area packing factor, construction and containment methods to be identical to SEPS.

Potential Modifications:

1) Interconnect routing geometry may require change to accommodate selected parallel by series configuration.

2) Depending on load input level specified to array base the PEP deployed blanket tension might increase over the SEP tension to preclude blanket/mast contact.

5.3.2 Container Assembly Modifications

Modification

1) Basic structural material will be aluminum rather than graphite-epoxy to minimize material, fabrication and testing costs.

5.3.3 Box Cover Locking Lever Modifications

Modification

1) Lever material will be aluminum rather than graphite-epoxy to minimize material, fabrication and testing costs.

5.3.4 Tensioning Mechanism Modification

Modification

1) Remove intermediate tensioning mechanism and associated hardware since no intermediate position specified.
2) Larger guide wire storage reel to accommodate longer length associated with increase in blanket panels.
3) Add redundant bearings to negator motors to increase reliability to R = .999.

Potential Modification

1) Increase size of negator motors and cables if increase in blanket tension is required.

5.3.5 Extension Mast Modifications

Modification

1) Increase mast moment capability to 150 ft-lbs by increasing boom radii from 7.2 inches to 9.28 inches

2) Design and test mast for multiple extension/retraction cycles

3) Incorporation into mast canister the structural integrity required for cantilevered attachment

4) Addition of redundant mechanical elements to minimize single points of failure and enhance its extension/retraction reliability through multiple deployments

5.3.6 Canister to Cover Linkage

This linkage is more of an addition than a modification to the SEP design. This addition consists of adding in series to the existing rigid SEP mast tip fitting a rotatable link which will allow the mast canister to rotate 90° relative to the box cover.

The linkage will be fabricated from aluminum using standard fabrication technology and is not foreseen as a significant cost or risk driver.

5.3.7 Canister Deployer and Support Structure

The PEP wings are unlike the modular self-contained SEP wings which lend themselves to be divorced from the basic solar array andbe integrated at the system assembly level. The canister deployer and support due to their unique latching, caging and deployment interaction with the basic solar array wings must now be considered an integral part of the solar array system. LMSC views the design, fabrication and test of the deployer and support structure as an integral structure as necessary from a system standpoint. It is LMSC's belief that the least complex and most cost efficient solar array system can be achieved if the wings, canister, deployer and support structure are incorporated into a single unit.

6.0 ASSESSMENT CONCLUSIONS

There are no known serious design limitations involved in the implementation of the recommended design modifications and additions summarized in Section 5.0. The work done in these phases of the contract has resulted in several conclusions related to the adaptability of the SEPS Solar Array design for use on the Power Extension Package Solar Array. The assessment of SEPS applicability relating to PEP requirements is given in Table 6-1. The general overall assessment conclusions are summarized below.

1. The structural modifications needed to the existing SEP solar array design to incorporate the rotating canister are minor in their nature and can be incorporated routinely.

2. All the significant risk factors are already inherent in the low-mass technology rather than in the modification of the SEP-type array.

3. The best choice of panel size appears to be the present SEP panel size with an increase from 41 to 48 panels to generate 15.3 kW.

4. The mast and its canister can be built to the calculated sizes, based on the present SEP coilable lattice mast. Able Engineering, the mast vendor, has verified the scale-up analysis of the mast.

5. The natural frequency requirement of $\leq .02$ Hz can be met by reducing blanket tension, however, blanket to mast contact results which is undesirable.

6. A more meaningful system load and dynamic analysis is needed to bound the magnitude of inputs to array base and to fully understand boom and blanket displacement regimes.

TABLE 6-1

PEP ASSESSMENT SUMMARY

ITEM	REQUIREMENT	ASSESSMENT
Design Requirements		
Output EOL, kWe	30	30,105
Altitude, km	370 - 556	No inherent limiations
Inclination, Deg	28.5, 57 & 90	
Array Orientation	Normal to Solar Vector ± 10°	
Life		
• Years	5	Must be demonstrated to determine refurbishment cycle
• Missions	30 (5 years)	
• Retraction Cycles (100%)	Orbit - 1 Per Mission	
• Retraction Cycles (Partial)	Ground - 1 Per Mission	
Mission Duration, Days	30	
Reliability (Extend/Retract)	0.999/Cycle	Achievable (see Figure 4-28)
Voltage, Volts		
• Vmp at 70°C	~120	Comply (see Table 3-4)
Intermediate Retraction Position	None	Could be provided if necessary
Replacement	Required	Inherent to SEPS design
Max. Weight, kg	612	See Table 3-5
Max. Size, m		
• Box	Max. Length - 4.5 m	Identical to SEP (4.27 m)
• Canister		Configuration Dependent
• Max. Blanket Length, m	50.0	38.6 m
• Max. Retracted Length, m	2.0	1.88 m

TABLE 6-1 (Continued)

ITEM	REQUIREMENT	ASSESSMENT
Deployed Natural Frequency, Hz		
• Bending	≧.04	Dependent on mast EI and blanket tension
• Torsion	≧.04	
Shuttle Launch Environment	Per 7700	
• G-Loads		To be verified by test and analysis
• Vibration		
• Acoustics		
Post-Mission Checkout	Required	Visual and Dark EI (Partial Extension Suggested)
Technical Risk	Low	SEPS technology enhances probability of technical success
Schedule Risk (24 months)	Low	High - due to manufacturing scale-up requirements
Magnetic Moment	TBD	Not assessed
RCS Thruster Loads	TBD	Cannot meet 7700 Table 3.1.2 acceleration levels - MDAC assessed
Independent Array Jettison	None	Suggest further study
On-Orbit Design Loads		
• Axial, Kg (Lb)	TBD	Thrustor pulsing dependent
• Lateral, Kg (Lb)	TBD	
• Bending, N-M (Ft-Lb)	135.58 (100)	
• Torsion, N-M (Ft-Lb)	TBD	

7.0 REFERENCES

1. HESP Technical Report AFAPL-TR-77-36, 1 June 1975 - 15 June 1977

2. Orbital Service Module Flyback Solar Array, Program Plan, LMSC-D665402, 30 October 1978

3. Space Shuttle Payload Accommodations, Level II Program Definition and Requirements, Volume XIV, JSC 07700, Rev E, June 17, 1977

4. Orbital Service Module Systems Analysis Study, Midterm Review, McDonnell Douglas Astronautics Company, Huntington Beach, CA, MDC-7518, 18 July 1978

5. Orbital Service Module Systems Analysis Study, Final Review, McDonnel Douglas Astronautics Company, Huntington Beach, CA, MDC-G7554, 1 November 1978

6. Orbital Service Module Analysis Contract, 20 March 1978, NAS9-15532

7. Fong, M. C. and C. K. Liu, "Contamination Control of Long Life Shuttle Payload," LMSC-D569577, Lockheed Missiles & Space Co., December 10, 1976

8. Etheridge, F. G. and R. A. Boudreaux, "Attitude-Control Rocket Exhaust Plume Effects on Spacecraft Functional Surfaces," J. Spacecraft, Vol. 7. No. 1, January 1970, pp. 44-48

9. Breisacher, P., H. H. Takimoto, G. C. Denaut, and W. A. Hicks, "Simultaneous Mass Spectrometric Differential Thermal Analyses of Nitrate Salts of MMH and Methylamine," Combustion and Flame, Vol. 14 No. 3, June 1970, pp. 397-404

APPENDIX A

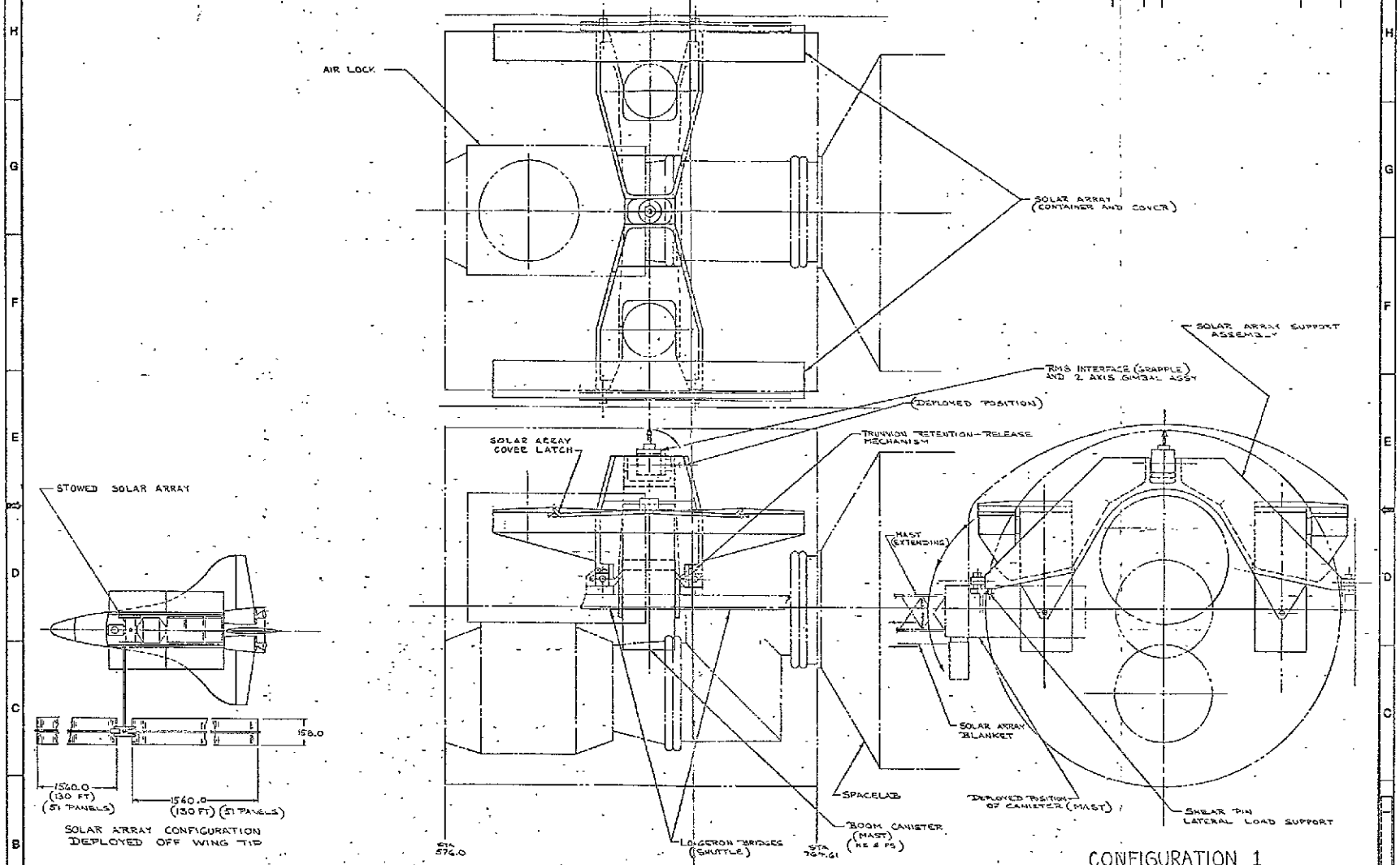

CONFIGURATION 1

CONFIGURATION 1

ORBITAL SERVICE MODULE
ARTICULATED SOLAR ARRAY
DOUBLE BOOM

JUNE 12, 1978 W. Murphy

SCALE: 3/4" = 1 FT.

ALL DIM'S. IN INCHES

SK612780

FOLDOUT FRAME

ORIGINAL PAGE IS OF POOR QUALITY

A-2a

FOLDOUT FRAME

ORIGINAL PAGE IS OF POOR QUALITY

A-2b

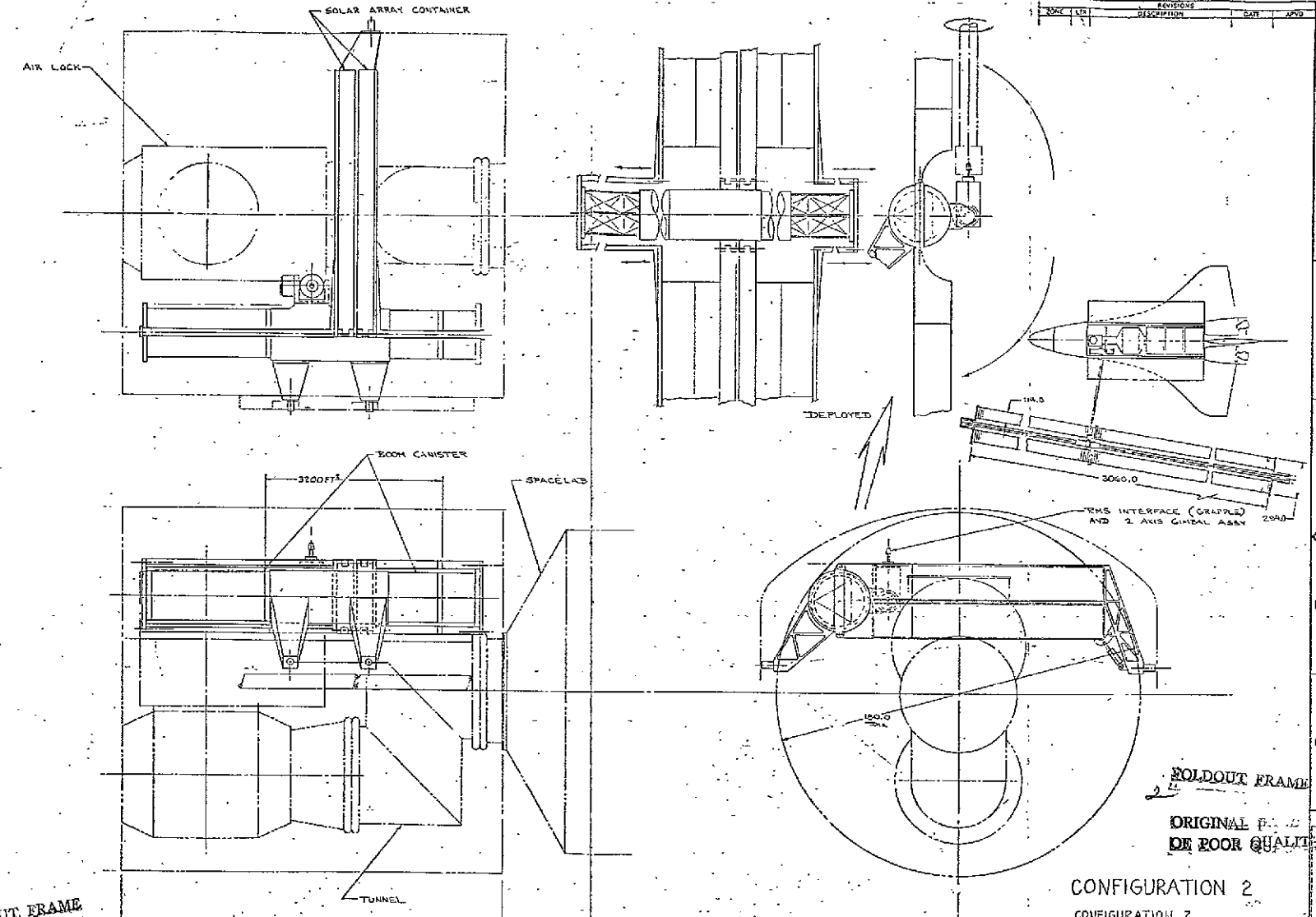
SOLAR ARRAY CONTAINER
AIR LOCK
DEPLOYED
BOOM CANISTER
3200FT²
SPACELAB
TUNNEL
STA 576.0
STA 744.61
RMS INTERFACE (GRAPPLE) AND 2 AXIS GIMBAL ASSY
114.0
3060.0
2940
180.0
FOLDOUT FRAME
FOLDOUT FRAME 2
ORIGINAL PAGE IS OF POOR QUALITY
CONFIGURATION 2
CONFIGURATION 2
ORBITAL SERVICE MODULE
ARTICULATED SOLAR ARRAY
DOUBLE BOOM
MAY 17, 1976
SCALE: 1/64=1 FT.
SK 517780
A-3 (a)
A-3 (b)

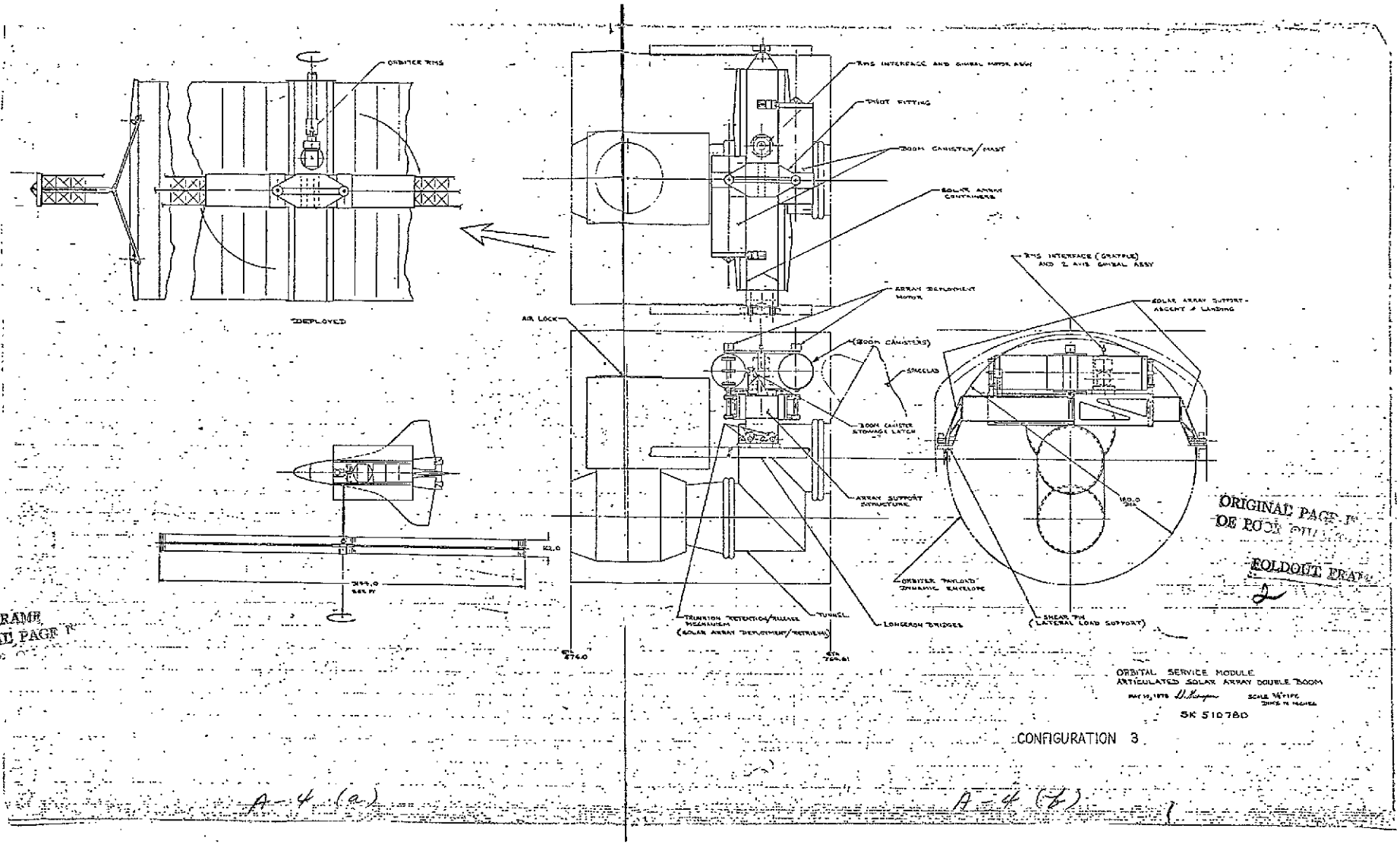

CONFIGURATION 3

FOLDOUT FRAME
ORIGINAL PAGE IS OF POOR QUALITY

FOLDOUT FRAME 2

A-4 (a)

A-4 (b)

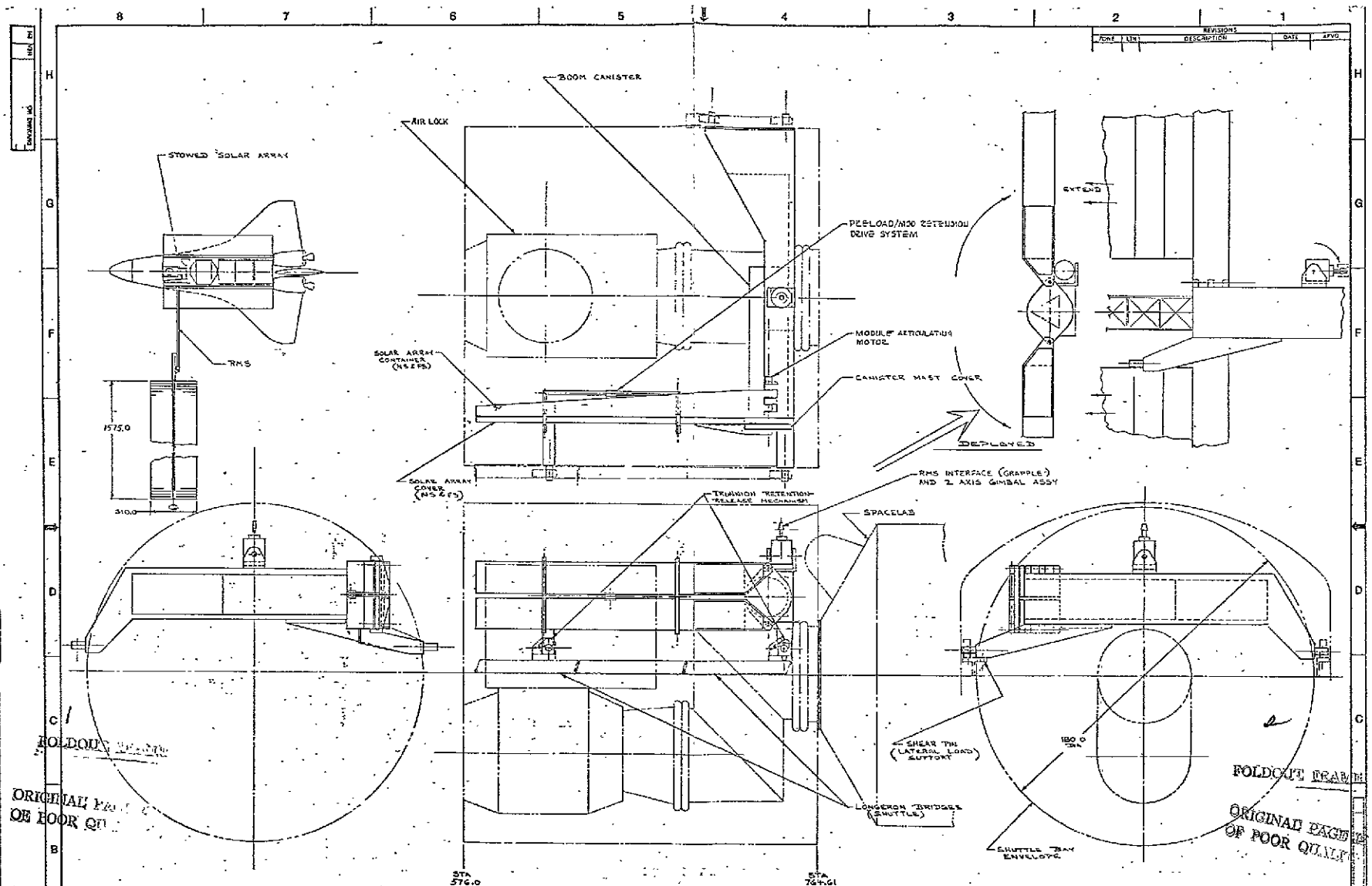

CONFIGURATION 4

CONFIGURATION 4

ORBITAL SERVICE MODULE
ARTICULATED SOLAR ARRAY
SINGLE BOOM

JUNE 2, 1978

SCALE: 3/4" = 1 FT

SK602780

A-5 (a)

A-5 (a)

APPENDIX B

AUTOMATICALLY DEPLOYABLE ABLE BOOMS

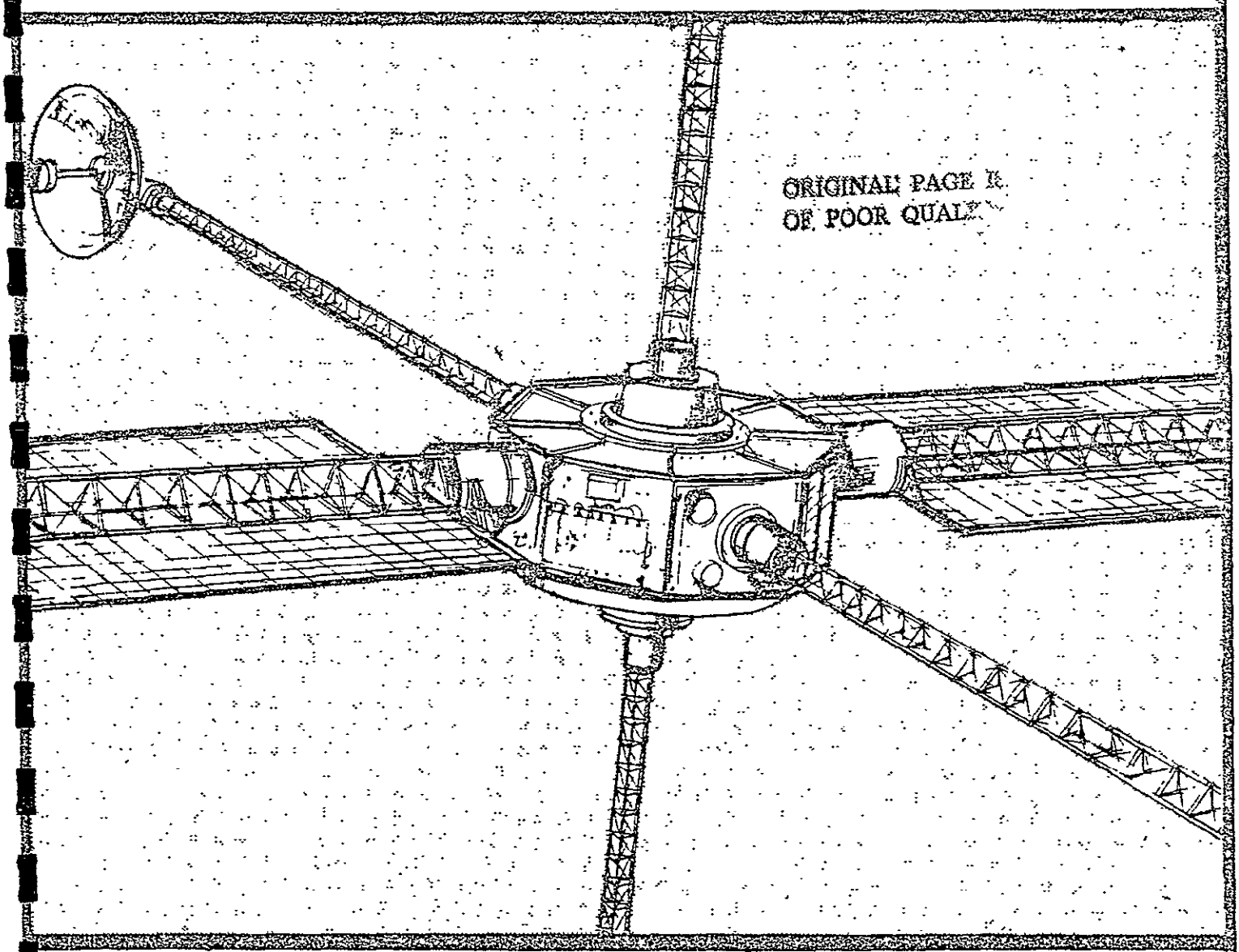

ABLE ENGINEERING COMPANY, Inc.

P.O. BOX C GOLETA, CALIFORNIA 93017 805/964-8707

INTRODUCTION

ABLE ENGINEERING COMPANY (ABLE) specializes in the design and manufacture of a variety of deployable lattice booms for ground, sea, air and space applications. These standard and custom-designed booms meet a broad range of structural and operational requirements, and they have been made in diameters ranging from 4 to 40 inches and in lengths over 100 feet. These booms can be deployed either manually, automatically or semiautomatically with high reliability and long life under repeated deployments and retractions. When retracted they are only a small fraction of their deployed length; therefore, they are highly portable.

This brochure describes and gives design information on several types of ABLE booms that are automatically deployed and retracted. These automated systems are especially useful in space and other hostile environments which demand stiff, strong and dimensionally stable booms that are highly portable and remotely deployable.

ABLE personnel have broad experience in engineering, manufacturing and testing these types of booms under U.S. Government contracts and for a great diversity of applications. This comprehensive experience will insure that you receive ABLE booms that are properly designed, manufactured and proof-tested to meet your most stringent requirements and specifications.

Because the specifications of particular applications usually dominate the design and price of automatic ABLE boom systems, no stardardized price-listed systems are offered. However, upon your request, ABLE will provide preliminary design data and prices for systems to meet your requirements.

AUTOMATIC ABLE BOOMS

Applications

Typical uses for automatically deployable ABLE boom systems are to deploy and support magnetometers, hydrophones, spectrometers, antennas, interferometers, solar-cell arrays, or gravity-gradient masses for spacecraft stabilization. Their light weight and compactness provide the portability needed for the listed applications. ABLE booms are also, potentially, a very useful element of remote manipulator systems for space, undersea and other unfriendly environments. Electrical conductors can be permanently attached to any of the several types of ABLE booms, without impairing their capability for repeated deployment and retraction. Because of their low susceptibility to thermal distortions (see later section), ABLE booms are especially useful for applications requiring high dimensional stability in the solar irradiation environment of space.

Descriptions and Design Data

ABLE booms are lightweight, open lattice structures that deploy from, and retract into, a very compact cylindrical volume. The cylindrical volume can be as short as 2% of the deployed boom length, and its diameter is nominally the same as the boom diameter. There are two basically different types of ABLE booms. One type has continuous-longeron members which are elastically coiled when the boom is retracted. The second type employs articulated longerons which hinge for retraction. Two different methods of hinging are offered and are described later.

Either the continuous- or articulated-longeron booms can be stowed in and deployed by a motorized canister. The canister diameter is slightly greater than the boom diameter. The canister height is governed by the stowed height of the boom plus the height of any one of several mechanisms that are used to enforce and control boom deployment. Alternatively, the continuous-longeron booms can be secured in their stowed configuration without a canister, and then self-deployed while using a lanyard to control their deployment rate. The canister-deployed booms can be deployed to and utilized at any fraction of their total length. Usually, the lanyard-deployed booms are utilized only when deployed to their full length.

Four different types of ABLE boom systems are offered to provide a broad range of operational and performance capabilities. They are:

- ACR Systems -- a lattice boom having articulated longerons and using a powered canister for deployment, retraction and support; the retracted part of the boom rotates in the canister during deployment and retraction.
- ACO Systems -- a lattice boom having articulated longerons and using a powered canister; but the retracted part of the boom does not rotate in the canister.
- CC Systems -- a lattice boom having continuous coilable longerons and which is deployed, retracted and supported by a powered canister.
- CL System -- a lattice boom having continuous coilable longerons but which is deployed by its own strain energy and utilizes a lanyard to control deployment.

Descriptive and design data for these four types of systems are given below.

ACR Systems -- These systems should be used for applications which require booms of large bending stiffness or strength but for which boom diameter is restricted; i.e., a coilable longeron boom of a prescribed diameter has severely limited bending stiffness and strength (as discussed later).

An ACR system, comprised of its boom and canister, is illustrated in Figure 1a. A detail of the articulated-longeron lattice

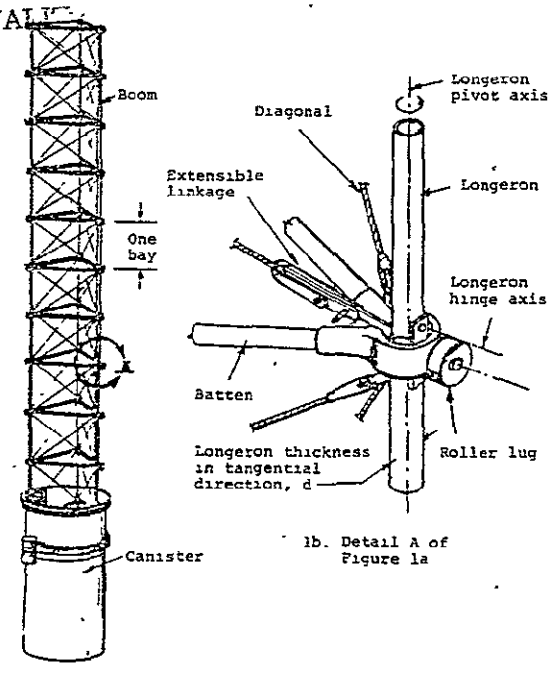

1a. Deployed ACR System Boom and Canister

1b. Detail A of Figure 1a

boom for ACR systems is illustrated in Figure 1b. The indicated longeron, batten and diagonal members comprise the principal structural components of the boom. Typically, the longerons are segments of metallic tubing which are articulated to the batten frames with universal hinge fittings. Six diagonal members, typically cables, provide shearing stiffness and strength for each bay of the boom (a bay is the boom portion between adjacent batten frames). Three of the six diagonals incorporate linkages which extend when unlatched. This combination of extendible diagonals and hinged longerons permits adjacent batten frames to be rotated differentially about the boom axis, thus collapsing the bay into the compact, retracted configuration shown in Figure 1c. Retraction and deployment of each bay proceeds independently of the extent to which adjacent bays are deployed. Any number of bays can be interconnected to provide a boom of a desired length.

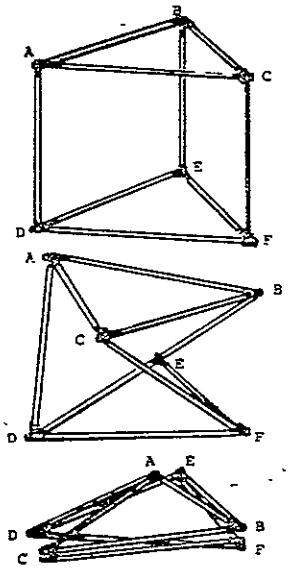

1c. Retraction Sequence for the ACR Articulated Boom

For a prescribed boom diameter, the longeron material and cross-sectional dimensions can be selected to provide the necessary bending stiffness or strength. Because the longerons of this type of boom are articulated, their materials and cross-sectional dimensions are not restricted by requirements for elastic coiling. However, to insure compact retraction, the distance between their hinge points must be no greater than about 0.75 times the boom diameter.

Following are formulas for the more common properties of the ACR booms:

Bending stiffness,

$$EI = 1.5C_1EA_lR^2$$

where E = Young's modulus of longeron material
A_l = cross-sectional area of one longeron
R = boom radius measured from boom axis to longeron centerline
C_1 = a reduction factor to account for flexibilities of articulating joints; typically $C_1 = 0.5$

Shearing stiffness,

$$\overline{GA} = 3\overline{EA}_d \sin \phi \cos^2 \phi$$

where $\overline{EA}_d$ = extensional stiffness of one diagonal member when pretensioned to its service load
ϕ = angle between a diagonal and a batten member; typically ϕ is about 42°

Torsional stiffness,

$$\overline{GJ} = 0.5\overline{GA}R^2$$

Bending strength,

$$M_{CR} = 1.5P_{CR}R$$

where P_{CR} = minimum strength of one longeron, whether that minimum is for Euler buckling between hinge pins, for bearing strength of joint, or for other limitations

This bending strength is for one longeron loaded in its weakest direction (tension or compression) and the other two longerons are each oppositely loaded to one-half the load of the critical longeron.

Shearing strength,

$$V_{CR} = \sqrt{3}T_d \cos \phi$$

where T_d = tensile strength of one diagonal

Torsional strength,

$$M_T = 1.5RT_d \cos \phi$$

Note that the formulas for V_{CR} and M_T are based on the assumption that diagonal strengths (rather than batten, longeron or joint strengths) are critical for pure shear or torsional loadings.

Boom weight,

$$W_B = 3C_2\rho A_l L$$

where ρ = density of longeron material
A_l = longeron cross-sectional area
L = boom length

and C_2 = an empirical coefficient, typically $C_2 = 2.5$ to 3.0 for articulated booms

Retracted height of boom,

$$H_B = 0.75\frac{Ld}{R}$$

where d = longeron thickness in tangent direction (see Figure 1b)

Because ACR booms are articulated, they have some mechanical deadband which allows them to bend freely until clearances are taken up. This deadband can result in operational problems for some applications, and one solution is to use, instead, the continuous-longeron ABLE boom which has no deadband. However, if an ACR boom is required for strength or stiffness, yet deadband is prohibited, then any one of several methods can be used to remove the deadband by prestressing the boom.

Devices used to stow, deploy and support lattice booms are referred to as canisters. One type of canister used to deploy ACR booms is shown in Figure 2. The retracted boom stows in the lower region, rails in the intermediate region guide the boom through its transitional configurations, and the upper region deploys and supports the boom. The upper region consists of a large, power-rotated three-threaded nut and three pairs of stationary, vertical guide rails. Round roller lugs which protrude from the boom at each batten corner (see Figure 1b) are engaged

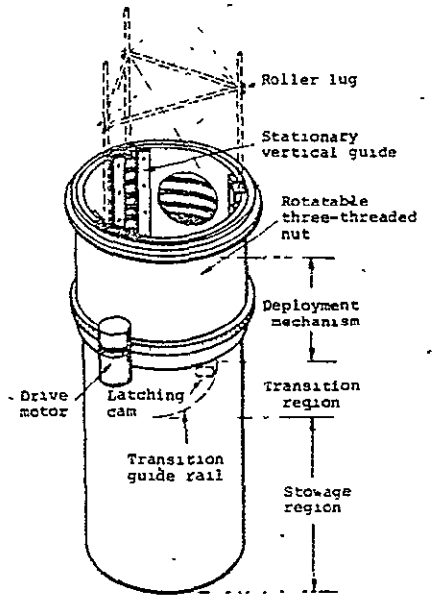

Figure 2. Canister for Deploying and Supporting ABLE Booms

between the stationary guides and the threads of the nut. When the nut is rotated by a drive motor, the boom is forced to deploy from or retract into the canister. The deployed part of the boom does not rotate as it deploys. As the boom is so deployed or retracted, cams located in the top of the transition region automatically latch or unlatch the boom diagonal linkages. Since one level of roller lugs is always engaged by the canister, the deployed portion of the boom is always supported. Therefore, the boom can be deployed to any fraction of its length and used there.

Since the ACR boom must be twisted to retract and since the deployed part of the boom does not rotate in the canister, the retracted part within the stowage region must and does rotate. To accommodate that rotation the bottom of the boom is mounted on a rotatable plate at the bottom of the canister.

The height of a canister for an ACR boom is*

$$H_{CAN} = H_B + 3R$$

H_B is the boom stowed height given by the previous formula and 3R is the height of the transition and deployer parts of the canister. The canister weight can be approximated by the empirical formula*

$$W_{CAN} = \frac{Ld}{14} + \frac{3}{5}R^2$$

where the weight is in pounds and the dimensions are in inches.

As can be seen from the preceding formula, the rotating-nut part of the canister becomes very heavy for booms of large radius. A lighter-weight deployment mechanism, incorporating three synchronously driven lead screws instead of the three-threaded nut, is recommended for large-diameter canisters. The lead screws are mounted 120° apart atop the transition region of the canister, and their threads engage the boom lugs in much the same manner as do the threads of the three-threaded nut. The boom is thus forced to deploy or retract as the lead screws are synchronously rotated. The heights of canisters with lead screws is about the same as those with three-threaded nuts. However, no empirical formula has been developed for their weight.

ACO Systems -- Booms used in ACO systems do not twist as they deploy and retract. ACO systems can be used for applications similar to those requiring ACR systems, but they are especially appropriate for applications which require that the base of the boom not rotate during deployment. Such nonrotating requirements arise, for instance, when a slip ring is not allowable as an electrical connection between a conductor on the boom and its outlet from the canister (as is required for ACR systems).

The ACO boom is illustrated in Figure 3. The longeron segments are singly hinged both at their connections to the batten frames and at their midlengths. The boom is retracted by simply folding the longerons inward. Latches are not required in the diagonal cables, but they are required for the longerons. The longeron midlength hinges are latched and unlatched by cams in the deployment canister.

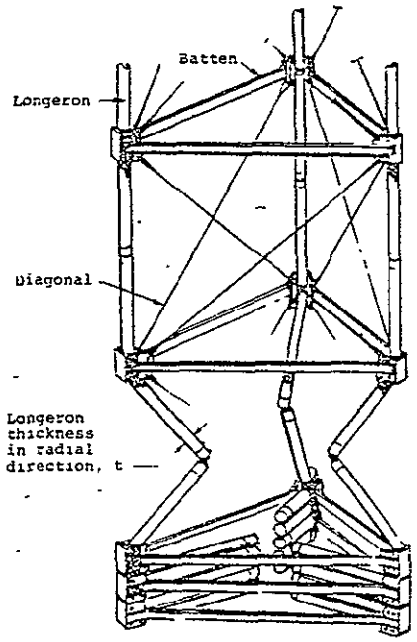

Figure 3. ABLE Boom for ACO Systems

Mechanical properties of ACO booms are calculated by the formulas listed previously for ACR booms, except that the retracted height of the ACO boom is

$$H_B = \frac{2t}{R}$$

where t = longeron thickness in radial direction (see Figure 3)

The stowed heights of ACO booms are generally larger than those of ACR booms.

*Crawford, R.F.: Structural Efficiency of Deployable Booms for Space Applications. AIAA Paper No. 71-396, April 1971.

Because the pretensioned diagonals precompress all hinge joints in the ACO booms, the joints have no mechanical deadband unless externally applied tensile loads cancel out the precompression.

Both the three-threaded nut and the lead screw types of canister mechanisms are used for ACO booms. Canister weights and heights are estimated using the previous formulas.

CC Systems -- This system is comprised of a continuous-longeron ABLE boom and a deployment canister. The continuous-longeron boom is used for applications which require high dimensional stability and/or a high ratio of bending stiffness to weight. However, the stowage envelope for the application must be sufficiently large that the continuous longerons of the resulting boom design can be elastically coiled. The coilable boom is used with a canister (a CC system) when the application also requires that the boom develop its full strength and stiffness at any stage of its deployment, or when the deployed portion must not rotate during deployment.

Figure 4 shows the principal parts of this boom and its retraction geometry. Its canister is indicated by dashed lines.

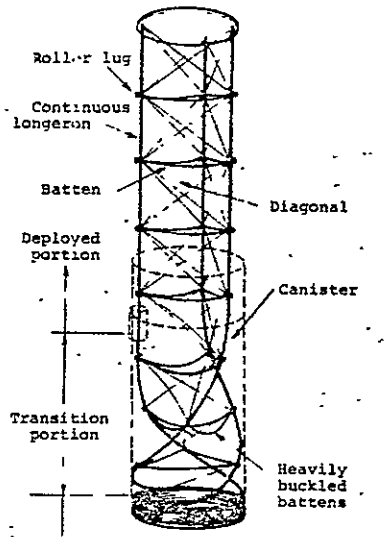

Figure 4. Deployment Geometry and Nomenclature for Continuous-Longeron ABLE Boom; CC System

The longerons are continuous over the boom length, and they are connected to the batten frames by radial pivots. Six relatively inextensible diagonals provide shearing strength and stiffness to each bay. When the boom is twisted about its axis, tension is increased in three of the six diagonals in each bay. This causes the batten members to buckle and shorten. As twisting proceeds, the longerons rotate about their pivots and assume a helical configuration. When fully retracted, the longerons are coiled in flat helices while the batten frames stack on one another. The distortions of the boom members are elastic. Therefore, the boom can withstand many cycles of deployment and retraction.

Formulas are presented below for the more common properties of these coilable booms. The data apply to booms with longerons that are solid and circular in cross section. Other cross sections may be used. Note that the following formulas are presented in terms of the allowable working strain ε of the longeron material because it is a critical material parameter for the coilable boom.

Bending stiffness,

$$EI = 1.5\pi ER^4\varepsilon^2$$

where ε = maximum bending strain of longerons when completely coiled ($\varepsilon = d/2R = F/E$ where F is the allowable working stress and d is longeron diameter)
E = Young's modulus of longeron material
R = boom radius

Shearing stiffness $\overline{GA}$ and torsional stiffness $\overline{GJ}$ are as previously defined for ACR booms.

Bending strength,

$$M_{CR} = 7.44ER^3\varepsilon^4$$

Note that Euler buckling of a compressed longeron limits the bending strength, and that the above formula is for bending in a direction which compresses one longeron and equally tensions the other two.

Shearing strength,

$$V_{CR} = 1.84ER^2\varepsilon^4$$

Torsional strength,

$$T_{CR} = 1.59ER^3\varepsilon^4$$

Euler buckling of battens limits V_{CR} and T_{CR}, and in the above formulas a typical batten design is assumed; batten diameter is 0.8 times the longeron diameter and of the longeron material.

Boom weight,

$$W_B = 9\pi\rho R^2\varepsilon^2 L$$

where ρ = density of longeron material

and L = boom length

Retracted height,

$$H_B = \frac{3}{\pi}L(\varepsilon + 0.005)$$

These formulas show that longeron material properties E and ε and the allowable boom radius R determine the performance that can be achieved with coilable ABLE booms. Principally, because of their high working strain, S-glass/epoxy rods with axially oriented fibers are very suitable for the longerons and battens. However, other materials can be used. Figure 5 shows the bending stiffness, bending strength, and weight versus the radius for coilable ABLE booms having S-glass/epoxy longerons for which

$$E = 7.5 \times 10^6 \text{ psi}$$

$$\varepsilon = 0.015$$

$$\rho = 0.075 \text{ pci}$$

The value of ε used here is typical and has resulted in highly reliable booms.

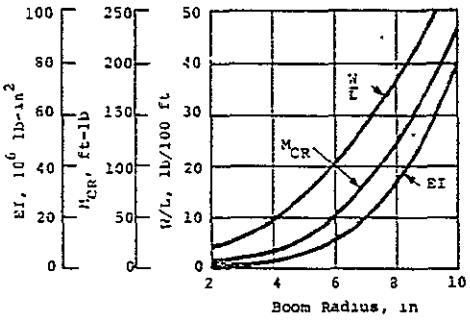

Figure 5. Mechanical Properties and Weights Versus Radii for S-glass/Epoxy, Continuous-Longeron ABLE Booms

Canisters for collable ABLE booms are essentially of the same design as those described for articulated booms. The retracted part of the boom (as indicated in Figure 4) rotates in the stowage region of the canister as the erected part deploys, without rotating, from the top of the canister. Roller lugs, which protrude from the longeron pivot fittings, are engaged by the canister to deploy and support the boom. Since a collable boom has no latches, its canister does not have latching cams. However, this difference is negligible inasmuch as the previous formulas can be used also to estimate heights and weights for collable-boom canisters.

CL Systems -- This type of system utilizes the previously described collable ABLE boom, but in this case the boom self-deploys by release of longeron strain energy. Deployment rate is controlled by a restraining lanyard which extends along the boom axis and between boom ends. This system is used in applications which have the same type of requirements and nonrestrictive stowage diameters as indicated for the CC systems. However, to use the CL system, the application must also permit the boom to deploy to its full length before it is used for vigorous operations. Advantages to be gained by using a CL rather than a CC system (assuming equal booms) are that a CL system is lighter in weight and stows in a shorter volume.

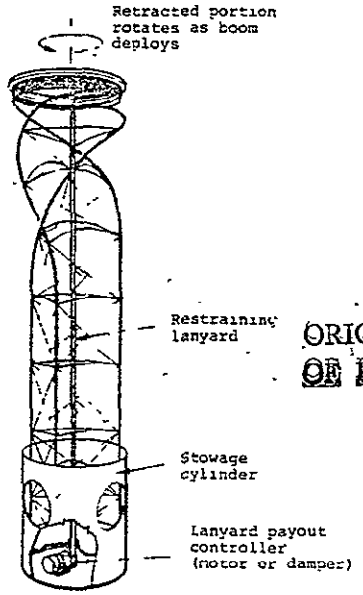

Figure 6. Continuous-Longeron Boom, Lanyard-Deployed; CL System

Figure 6 is a sketch of a CL system when the boom is partially deployed. The boom transition region, between its retracted and deployed parts, propagates upward as the lanyard is payed out. The retracted part rotates as deployment proceeds. Since roller lugs are not used in the lanyard method, boom weights are slightly less than those for CL systems. Note that the transition region lacks bending stiffness. Therefore, some operations are prohibited when the boom is partially deployed.

The lanyard is usually a metallic or fibrous tape and is wound on a reel. Lanyard payout rate is controlled, typically, by a viscous damper or an electric motor. When an electric motor is used, the boom can be retracted by reeling in the lanyard. However, a bridle is then incorporated in the outboard end of the lanyard to twist the boom tip as necessary to initiate retraction.

The preceding formulas and graphs for mechanical properties and weights of collable ABLE booms apply also to CL boom systems. When the longerons are solid circular rods, the self-deployment force P developed by collable ABLE booms is

$$P = 1.178E\varepsilon^4R^2$$

Because CL system designs can vary widely, depending on specific requirements of applications, lanyard mechanism weights and stowage weights are not standardized. However, those parts of CL systems generally weigh much less than the canisters of CC systems.

THERMAL DISTORTIONS OF ABLE BOOMS

Because all types of ABLE booms can be made so that they undergo very little thermal twisting or bending in the environment of solar irradiation, ABLE booms are especially useful for space applications that require high dimensional stability. To meet such requirements, ABLE booms are fabricated with a uniform rate of pretwist over their lengths. The pretwist is used primarily to preclude thermal twisting, as explained later, but it also precludes the excessive thermal bending that would occur if one longeron shadowed another. Thermal distortions of ABLE booms are also minimized by careful selection of materials.

If sun rays are directly in line with one set of diagonals of an initially straight lattice boom, then that set of diagonals would have a significantly lower temperature than the intersecting set which are nearly perpendicular to the rays. Shear distortions would result in the panels surrounding those intersecting diagonals, and those distortions would lead to both shearing and twisting of the overall boom. The rate of thermal twisting β' for a boom segment has been determined* to be

$$\beta' = \frac{a T_o F}{3R \sin\phi \cos\phi}$$

where
- a = coefficient of linear expansion for the diagonal material
- T_o = diagonal temperature when oriented perpendicular to sun rays
- F = a function depending on the orientation of the boom relative to the sun rays
- R = boom radius
- ϕ = angle between diagonals and battens

The function F varies cyclically with the sun azimuth angle (angular position of radial components of sun rays). The period of F is 120° and the integral of F over the period is zero. Therefore, to nullify thermal twisting, a lattice boom is manufactured with pretwist over its length equal to an integer multiple of 120°. The result is a greatly reduced net thermal twist

*IBM Corporation: Development of a Microwave Interferometer Position Locator. NASA CR-112188, August 1973.

between the base and tip of the boom. For instance, for booms with fiberglass-rod diagonals Figure 7 shows the maximum possible

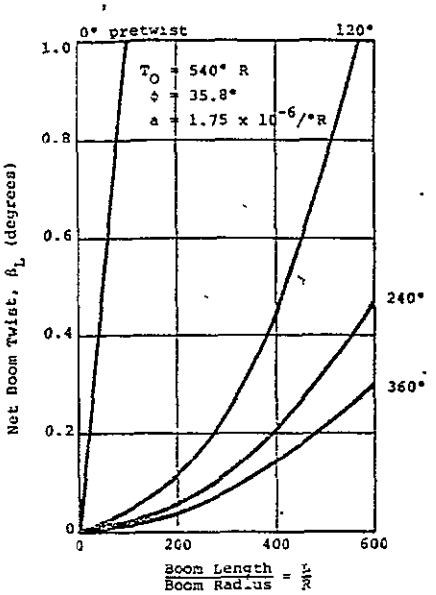

Figure 7. Net Thermal Twist Between Ends of ABLE Booms with Fiberglass Diagonals; Worst Sun Orientation and Various Amounts of Pretwist

thermal twist β_L versus length-to-radius ratio and various pretwists. Figure 7 illustrates that β_L is very large when no pretwist is used, and that although β_L is small for pretwisted booms it does increase as L/R increases. Note that bending stiffness and strength of booms are not significantly reduced by pretwists resulting in longeron helix angles as large as 10°.

The data in Figure 7 exclude an additional source of thermal twisting that is possible for pretwisted booms. If there is a difference between the average thermal strains of the longerons and diagonals, then an additional uniform twisting or untwisting $\Delta\beta_L$ occurs;

$$\Delta\beta_L = \frac{2}{3}\left(\frac{\ell}{R}\right)^2 (\varepsilon_d - \varepsilon_\ell)\beta_O$$

where ℓ = bay length
R = boom radius
ε_d = diagonal thermal strain
ε_ℓ = longeron thermal strain
β_O = initial pretwist of total boom length

This effect is seen to be absent if $\beta_O = 0$. The effect is generally quite small when longerons and diagonals are made of materials (e.g. fiberglass rods) with low coefficients of thermal expansion and whose surface properties do not permit excessive heating. As an example, consider an ABLE boom with fiberglass longerons and diagonals ($\alpha = 1.75 \times 10^{-6}$/°R), with an average temperature difference of 300°R between those members, and with a pretwist of 240° and $\ell/R = 125$. Then $\Delta\beta_L = 0.131°$.

Formulations have also been made for predicting thermal shearing distortions of ABLE booms, but they have not been integrated and otherwise evaluated to provide general parametric data. However, as a single-point example, the thermal shear deflection of the tip of a 62-foot-long cantilevered boom with 120° pretwist and fiberglass diagonals was calculated to be about 0.2 inches. It is noted that shear deflections are independent of both R and longeron thermal strains.

Also undeveloped are parametric data for thermal bending due to mutual shadowing among the parts of ABLE booms. However, consider the boom in the previous example. Assume its radius is 4 inches and its fiberglass longeron, batten and diagonal diameters are respectively 0.120, 0.100 and 0.032 inches. The tip deflection due to thermal bending is calculated to be 1.20 inches and the corresponding tip slope is 0.095°.

All the thermal distortions in the above examples could be reduced even further by using, for instance, carbon/epoxy longerons and diagonals for which $\alpha < 0.5 \times 10^{-6}$/°R .

The above formulas and trends for thermal distortions apply to both articulated- and continuous-longeron ABLE booms. Either type can be uniformly pretwisted by simply making all intersecting diagonals of the same unequal lengths. Note that when materials and dimensions are selected to minimize thermal distortions, the effect on mechanical properties can be serious; however, that effect can be evaluated by the foregoing formulas for the mechanical and dimensional properties of the various types of booms.

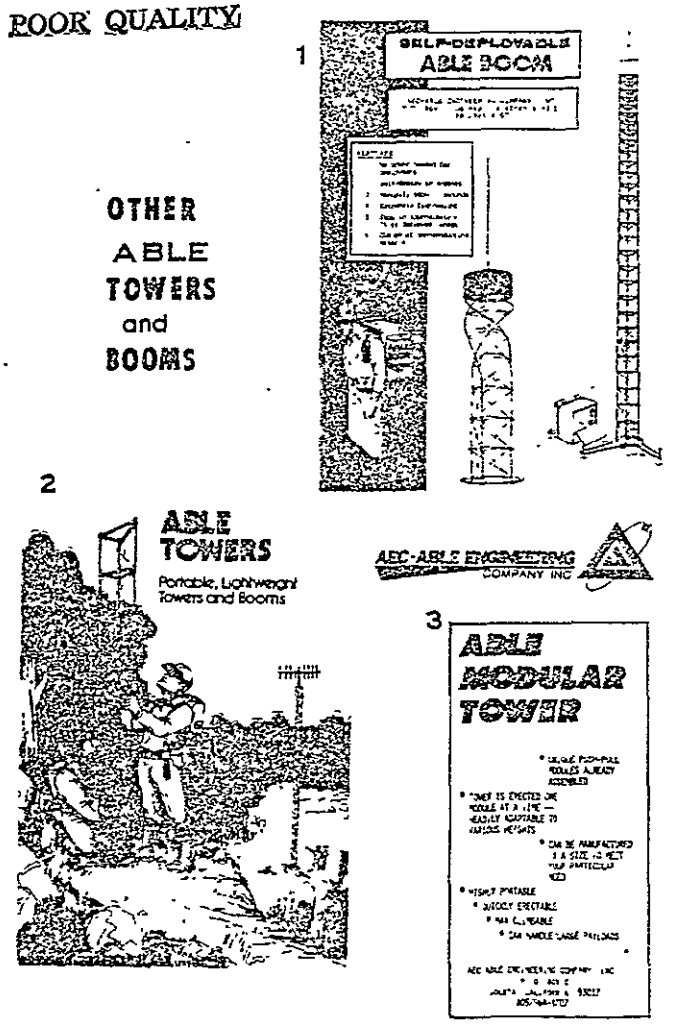

APPENDIX C

Enclosed are plots of the first 20 cantilever mode shapes of the PEP solar array model. Each has been normalized such that the generalized mass is 1.0, and the corresponding frequencies are listed with each plot. In each case, the solid line represents the boom, and the dashed line is the solar panel.

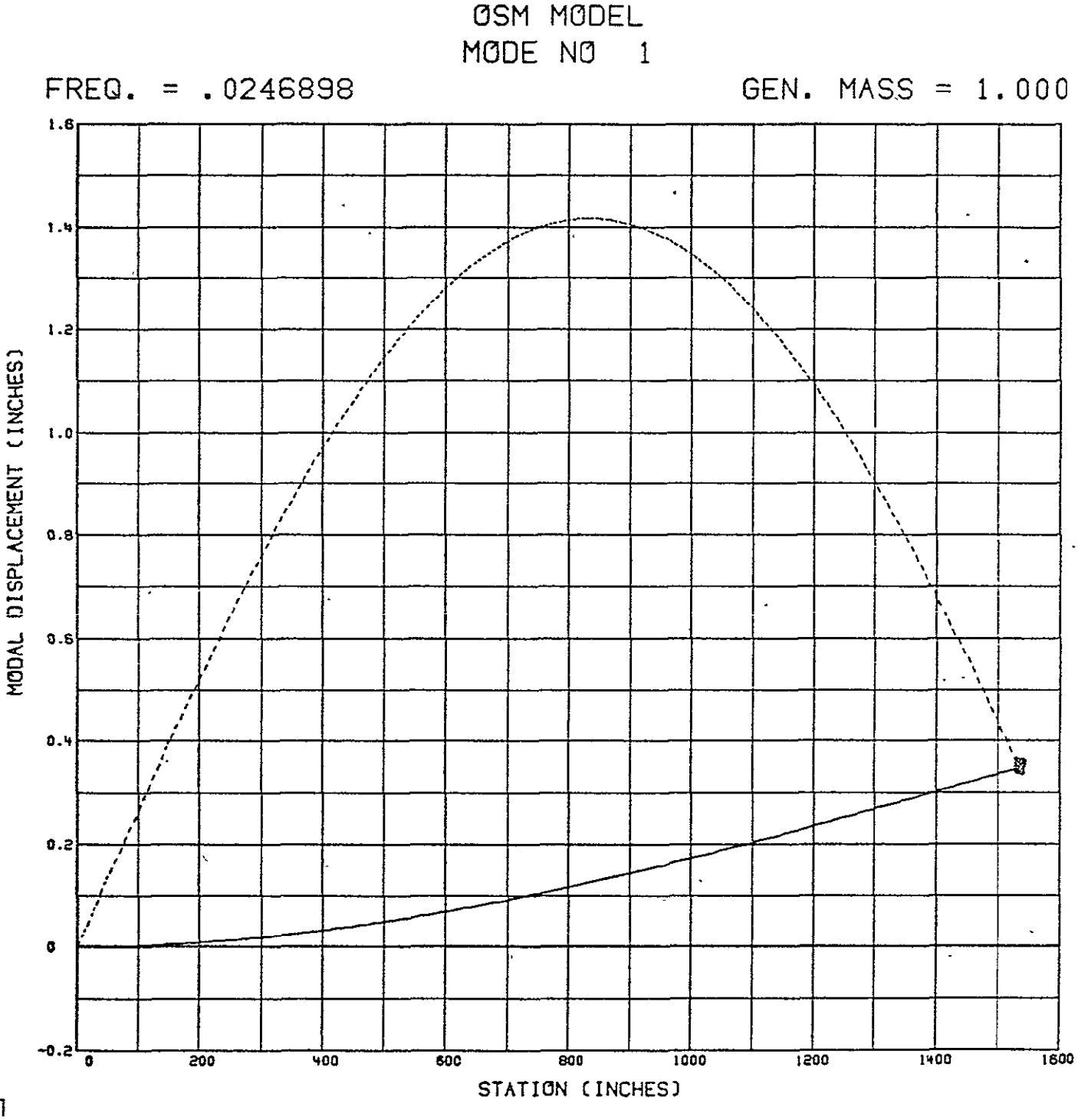
OSM MODEL
MODE NO 1
FREQ. = .0246898
GEN. MASS = 1.000
MODAL DISPLACEMENT (INCHES)
1.6
1.4
1.2
1.0
0.8
0.6
0.4
0.2
0
-0.2
0
200
400
600
800
1000
1200
1400
1600
STATION (INCHES)

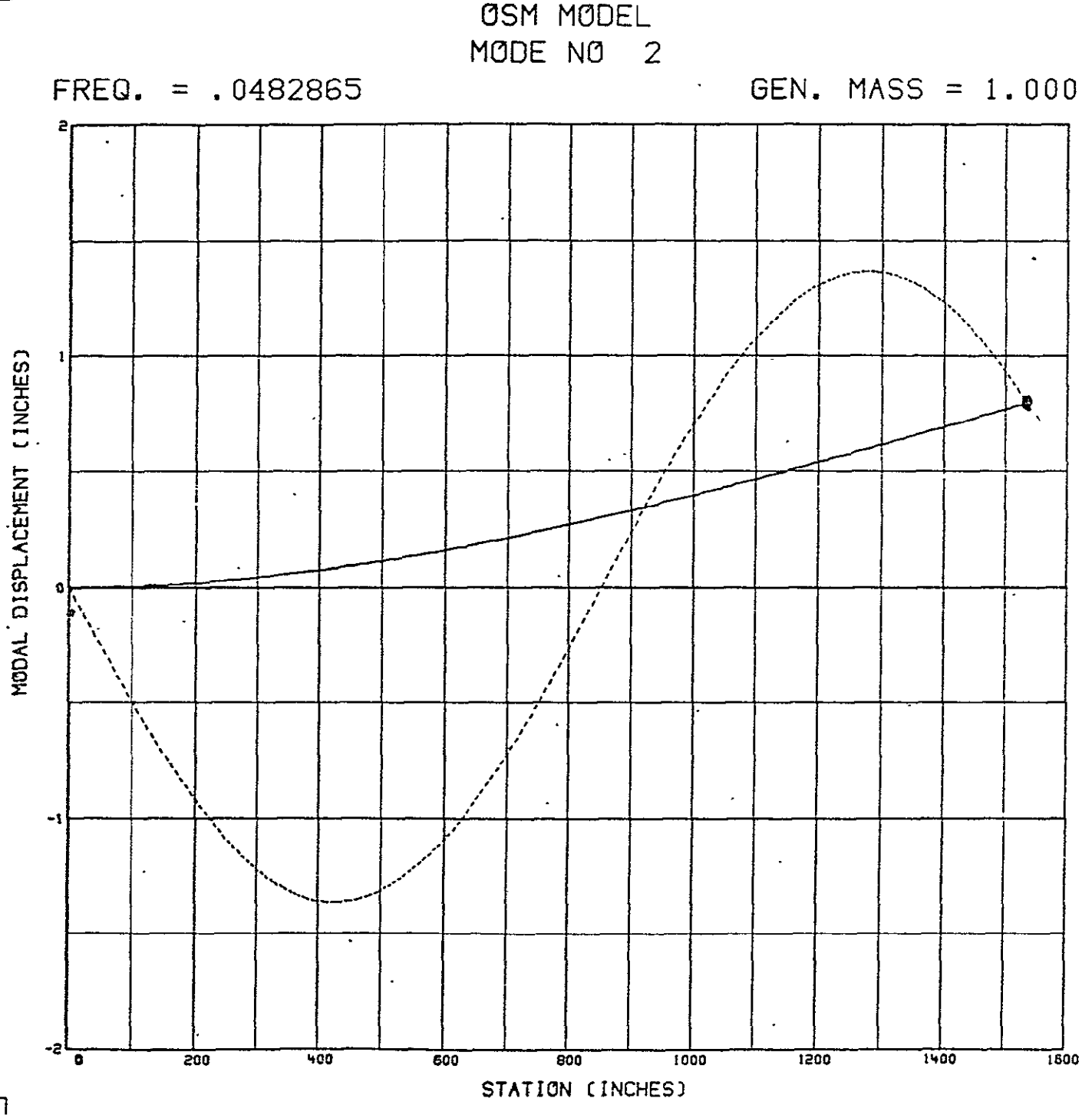
ØSM MØDEL
MØDE NØ 2
FREQ. = .0482865
GEN. MASS = 1.000
MØDAL DISPLACEMENT (INCHES)
2
1
0
-1
-2
0
200
400
600
800
1000
1200
1400
1600
STATION (INCHES)

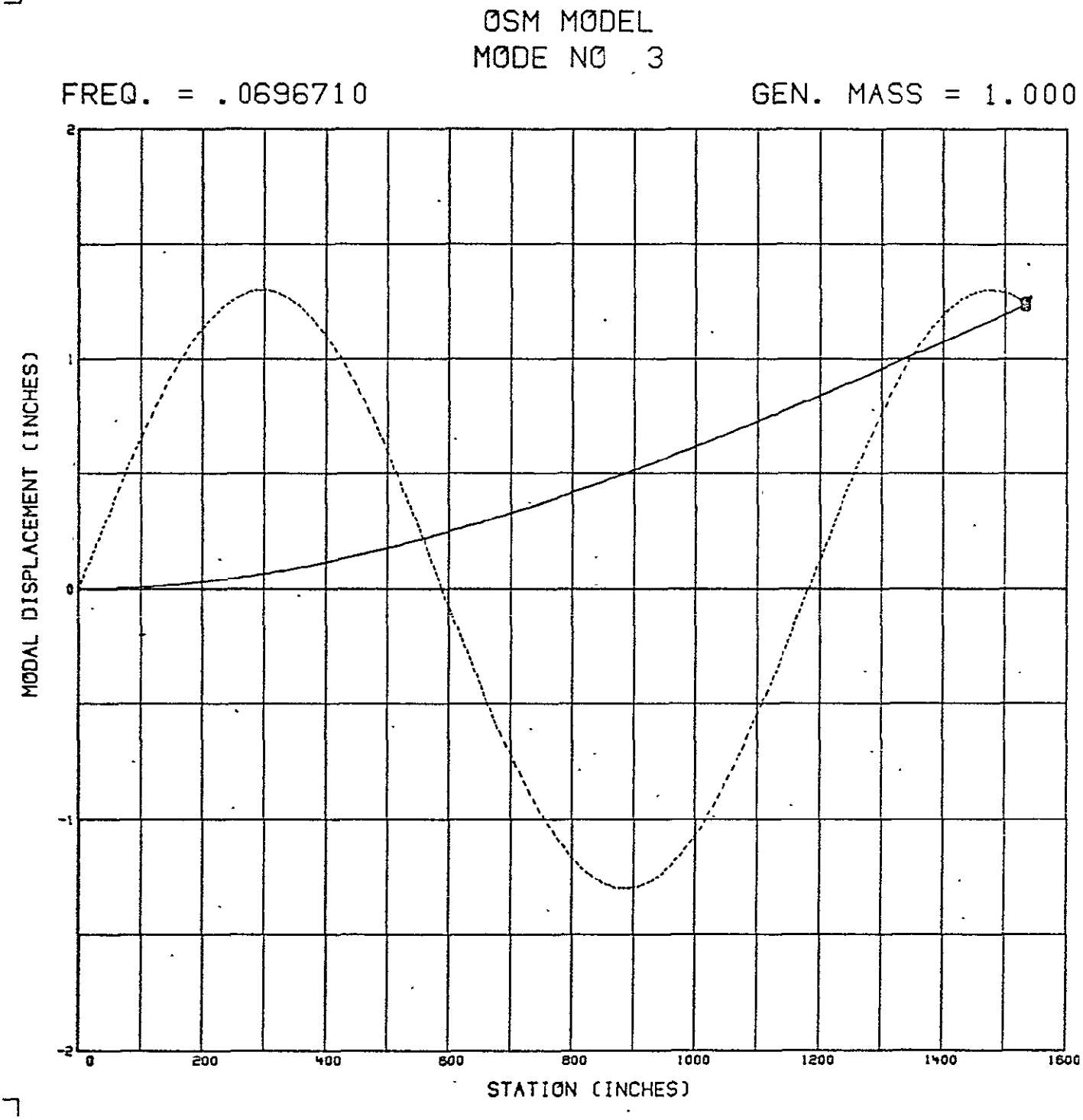
OSM MODEL
MODE NO 3
FREQ. = .0696710
GEN. MASS = 1.000
MODAL DISPLACEMENT (INCHES)
2
1
0
-1
-2
0
200
400
600
800
1000
1200
1400
1600
STATION (INCHES)

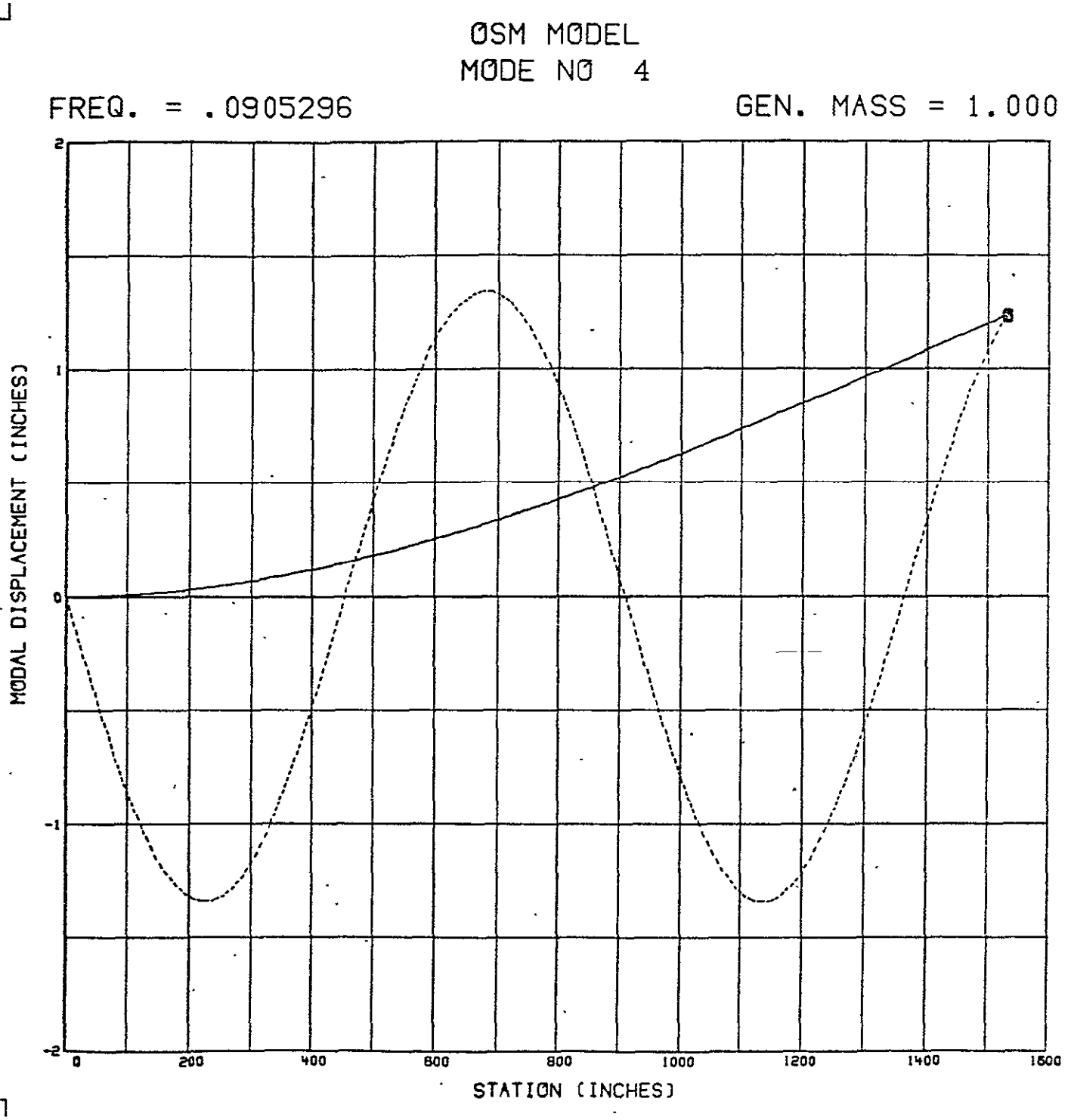
OSM MODEL
MODE NO 4
FREQ. = .0905296
GEN. MASS = 1.000
MODAL DISPLACEMENT (INCHES)
2
1
0
-1
-2
0
200
400
600
800
1000
1200
1400
1600
STATION (INCHES)

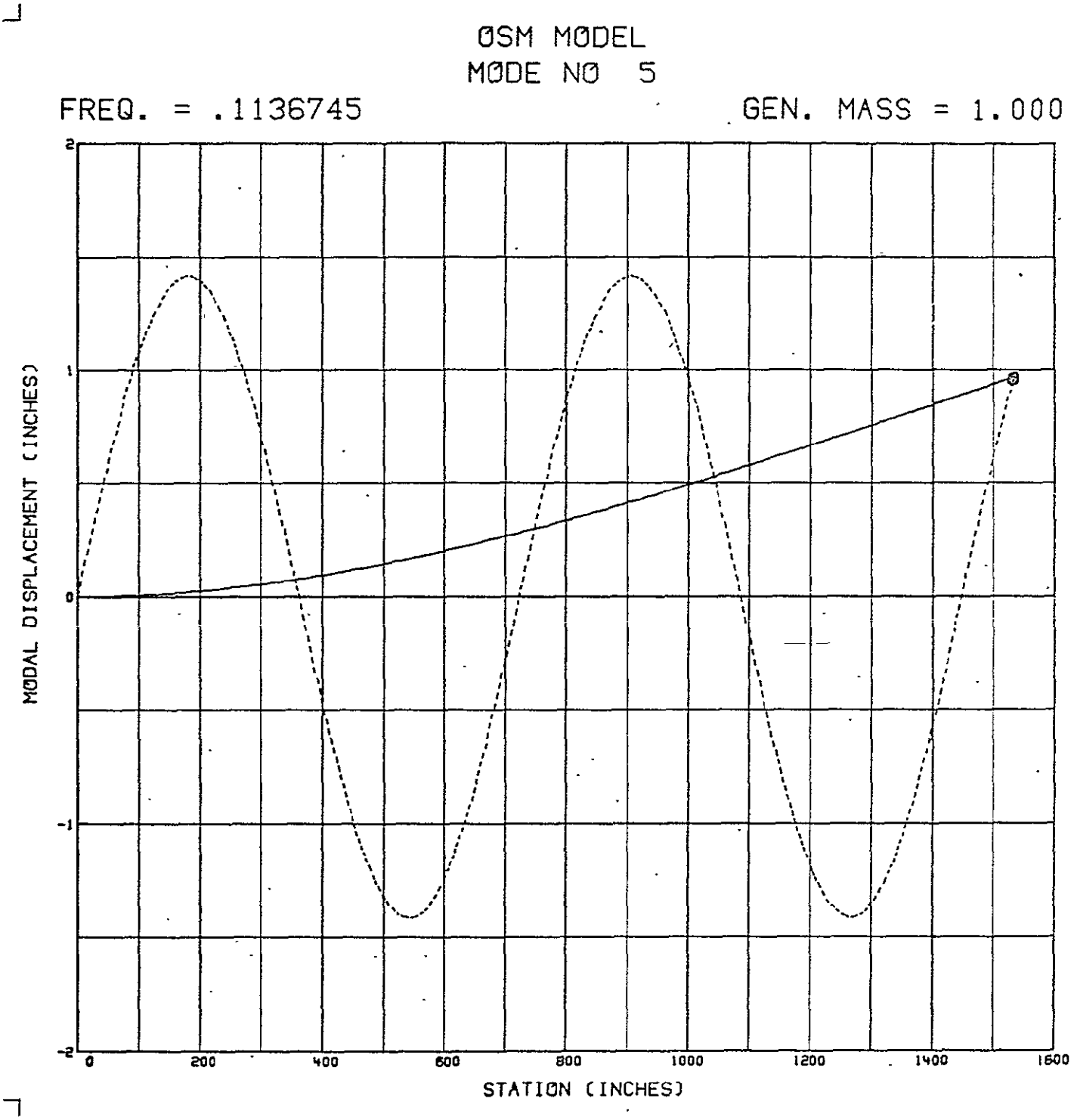
ØSM MØDEL
MØDE NØ 5
FREQ. = .1136745
GEN. MASS = 1.000
MØDAL DISPLACEMENT (INCHES)
2
1
0
-1
-2
0
200
400
600
800
1000
1200
1400
1600
STATION (INCHES)

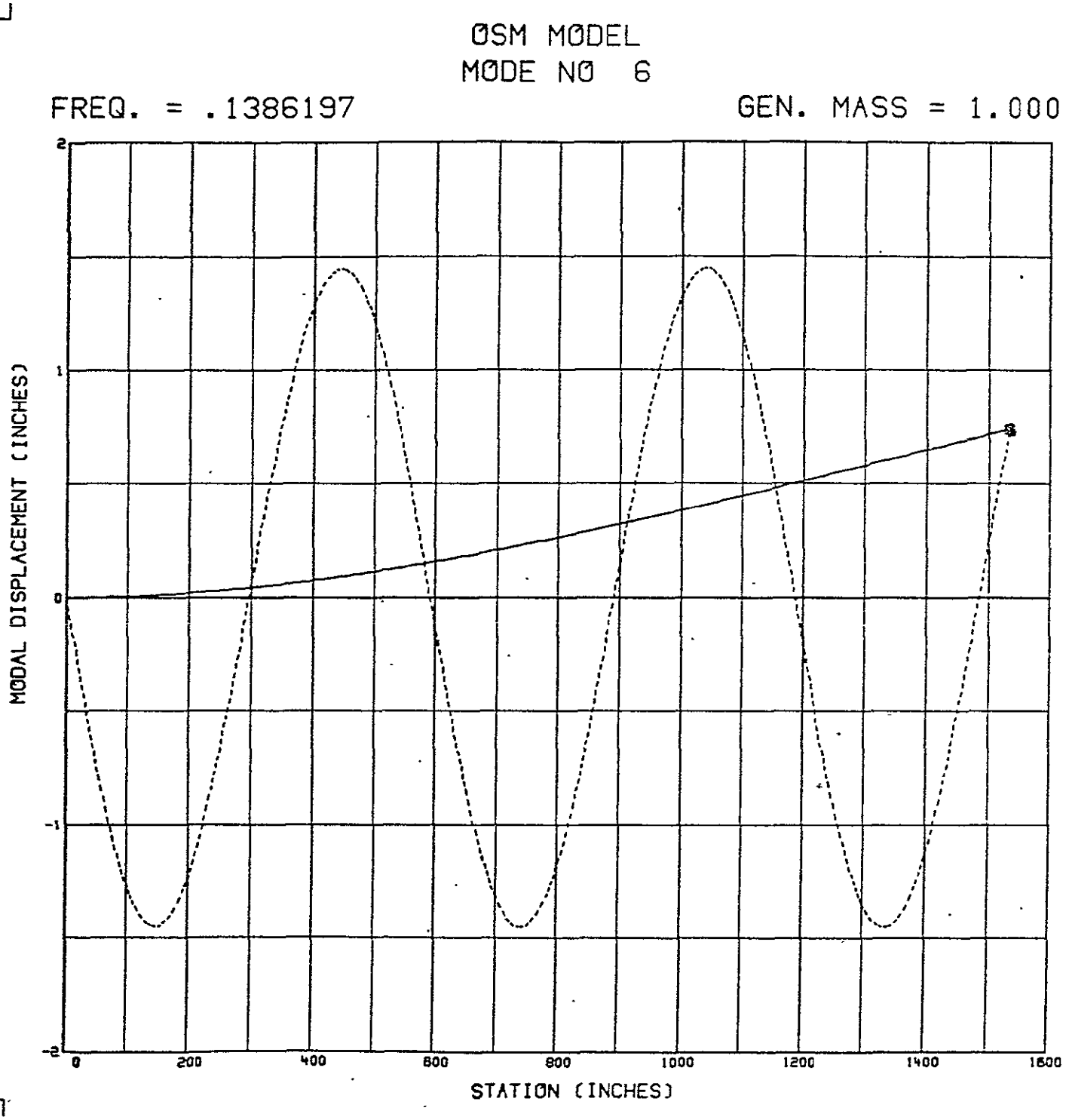
OSM MODEL
MODE NO 6
FREQ. = .1386197
GEN. MASS = 1.000
MODAL DISPLACEMENT (INCHES)
2
1
0
-1
-2
0
200
400
600
800
1000
1200
1400
1600
STATION (INCHES)

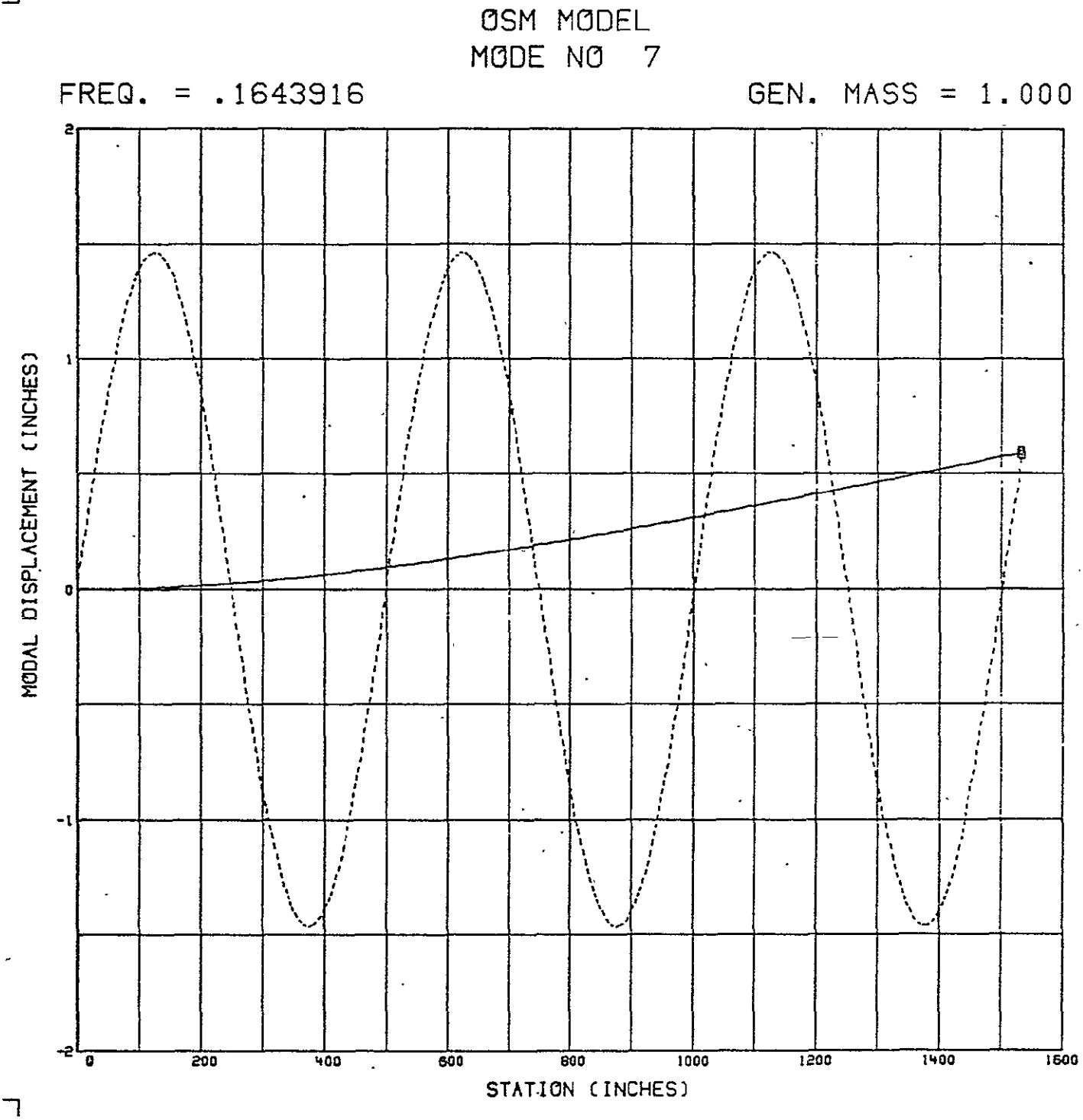
OSM MODEL
MODE NO 7
FREQ. = .1643916
GEN. MASS = 1.000
MODAL DISPLACEMENT (INCHES)
STATION (INCHES)
2
1
0
-1
-2
0
200
400
600
800
1000
1200
1400
1600

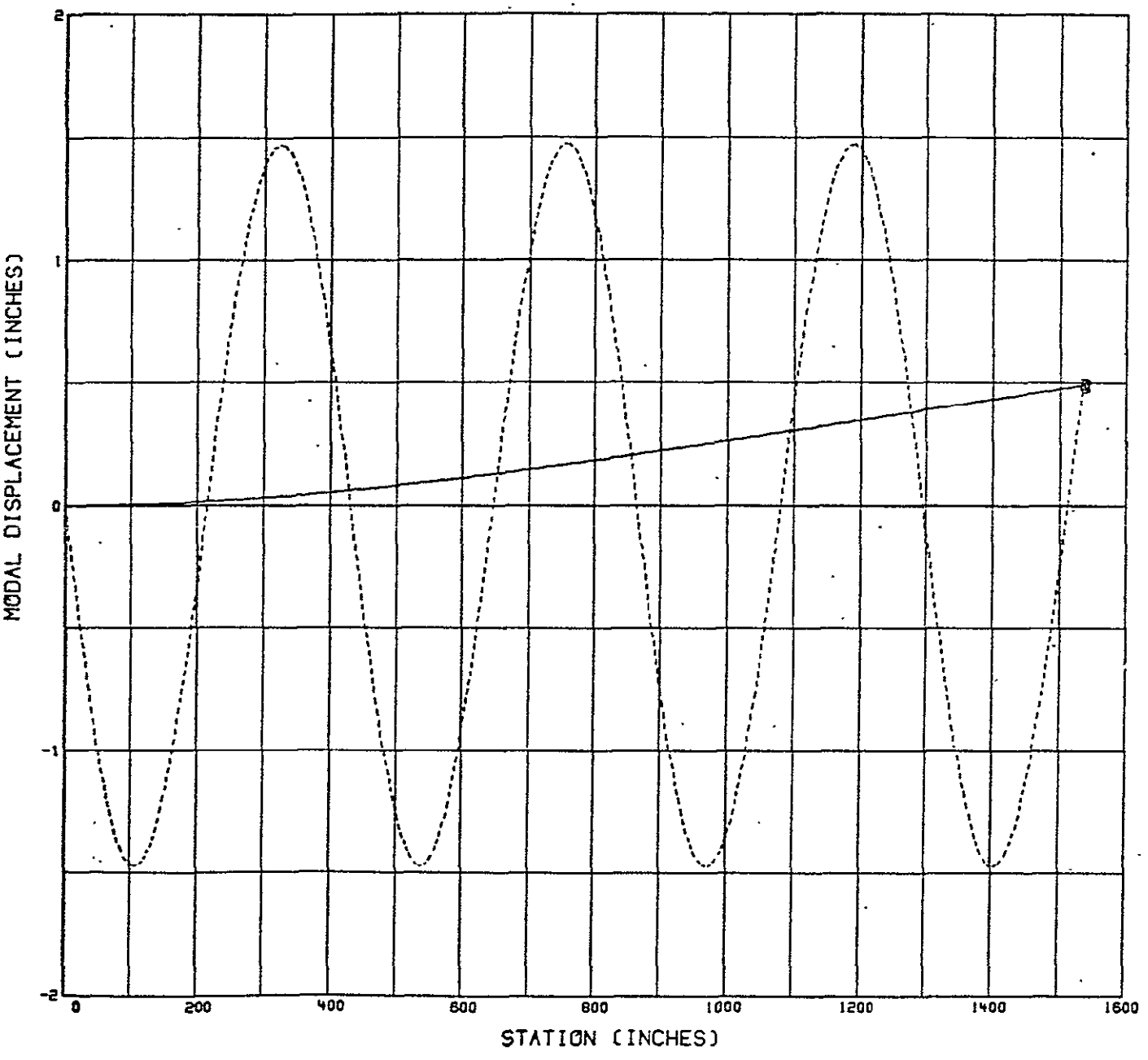
OSM MODEL
MODE NO 8
FREQ. = .1905504
GEN. MASS = 1.000
MODAL DISPLACEMENT (INCHES)
2
1
0
-1
-2
0
200
400
600
800
1000
1200
1400
1600
STATION (INCHES)

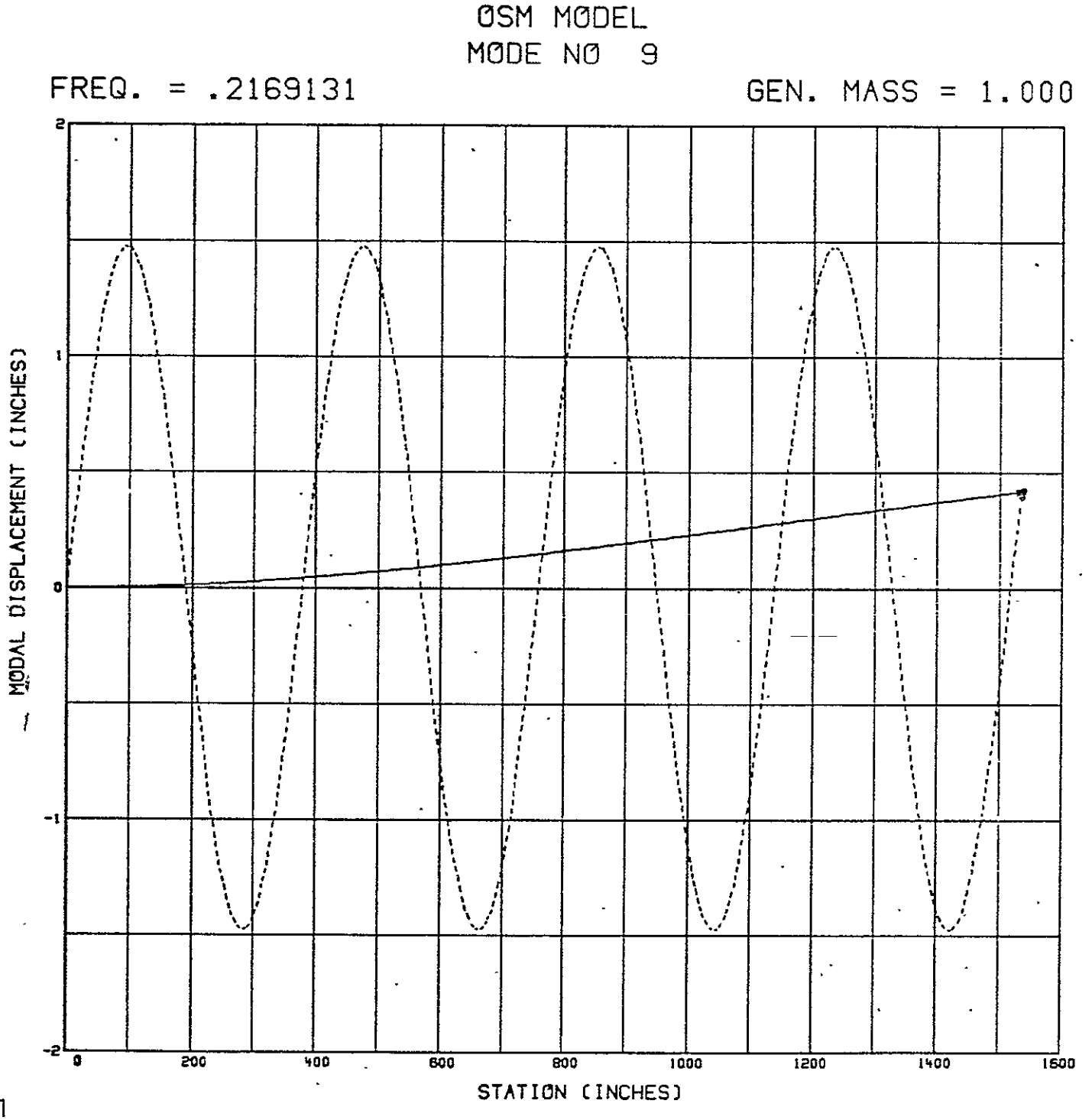
0SM M0DEL
M0DE N0 9
FREQ. = .2169131
GEN. MASS = 1.000
MODAL DISPLACEMENT (INCHES)
2
1
0
-1
-2
0
200
400
600
800
1000
1200
1400
1600
STATION (INCHES)

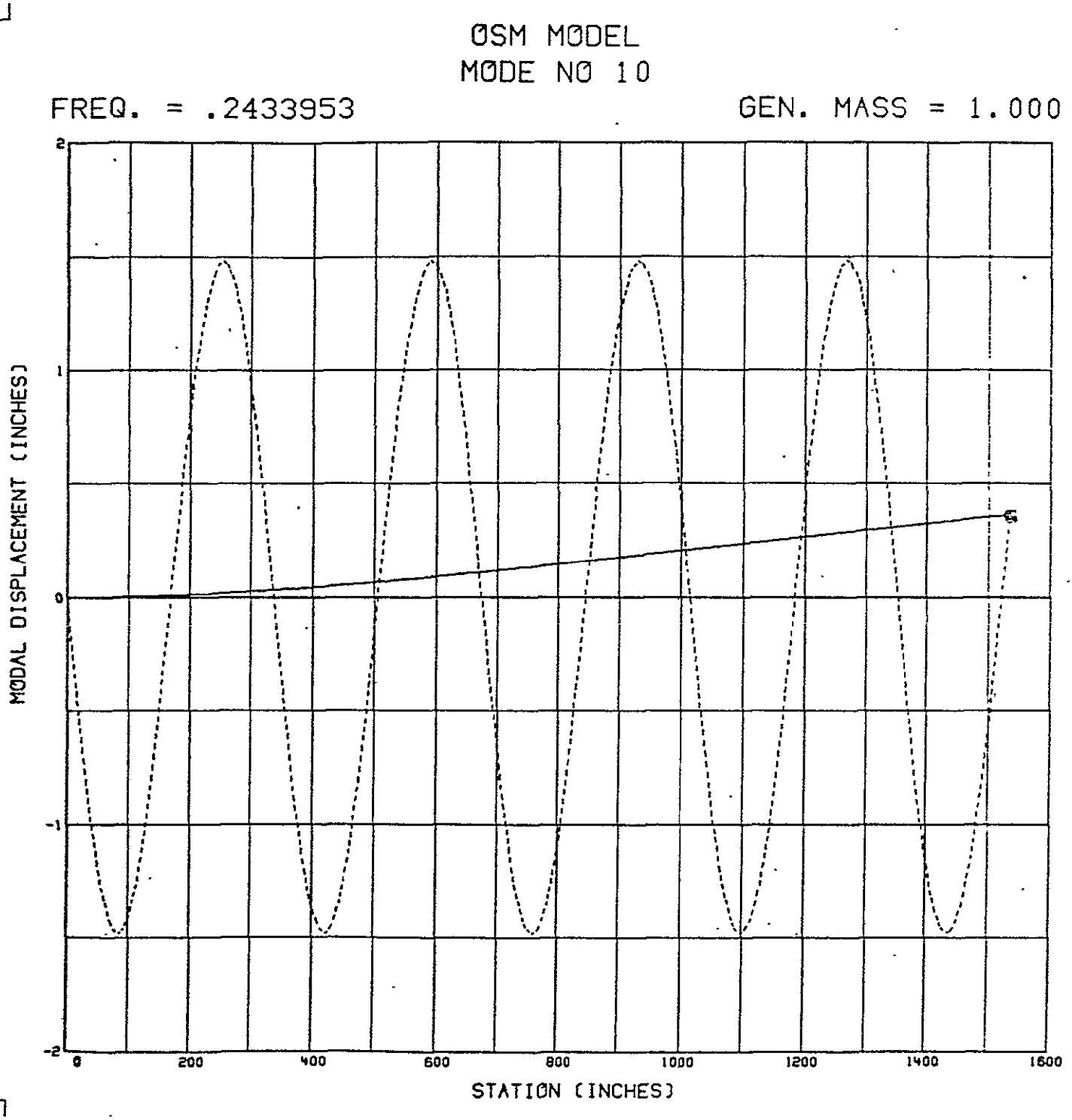
OSM MODEL
MODE NO 10
FREQ. = .2433953
GEN. MASS = 1.000
MODAL DISPLACEMENT (INCHES)
2
1
0
-1
-2
0
200
400
600
800
1000
1200
1400
1600
STATION (INCHES)

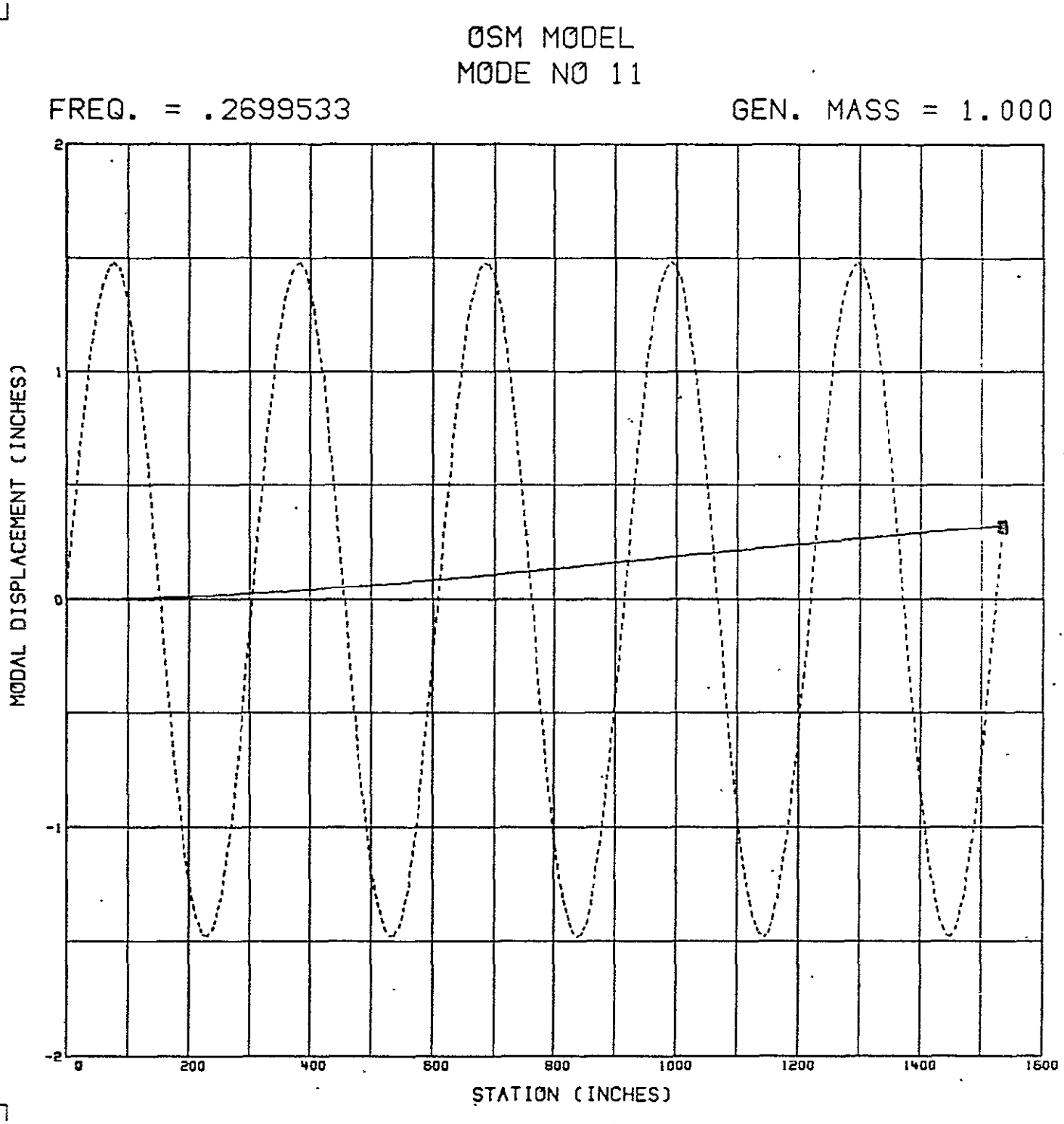
OSM MODEL
MODE NO 11
FREQ. = .2699533
GEN. MASS = 1.000
MODAL DISPLACEMENT (INCHES)
2
1
0
-1
-2
0
200
400
600
800
1000
1200
1400
1600
STATION (INCHES)

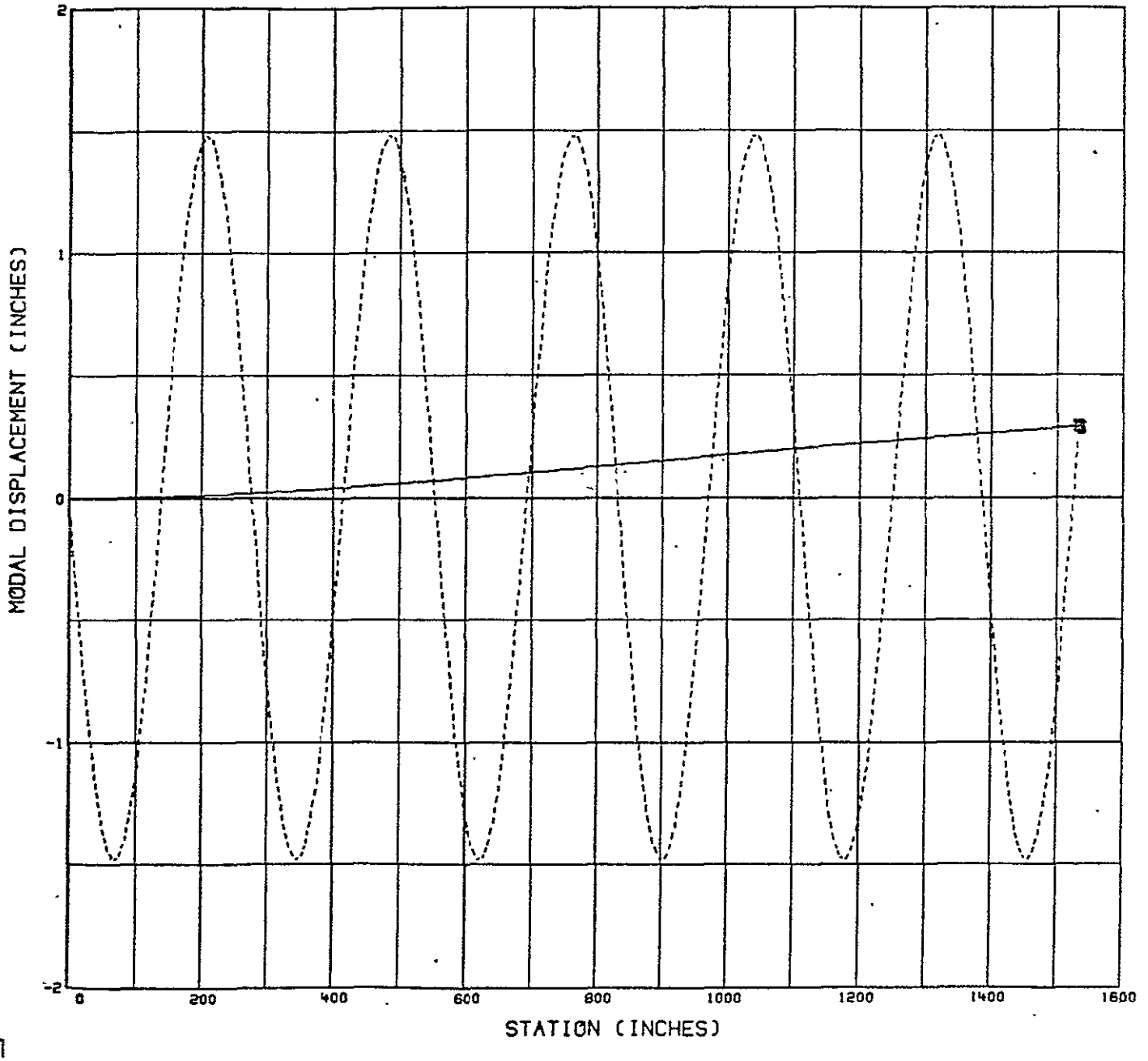
ØSM MØDEL
MØDE NØ 12
FREQ. = .2965624
GEN. MASS = 1.000
MØDAL DISPLACEMENT (INCHES)
2
1
0
-1
-2
0
200
400
600
800
1000
1200
1400
1600
STATION (INCHES)

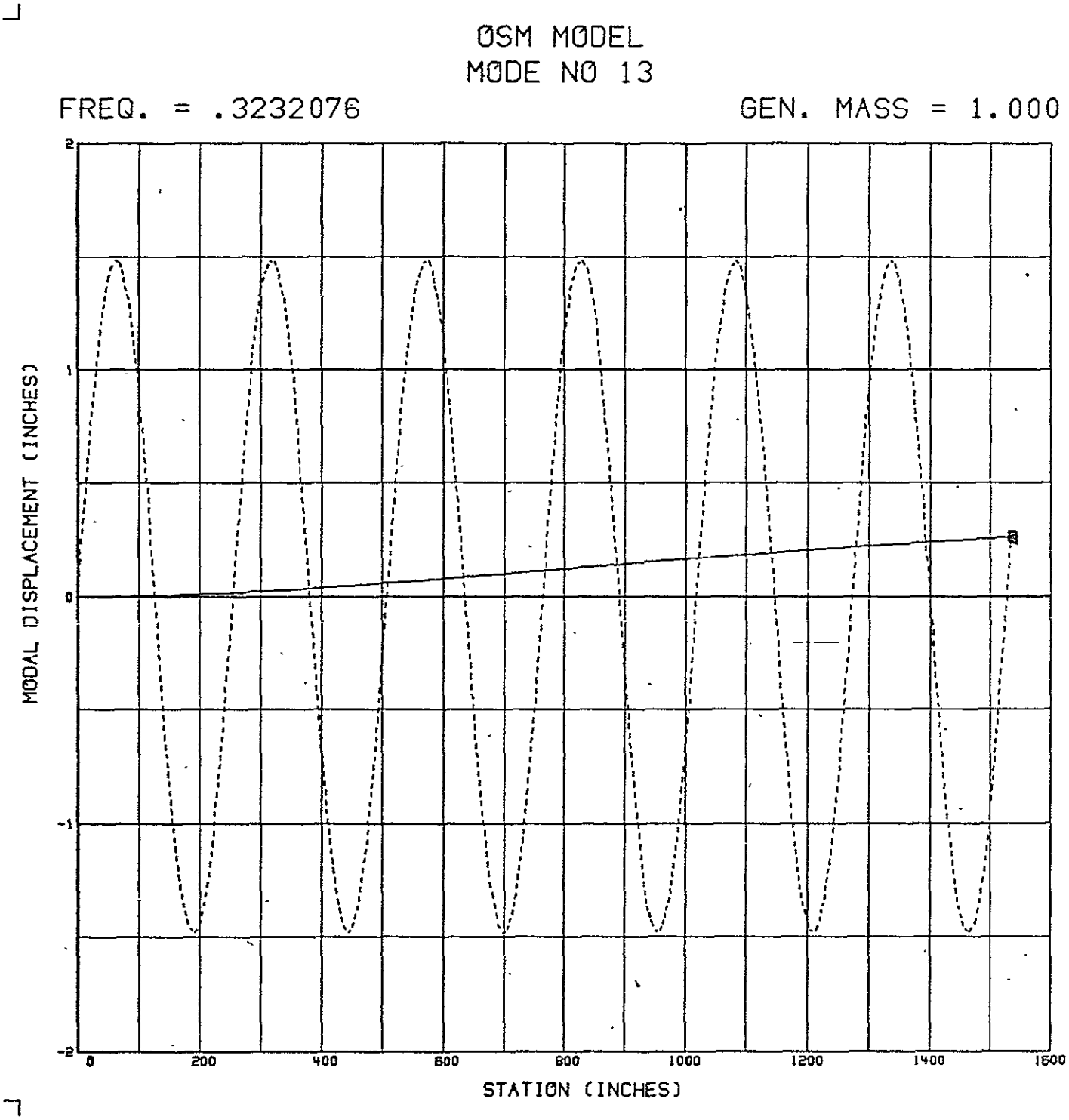
ØSM MØDEL
MØDE NØ 13
FREQ. = .3232076
GEN. MASS = 1.000
MODAL DISPLACEMENT (INCHES)
2
1
0
-1
-2
0
200
400
800
800
1000
1200
1400
1600
STATION (INCHES)

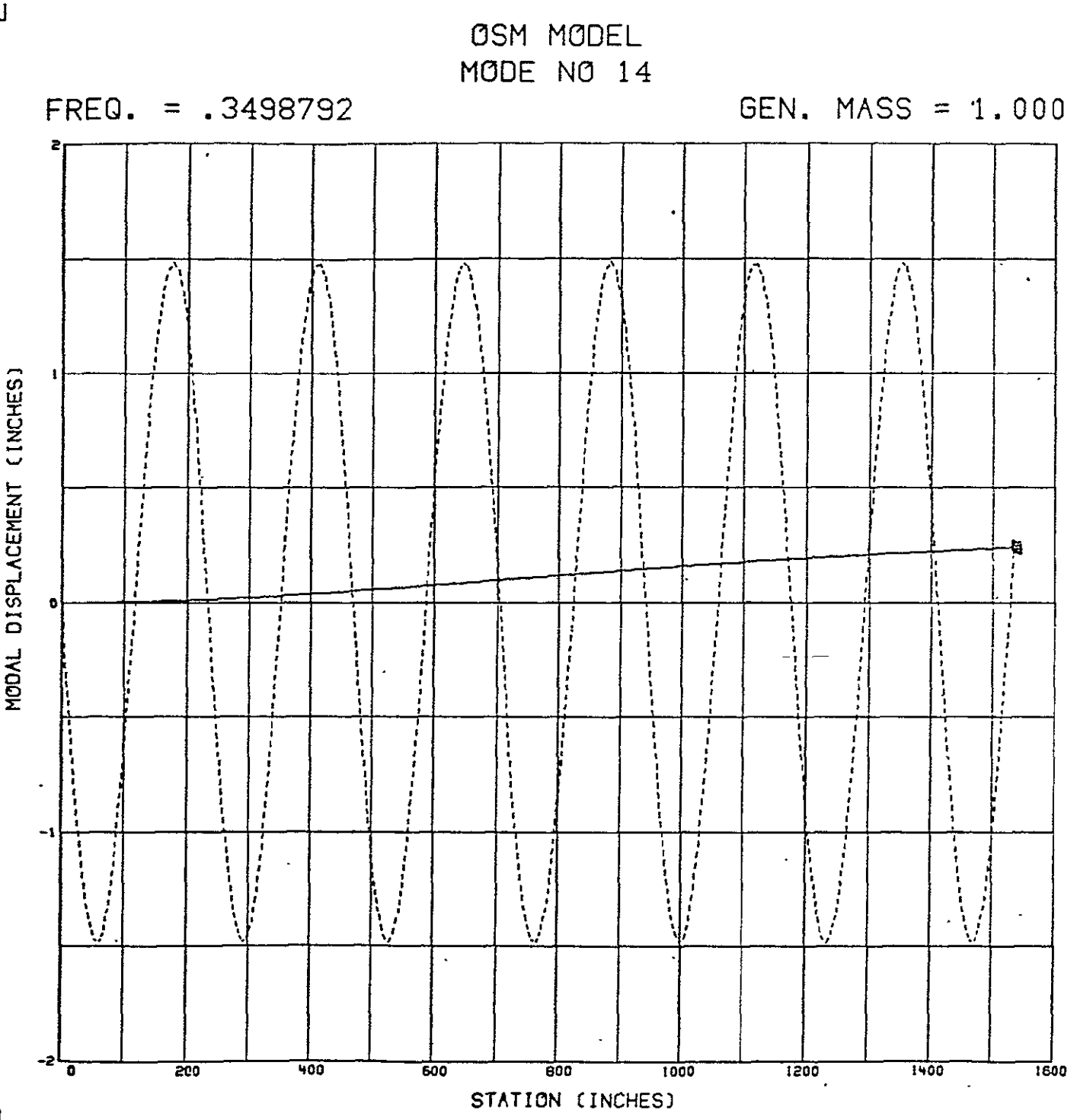
OSM MODEL
MODE NO 14
FREQ. = .3498792
GEN. MASS = 1.000
MODAL DISPLACEMENT (INCHES)
2
1
0
-1
-2
0
200
400
600
800
1000
1200
1400
1600
STATION (INCHES)

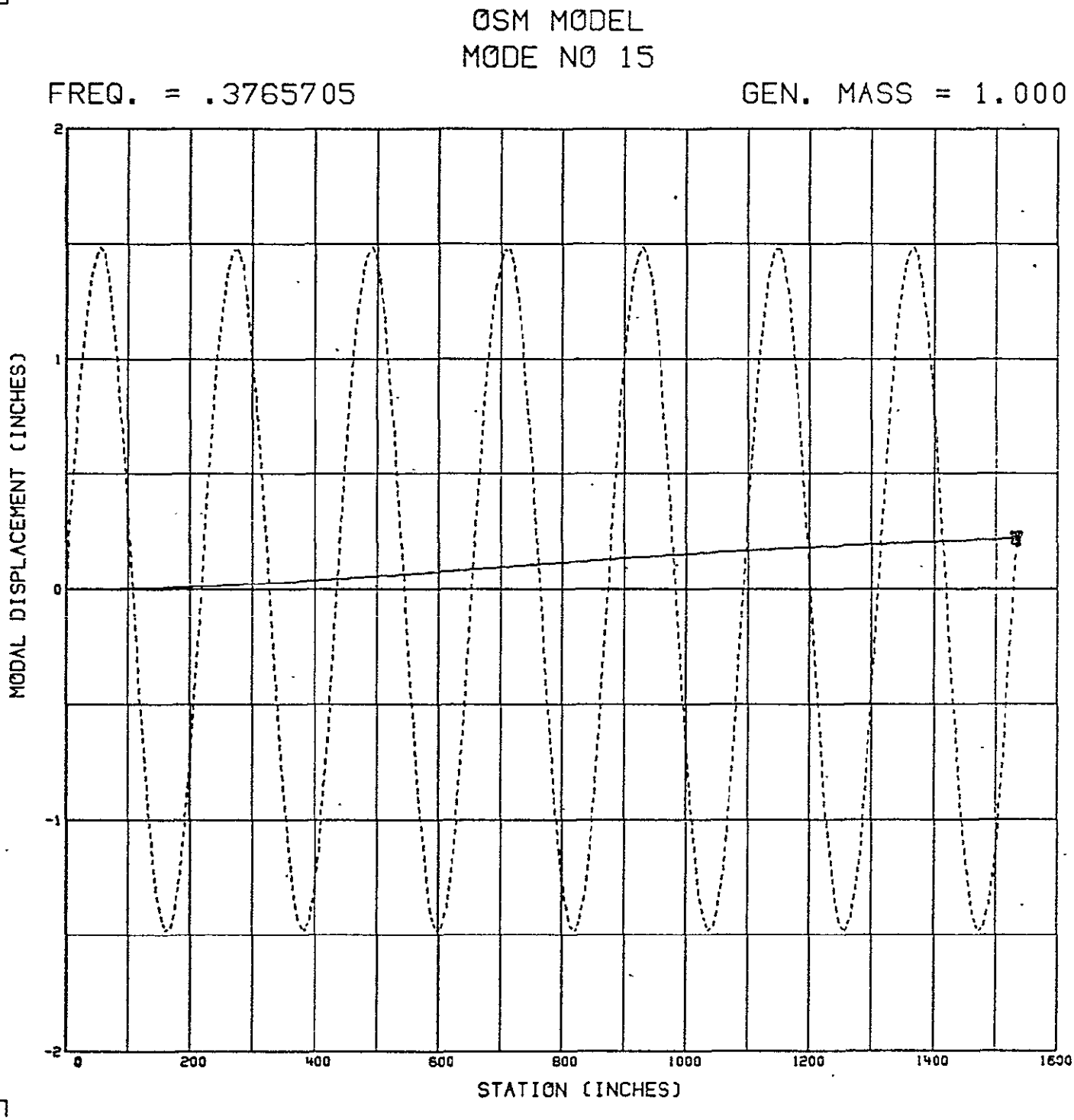
OSM MODEL
MODE NO 15
FREQ. = .3765705
GEN. MASS = 1.000
MODAL DISPLACEMENT (INCHES)
2
1
0
-1
-2
0
200
400
600
800
1000
1200
1400
1600
STATION (INCHES)

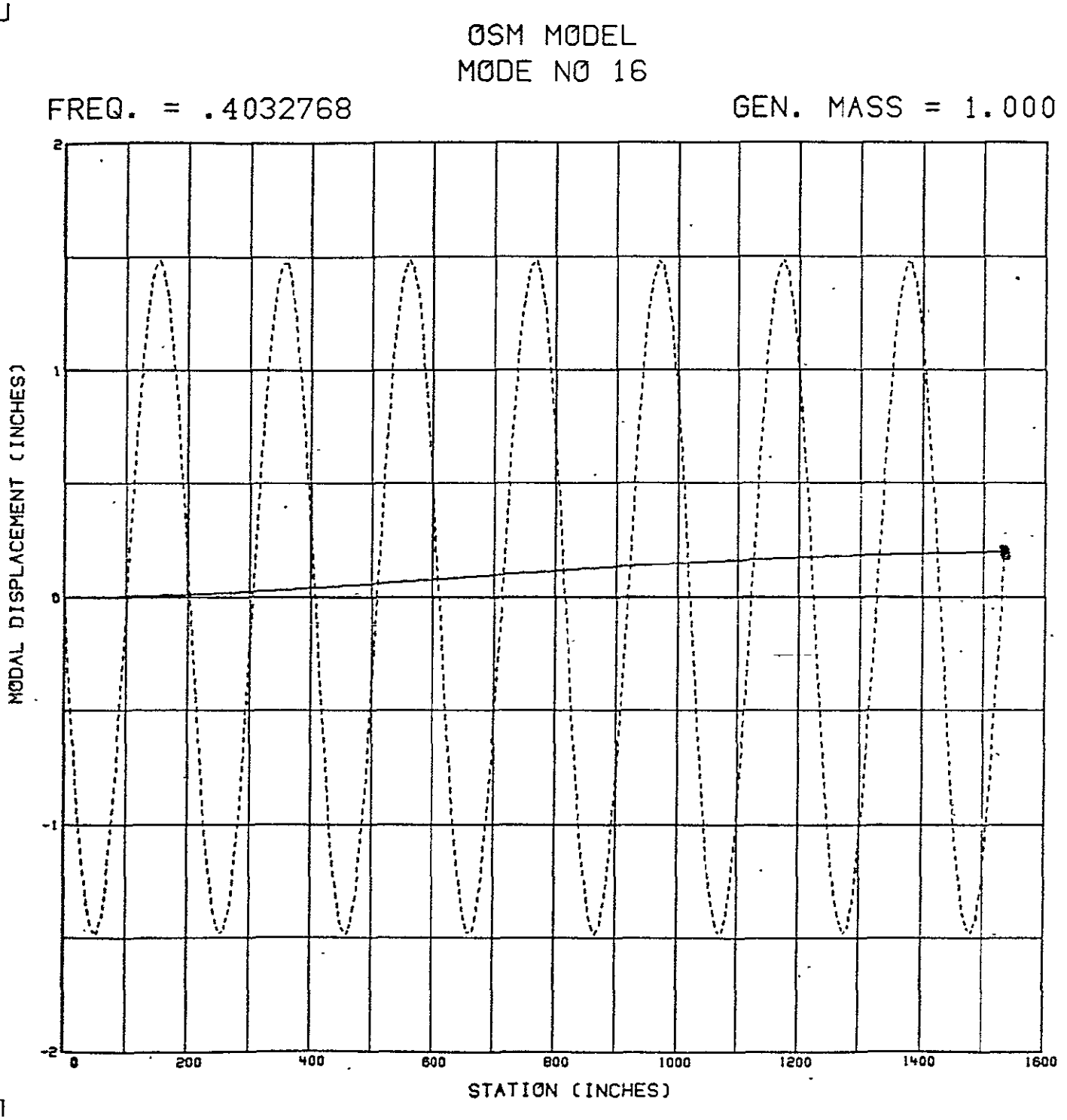
OSM MODEL
MODE NO 16
FREQ. = .4032768
GEN. MASS = 1.000
MODAL DISPLACEMENT (INCHES)
2
1
0
-1
-2
0
200
400
600
800
1000
1200
1400
1600
STATION (INCHES)

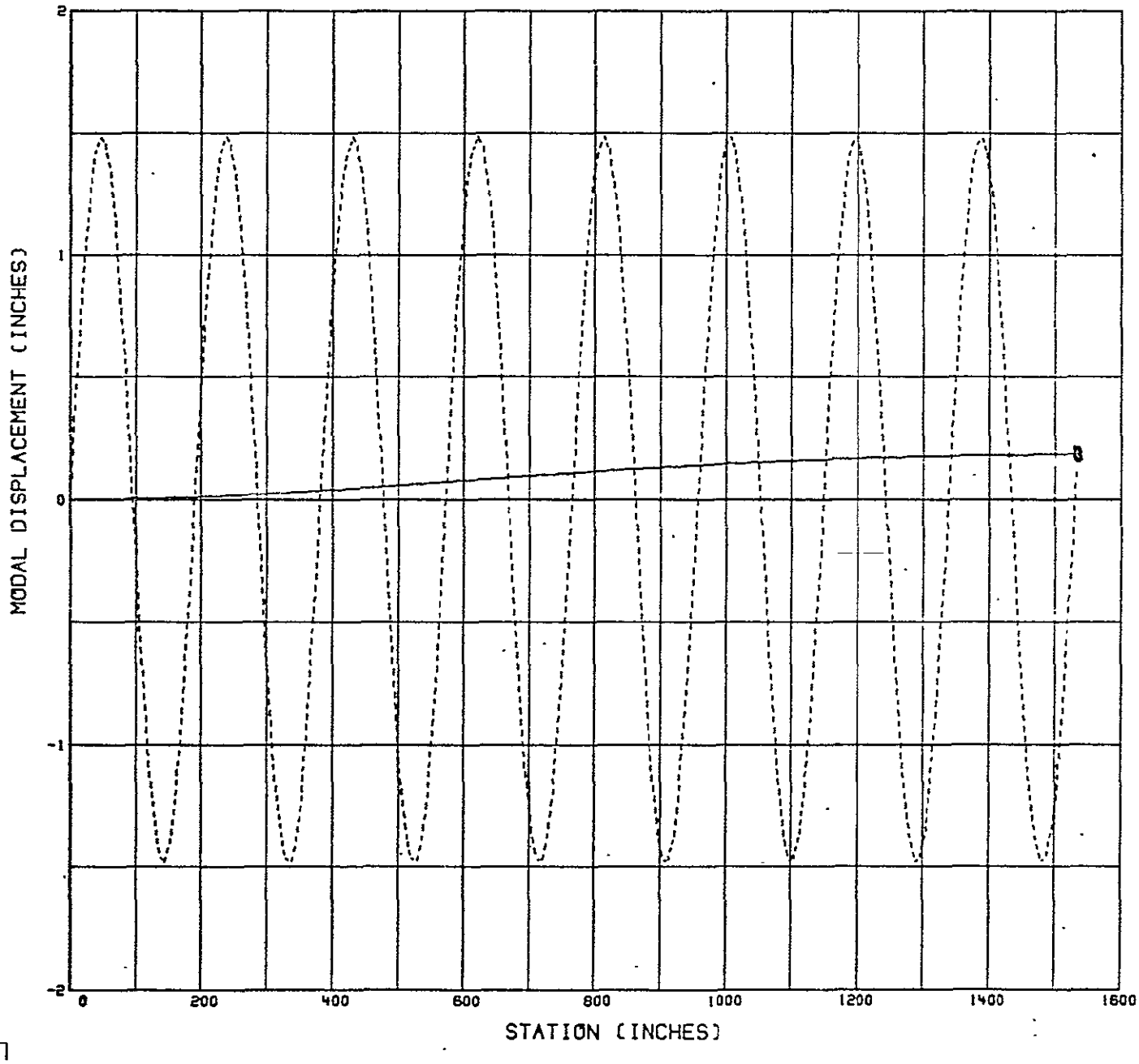
0SM M0DEL
M0DE N0 17
FREQ. = .4299948
GEN. MASS = 1.000
MODAL DISPLACEMENT (INCHES)
2
1
0
-1
-2
0
200
400
600
800
1000
1200
1400
1600
STATION (INCHES)

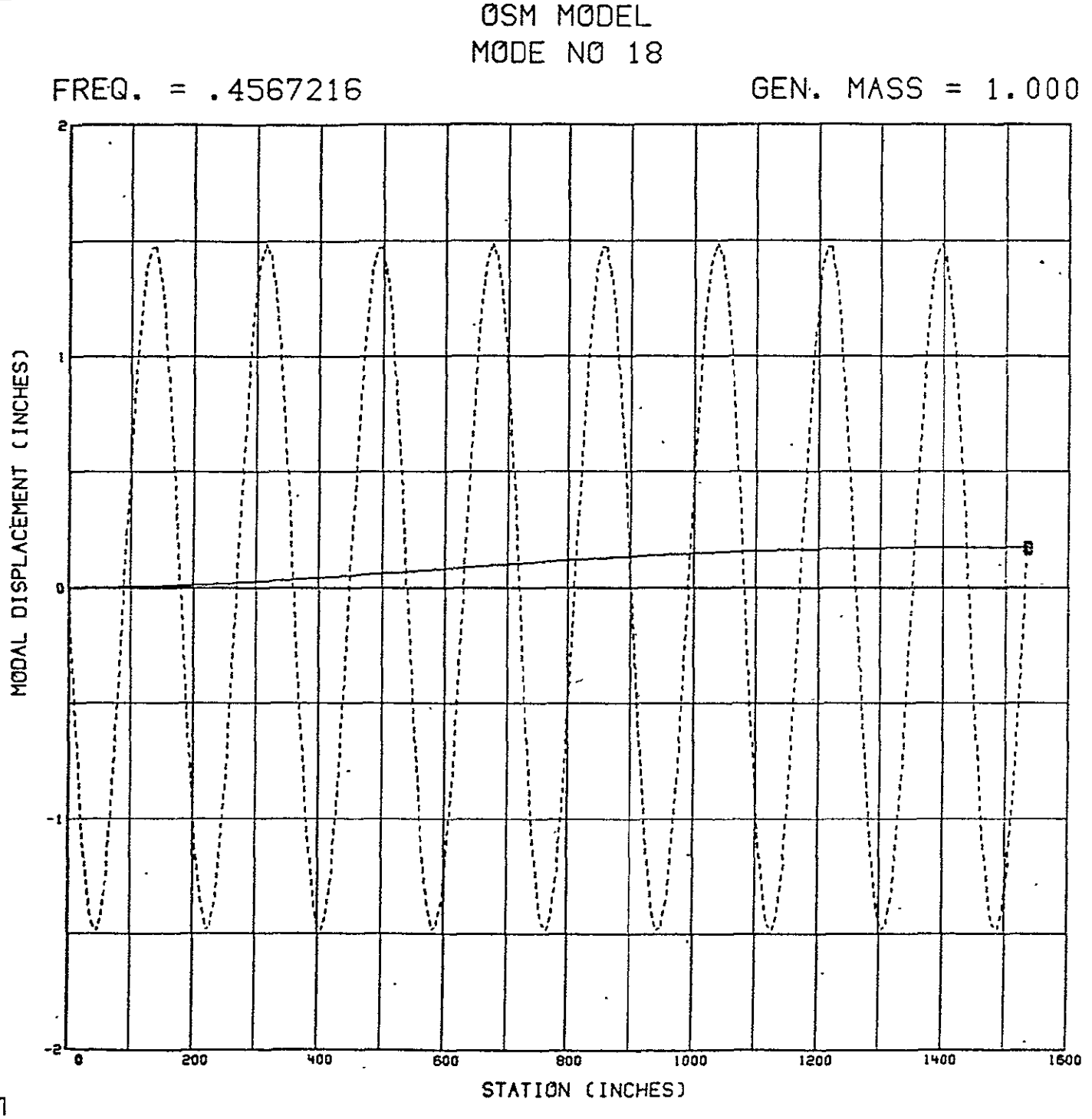
OSM MODEL
MODE NO 18
FREQ. = .4567216
GEN. MASS = 1.000
MODAL DISPLACEMENT (INCHES)
2
1
0
-1
-2
0
200
400
600
800
1000
1200
1400
1600
STATION (INCHES)

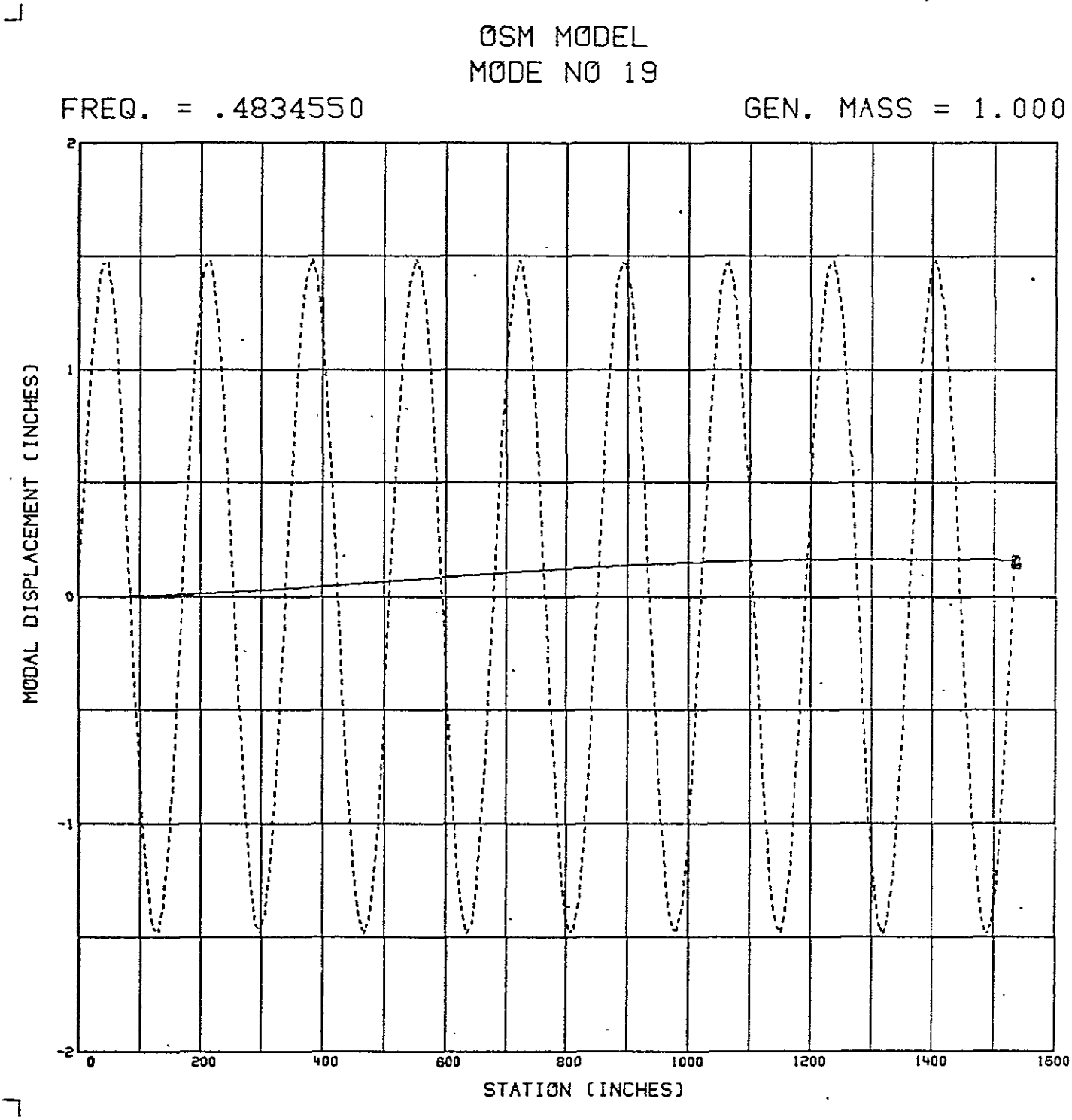
ØSM MØDEL
MØDE NØ 19
FREQ. = .4834550
GEN. MASS = 1.000
MØDAL DISPLACEMENT (INCHES)
2
1
0
-1
-2
0
200
400
600
800
1000
1200
1400
1600
STATION (INCHES)

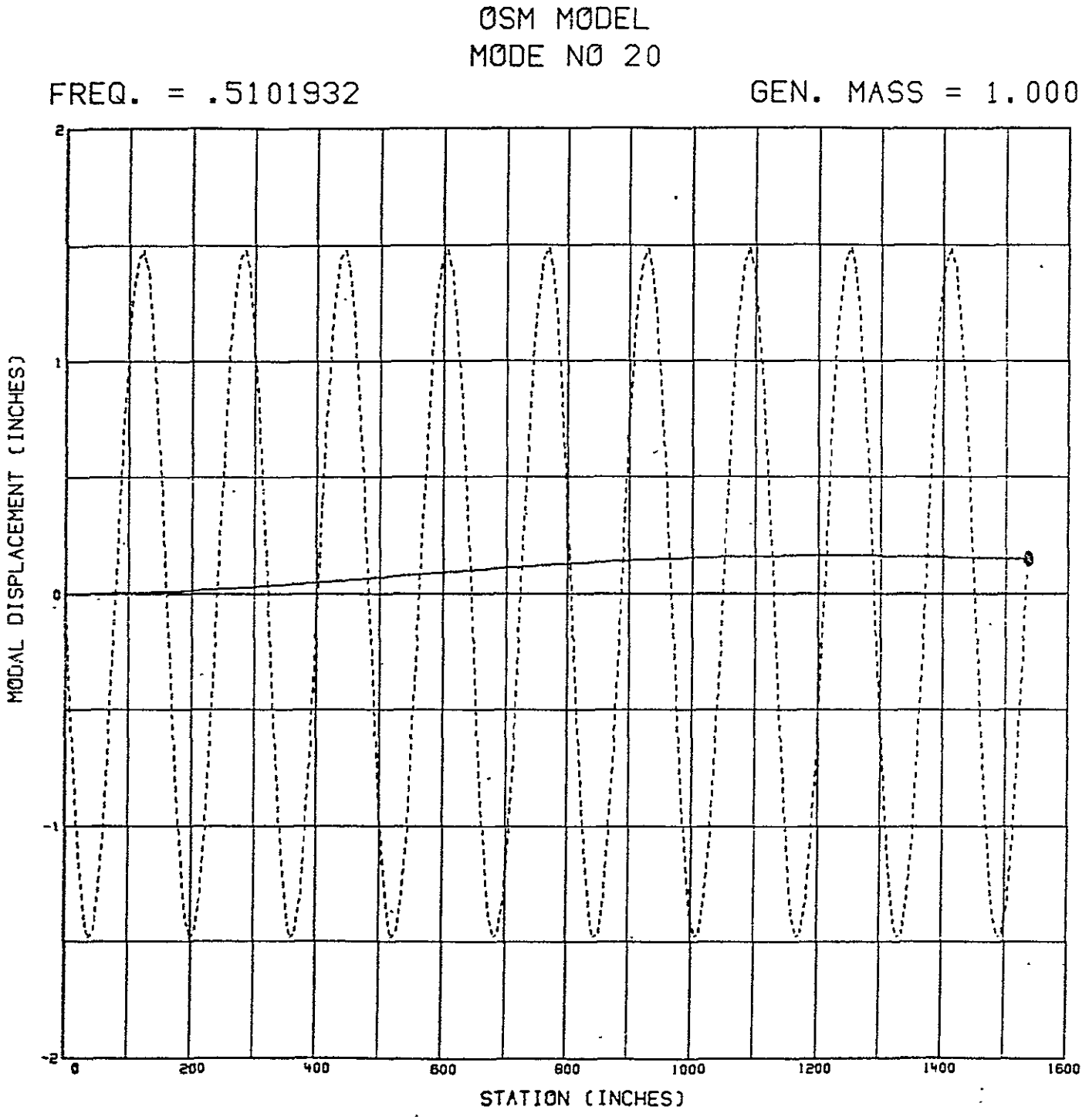
ØSM MØDEL
MØDE NØ 20
FREQ. = .5101932
GEN. MASS = 1.000
MØDAL DISPLACEMENT (INCHES)
2
1
0
-1
-2
0
200
400
600
800
1000
1200
1400
1600
STATION (INCHES)